Energetics of ligand binding to the active site of glutathione transferase M1-1

Nichole Michelle Kinsley

A thesis submitted to the Faculty of Science, University of the Witwatersrand, Johannesburg, in fulfilment of the requirement for the degree of Master of Science.

Johannesburg, August 2005

DECLARATION

I declare that this thesis is my own, unaided work. It is being submitted for the degree of Master of Science in the University of the Witwatersrand, Johannesburg. It has not been submitted before for any degree or examination in any other University.

Nichole Michelle Kinsley

this day of 2005

This work is dedicated to the love of my life, Carlo

To my family, Mom, Dad and Tanya thank you for your support, love and confidence in me

To Ernie and Colleen, thank you for your support

'Bernard of Chartres used to say that we are like dwarfs on the shoulders of giants, so that we can see more than they, and things at a greater distance, not by virtue of any sharpness of sight on our part, or any physical distinction, but because we are carried high and raised up by their giant size.'

John of Salisbury, 1159

'If I have seen further it is by standing on the shoulders of giants.'

Sir Isaac Newton, 1675

ABSTRACT

Isothermal titration calorimetry was used to investigate the forces that drive ligand binding to the active site of rGST M1-1. In an attempt to gain insight into the recognition of non-substrate ligands by GSTs, this study also investigates interactions between rGST M1-1 and ANS, a non-substrate ligand. At 25 °C, complex formation between rGST M1-1 and GSH, GSO_3^-, and *S*-hexylglutathione is characterised by a monophasic binding isotherm with K_d values of 38.5 μM, 2.1 μM and 0.2 μM, respectively. One molecule of each ligand is bound per monomer of rGST M1-1. Binding of these ligands is enthalpically favourable and entropically unfavourable with a resultant favourable Gibbs free energy, overall. The effects of temperature and buffer ionisation on the energetics of binding were studied. The enthalpic and entropic contributions for all three ligands exhibited temperature dependence over the temperature range investigated (5-30 °C). The Gibbs free energy showed negligible changes with increasing temperature due to enthalpy-entropy compensation. The temperature dependence of the binding enthalpy yielded heat capacity changes of –2.69 kJ/mol/K and –3.68 kJ/mol/K at 25 °C for GSH and *S*-hexylglutathione binding and –1.86 kJ/mol/K overall for GSO_3^-. The linear dependence of ΔH on temperature for GSO_3^- binding to rGST M1-1 suggests the formation of a more constrained complex which limits the fluctuations in conformations of the mu-loop at the active site. The non-linear dependence of ΔH on temperature for GSH and *S*-hexylglutathione binding to the enzyme suggests the formation of a complex that samples different bound conformations due to the mobility of the mu-loop even after ligand is bound. Calorimetric binding experiments in various buffer systems with different ionisation enthalpies suggest that the binding of GSH to rGST M1-1 is coupled to the deprotonation of the thiol of GSH while GSO_3^- binding to rGST M1-1 is independent of the buffer ionisation. At 25 °C, the rGST M1-1●ANS association is represented by a monophasic binding isotherm with one molecule of ANS bound per monomer of rGST M1-1. The interaction is both enthalpically and entropically driven with a K_d value of 27.2 μM representing moderate affinity. The effect of temperature on the interaction was investigated over the temperature range of 5-30 °C. The linear dependence of the binding enthalpy on temperature indicates that no significant structural changes occur upon binding of ANS to the enzyme (ΔC_p = -0.34 kJ/mol/K). The change in heat capacity associated with the interaction can be attributed to the

burial of the polar sulphonate group of ANS and the exposure of the anilino and naphthyl rings to solvent as well as the possibility of weak electrostatic interactions between ANS and residues at the active site. The effect of ethacrynic acid, GSH, GSO_3^- and *S*-hexylglutathione on the fluorescence of ANS was investigated in order to obtain some idea as to the location of the ANS binding site on rGST M1-1. ANS was displaced by GSO_3^-, *S*-hexylglutathione and ethacrynic acid, while no displacement occurred upon binding of GSH to the active site of rGST M1-1. Displacement studies and molecular docking simulations indicate that ANS binds to the H-site of rGST M1-1 and the possibility of a second binding site for the molecule cannot be ruled out.

ACKNOWLEDGEMENTS

To my supervisor, Professor Heini Dirr for his guidance and amazing enthusiasm and passion for Science. Thank you for the opportunity of working in your laboratory.

To my co-supervisor, Doctor Yasien Sayed, thank you for your understanding and discussion.

To all the members of the Protein Structure-Function Research Unit for their help and individuality.

The University of the Witwatersrand and the National Research Foundation of South Africa for financial assistance.

TABLE OF CONTENTS

LIST OF FIGURES

LIST OF TABLES

ABBREVIATIONS

A_{280}	absorbance at 280 nm
ANS	8-anilino-1-napthalene sulphonate
ASA	solvent accessible surface area
CD	circular dichroism
CDNB	1-chloro-2,4-dinitrobenzene
ΔC_p	change in heat capacity
EA	ethacrynic acid
EDTA	ethylenediaminetetra-acetic acid
ΔG	change in Gibbs free energy
GSH	reduced glutathione
G-site	glutathione binding site in GSTs
GSO_3^-	glutathione sulphonate
GSTs	glutathione transferases
H-site	hydrophobic, electrophilic substrate binding site in GSTs
ΔH	change in enthalpy
ITC	isothermal titration calorimetry
K_d	dissociation constant
K_a	association constant
kDa	kilodalton
L-site	non-substrate ligand binding site in GSTs
rGST M1-1	rat mu class glutathione transferase with two type 1 subunits
N	stoichiometry
NMR	nuclear magnetic resonance
OD_{600}	optical density at 600 nm
PDB	Protein Databank
rpm	revolutions per minute
ΔS	change in entropy
SDS-PAGE	Sodium dodecyl sulphate – polyacrylamide gel electrophoresis
SEC-HPLC	Size exclusion high performance liquid chromatography
TCEP	Tris(2-carboxyethyl)phosphine hydrochloride

The IUPAC-IUBMB three and one letter codes for amino acids are used

1 INTRODUCTION

1.1 Protein-ligand interactions and molecular recognition

The structural assembly and functional regulation of biological systems is dependent on the association of biological macromolecules with one another, as well as their association with small ligand molecules (Freire et al., 1990). The primary function of proteins is to interact with other molecules (ligands), be it a substrate, transition state, effector, hormone, ion, lipid, nucleic acid, or another protein (Eftink et al., 1983).

1.1.1 Lock-and-key versus induced-fit mechanism of ligand binding

In 1894, Emil Fischer formulated the lock-and-key hypothesis stating that the specificity of an enzyme (lock) for its substrate (key) arises from their geometric complementary shapes. This implies that the substrate binding site appears as a pre-formed cavity on the surface of the enzyme upon inspection. This cavity is complementary in shape to the substrate and the amino acids involved in cavity formation are arranged to interact specifically with the substrate in an attractive manner (Caret et al., 1993). Slight alterations in the position of these residues constituting the binding pocket would be expected to alter the affinity of the ligand. This allows enzymes to discriminate against molecules that differ in shape and functional group distribution from their designated substrates. The lock-and-key hypothesis assumes that the substrate binding site is rigid and exists in the absence of bound ligand (Caret et al., 1993). However, most proteins are highly flexible and regions within the binding sites are dynamic and often undergo conformational changes while carrying out their specific functions (Ishima and Torchia, 2000). Daniel Koshland later introduced the induced-fit model which states that the binding of a substrate induces conformational changes in the enzyme resulting in a complementary interaction (Koshland, 1994). The substrate binding site is therefore, a flexible pocket that approximates the shape of the substrate (Caret et al., 1993). The substrate enters the binding site and the attraction between its groups and those of the enzyme cause a change in the three-dimensional structure of the binding site, resulting

in a binding site that fits to the surface of the substrate (Caret et al., 1993). Many proteins undergo conformational adjustments, to some extent, upon ligand binding e.g., the C-terminal region in hGST A1-1 which forms an amphipathic α-helix is disordered in apo protein and upon ligand binding, becomes structured and localised (Kuhnert et al., 2005). Studies suggest that the globular structure of proteins in solution is quite delicate, being marginally stabilised by a large number of individually weak intramolecular interactions (hydrogen bonds, van der Waals contacts, etc.) (Eftink et al., 1983). Rapid fluctuations in the structure of proteins may involve the rotation of side chains, vibration of bonds, and the making/breaking of hydrogen bonds and van der Waals contacts (Eftink et al., 1983). These structural fluctuations imply that a protein exists as a macroscopic ensemble of a number of closely related microstates (Eftink et al., 1983). In addition to these different structural states, a protein may also exist in various states of protonation. All these states (structural, aggregation, protonation) of a protein may be characterised by a different enthalpy level and it is likely that each state will have different abilities to interact with ligand (Eftink et al., 1983).

1.1.2 Protein-ligand interactions

1.1.2.1 Hydrophobic interactions

Hydrophobic interactions result due to the tendency of nonpolar groups to interact with each other rather than with the surrounding polar solvent i.e., like attracts like. The inability of nonpolar groups to participate in hydrogen bonding interactions with surrounding water molecules, forces the water molecules to assume an ordered network thereby satisfying their hydrogen bonding potential. These water molecules are ordered around nonpolar groups, resulting in unfavourable entropy compared to water molecules in bulk solvent. Hydrophobicity is currently thought to be the dominant force that drives the folding of proteins (Dill, 1990; Pace, 1992). The importance of hydrophobicity was first identified by Kauzmann (1959), who proposed that a protein structure would tend to bury the amino acids with nonpolar side chains, while those with polar or charged side-chains would be orientated to interact with the solvent. It has been suggested that hydrophobic interactions drive ligand binding to proteins, i.e., the hydrophobic effect is the major source of stabilisation in protein

associations (Goto, 1995; Tsai et al., 1997). The observation that the binding surfaces, where the hydrophobic effect drives ligand binding, are enriched with hydrophobic residues but are more hydrophilic than protein cores (Tsai et al., 1997; Xu et al., 1997), suggests that the hydrophobic effect could play less of an important role in certain proteins. The hydrophobic effect is likely to play an important role where significant structural rearrangements occur as a result of ligand binding because these arrangements are likely to involve the exposure of hydrophobic residues normally buried when the protein is in its unbound state (Tsai et al., 1997).

1.1.2.2 Electrostatic interactions

Electrostatic interactions may be defined as interactions occurring between oppositely charged groups that are in close proximity (Barlow and Thornton, 1983; Dill, 1990). These interactions can be both stabilising and destabilising. Destabilising effects originate from the non-specific repulsion between groups with like charges. Stabilising effects occur due to the formation of ion pairs/salt-bridges between two oppositely charged groups within 4 Å of each other (Barlow and Thornton, 1983). The formation ion pairs/salt-bridges comes at a lower desolvation cost because hydrophilic pairs and their surrounding polar groups mimic the interactions between hydrophilic groups and their solvation shell before the binding interaction (Xu et al., 1997). In proteins, these electrostatic interactions can take place between the amino and carboxyl termini of the ionisable side chains of lysine, arginine, aspartic acid, glutamic acid and histidine. The strength of these interactions decreases in aqueous environments due to the tendency of water molecules to hydrate these groups, hence shielding ionisable groups from one another. In a study of rigid-body associations, where complex formation does not result in any major conformational changes, it was discovered that hydrophilic pairs within the binding site play an important role in stabilisation of the complex (Xu et al., 1997). The frequency of charged and polar amino acid groups seems to be higher in the interior of protein-protein interfaces rather than the interior of individual proteins thereby suggesting that hydrophilic pairs may be contributors to complex stability (Tsai et al., 1997). Binding electrostatics, therefore, not only provides specificity but also contributes toward the binding affinity (Xu et al., 1997).

1.1.2.3 Hydrogen bonding

A hydrogen bond is a weak attraction between electronegative atoms involving hydrogen. The hydrogen atom is covalently linked to one electronegative atom (the donor) and electrostatically bonded to another (the acceptor) (Dill, 1990; Creighton, 1993). Hydrogen bond donors and acceptors include sulphur, nitrogen and oxygen atoms. Weak non-conventional CH---O hydrogen bonds are now becoming widely accepted as genuine hydrogen bonds. This is due to the increasing recognition of their importance in the stabilisation and function of biological molecules (Jiang and Lai, 2002). In proteins, hydrogen bonding is most prevalent between the carbonyl oxygen and the amide nitrogen of peptide bonds, and forms the basis for stabilisation of secondary structures. When the three atoms involved in a hydrogen bond assume a linear configuration, the hydrogen bond is said to be at the most energetically favourable level (Creighton, 1993).

1.2 Thermodynamics and isothermal titration calorimetry

Modern NMR and crystallographic techniques have provided the scientific community with a rapidly expanding library of structures of biologically significant molecules (Plum and Breslauer, 1995). It is becoming increasingly clear that a correlation between thermodynamic and structural information is required to develop an appreciation of the critical inter-relationships that exist among structure, energetics, and biological function (Plum and Breslauer, 1995). A recent study of the structures of protein complexes with low molecular weight ligands has revealed that, in the unbound proteins, the binding sites are characterised by the presence of regions with low structural stability (Luque and Freire, 2000). Because these regions become stabilised upon ligand binding, the energetics of ligand binding is a function not only of the interactions established between ligand and protein (as depicted in the structure of the bound complex), but also of the energy required to bring the protein into its bound conformation (Leavitt and Freire, 2001). According to the principles of thermodynamics, to predict how molecules act we must account for the free energies (Dill, 1997). Free energies are expressed as van der Waals interactions, hydrogen bonding, ion pairing, solvation and hydrophobic interactions, and entropies due to translations, vibrations, rotations, and configurations (Dill, 1997).

In order to fully understand the driving forces behind molecular recognition between protein-ligand complexes, a detailed thermodynamic profile of the binding process is essential. Due to its high accuracy and precision, rapid calorimetric response and very high sensitivity, ITC has found application in a wide range of chemical and biochemical reactions (Wiseman et al., 1989; Doyle, 1997). Calorimetry is a procedure wherein a heat signal is measured in proportion to the advance of a reaction (i.e., the formation of a macromolecule/ligand complex). Calorimetry directly measures the heat associated with a given process, which, at constant pressure, is equal to the enthalpy change in that process, ΔH (Velazquez-Campoy and Freire, 2005). Calorimeters used to characterise binding processes belong to the category of titration calorimeters with dynamic power compensation operating at constant temperature (isothermal titration calorimeter, ITC) (Velazquez-Campoy and Freire, 2005). In following is a brief description of the ITC practice.

The macromolecular solution is located inside the sample cell and the ligand solution in the injector syringe. A feedback control system supplies thermal power continuously to maintain the same temperature in both reference and sample cells (Wiseman et al., 1989). Any event taking place in the sample cell, usually accompanied by heat, will change the temperature in that cell and the feedback control system will adjust the power supplied in order to minimise such temperature imbalance (Velazquez-Campoy and Freire, 2005). A sequence of injections is programmed and the ligand solution is injected at regular intervals into the sample cell. The value of the association constant (or binding affinity), K_a, governs the equilibrium, i.e., the partition between bound and unbound species. After each injection, the composition inside the sample cell changes causing the rearrangement of populations and complex formation (Velazquez-Campoy and Freire, 2005). The system will pass through different states of equilibrium each differing in composition, as the sequence of injections proceeds. The heat associated with each injection is proportional to the increase in complex concentration (advance of the reaction) and it is calculated by integrating the area under the deflection of the signal measured (amount of heat per unit of time provided to maintain both cells, sample and reference, at the same temperature) (Velazquez-Campoy and Freire, 2005). At the end of the experiment, saturation of the macromolecule is reached and it is possible to estimate the association constant or binding affinity, K_a, the binding enthalpy, ΔH,

and the stoichiometry, N, in a single experiment (independent variables). Knowing the binding affinity, it then holds that:

$$\Delta G = -R\mathrm{T}\ln K_a \quad (1)$$

where R is the universal gas constant (8.3 J/mol/K) and T is the experimental temperature in kelvin. The Gibbs free energy is the parameter that influences the determination of biomolecular equilibria: it indicates the direction in which a process will tend to go, or the amount of work that needs to be done to make them go (Cooper, 1999). The entropy change is obtained by using the standard thermodynamic expression:

$$\Delta G = \Delta H - \mathrm{T}\Delta S \quad (2)$$

At the molecular level, this reflects the opposition of two fundamental effects – the tendency to fall to lower energy (bond formation, negative ΔH), offset by the equally natural tendency for thermal (Brownian) motion to disrupt things (bond breakage, positive ΔS) (Cooper, 1999).

By repeating a titration at different temperatures (and constant pressure), it is also possible to determine the change in heat capacity (ΔC_p) associated with the binding reaction:

$$\Delta C_p = \delta\Delta H/\delta\mathrm{T} \quad (3)$$

The magnitude and signs of the thermodynamic parameters obtained provide insight into the nature of interactions involved in the binding process.

The strength of an interaction and whether or not it is thermodynamically favourable is determined by the Gibbs free energy. Since this function is dependent on enthalpy and entropy (Equation 2), these two parameters are of equal importantance. If two binding processes that are characterised by the same Gibbs free energy and have different enthalpy and entropy, they correspond to different binding modes and therefore, the main underlying intermolecular interactions are different. For that reason, the Gibbs free energy (or binding affinity) is only 'half of a story' (Velazquez-Campoy and Freire, 2005). Since the native state of a protein exists as an ensemble of conformational states, the Gibbs free energy stabilising a protein will not uniformly be distributed throughout its three-dimensional structure (Luque and Freire, 2000). Some regions of the protein will exhibit high stability (e.g., the hydrophobic core) and other regions exhibit low stability (e.g., loops and turns) with the majority of proteins

exhibiting dual character (Luque and Freire, 2000). Since low molecular weight ligands are in general not found 'stuck' to the surface of proteins but are often buried in preformed cavities covered by loops or other structural components of the protein, the number of contacts between ligand and protein are maximised and hence, a significant surface area is buried from the solvent (Luque and Freire, 2000). This structural arrangement makes a favourable contribution to the Gibbs free energy of binding. If the rearrangements are only transient and the free and bound sates of the protein are the same, only the binding kinetics will be affected (Luque and Freire, 2000). If, however, the free and bound conformations of the protein are different, the binding affinity will be affected (Luque and Freire, 2000). The Gibbs free energy associated with the change in protein conformation from its free to its bound form needs to be included in the computation of the effective binding Gibbs free energy and corresponding binding affinity (Luque and Freire, 2000).

$$\Delta G_{\text{bind}} = \Delta G_{\text{bind}} + \Delta G_{\text{conf}} \quad (4)$$

where ΔG_{bind} is the Gibbs free energy of binding obtained under the assumption that the free and bound conformations of the protein are identical, and ΔG_{conf} is the Gibbs free energy associated with the protein change from its free to its bound conformation (Luque and Freire, 2000). In general, the Gibbs free energy associated with the change from a low stability region to the bound conformation will be more negative than that associated with the change from a stable conformation to the bound conformation (Luque and Freire, 2000). The presence of low stability regions in the binding sites also serves to facilitate the occurrence of ligand-induced conformational changes if the binding site is not binding-competent in the unligated protein (Luque and Freire, 2000). The presence of regions of low stability appears to provide a mechanism for eliciting high binding affinity for low molecular weight ligands and serves as an initiation point for the transmission of binding signals to distal sites (Luque and Freire, 2000).

The binding enthalpy is related to bond formation (exothermic reaction) and bond breaking (endothermic reaction) during the binding process, including bonds associated with the solvent. Processes that result in favourable enthalpy (negative ΔH) include hydrogen bond formation and van der Waals interactions (Ross and Subramanian, 1981). A favourable enthalpy contribution is an indication of specific interactions between binding partners and a good way to measure ligand specificity,

selectivity and adaptability. On the other hand, an unfavourable enthalpy contribution is an indication of non-specific interactions between the binding partners, making it very difficult to provide specificity, selectivity and adaptability. As a ligand enters the surface of a macromolecule's binding site, the more strongly it is bound (the more negative the ΔH of binding), the more its rotational and translational freedom will be restricted (the more negative the ΔS) (Eftink et al., 1983). Many internal intramolecular hydrogen bonds in a globular protein may be distorted, requiring less energy to be broken (Eftink et al., 1983). The breaking of certain hydrogen bonds, particularly those involving solvent molecules, may lead to an increase in rotational and/or translational freedom (i.e., increase in entropy) (Eftink et al., 1983). This would result in an increase in the probability of such bonds being broken thus allowing these bonds to contribute to the heat capacity of a protein (Eftink et al., 1983).

Calorimetry is an experimental technique providing only global information (change in thermodynamic parameters upon binding), with no possibility of obtaining detailed knowledge regarding the source or physical localisation of the individual interactions. It is possible to modify either the experimental conditions (e.g., pH, ionic strength) or the functional groups in the binding molecules (e.g., mutant proteins or structurally related ligands) in order to shed light into which are the driving forces and the structural determinants of the interaction (Velazquez-Campoy and Freire, 2005). The observed enthalpy change often includes contributions not only from the binding event, but also the heat due to conformational changes as well as the heat of ionisation of the buffer and reactants. Although conformational changes are often regarded as part of the binding process, efforts have been made to distinguish contributions of the buffer effects from the heat of the binding event (Gomez and Freire, 1995; Baker and Murphy, 1996, 1997). Binding processes for which ligand binding is accompanied by the transfer of protons between the solvent and protein-ligand complex are coupled to a protonation/deprotonation process. The linkage between ligand binding and proton transfer is quantified as a change in ligand binding constant with pH, as a change in the pK_a of an ionisable group upon ligand binding or as the dependence of measured enthalpy on the ionisation enthalpy of the buffer in which the reaction takes place (Gomez and Freire, 1995; Baker and Murphy, 1996; Velazquez-Campoy et al., 2000). By performing binding experiments as a function of pH in buffers with varying ionisation enthalpies, one can determine the intrinsic energetics of ligand binding, pK_a

values of ionisable groups responsible for proton linkage in the free and liganded states, and the number of protons that are coupled to the binding process (Baker and Murphy, 1996).

The binding entropy refers to the degree of disorder accompanying complex formation. The major contributions to the entropy change are the solvation and conformational entropies. Unfavourable binding entropy arises due to the loss of conformational degrees of freedom of both the protein and the ligand upon complex formation. Favourable binding entropy results due to the gain in solvent entropy originating from the burial of hydrophobic surfaces upon binding (Sturtevant, 1977; Ross and Subramanian, 1981). Entropically driven ligand binding reactions are characterised by a large, favourable entropic contribution and these ligands bind because they have the correct shape and geometry and are hydrophobic (not because of favourable interactions with the target). Since shape and hydrophobicity represent non-specific interactions, this would lead to a reduction in affinity when the target binding site is distorted by mutations (even conservative ones), thus, appearing the phenomenon of drug resistance (Velazquez-Campoy and Freire, 2005).

Changes in heat capacity upon formation of a complex can provide information on non-local effects. Although most interactions will provide some change in heat capacity, it seems that hydrogen-bonded networks of water molecules are particularly sensitive to environmental changes upon complex formation (Ladbury and Williams, 2004). Experimental determinations of ΔC_p can be used to quantify the amount of nonpolar surface removed from water upon binding and the contribution of the hydrophobic driving force to protein stability and other non-covalent self-assembly processes (Livingstone et al., 1991). A large negative ΔC_p is a distinctive feature of site-specific binding, and the sign of ΔC_p is determined by the removal of large amounts of nonpolar surface from water upon complex formation. When the amount of nonpolar surface involved in ligand binding appears too large to be accounted for in a 'rigid body' association, it has been proposed that conformational changes in protein that bury large amounts of nonpolar surface are coupled to binding (Spolar et al., 1989). A large contribution to the heat capacity must be due to vibrational and rotational contributions from the peptide bonds and residue side chains and from interactions between the protein and water (Eftink et al., 1983). The transfer of ligand from water to the binding site of the protein and the removal of water from the

binding site may contribute to the apparent ΔC_p due to the release of electrorestricted water or "hydrophobic water" (Sturtevant 1977).

1.3 Glutathione transferases

The glutathione transferases (EC 2.5.1.18) are a superfamily of multifunctional enzymes responsible for phase II metabolism of endogenous and xenobiotic electrophilic substances (Sheehan et al., 2001). The glutathione transferases (GSTs) protect cells against chemically induced toxicity and stress by catalysing the *S*-conjugation between the thiol group of glutathione (GSH) and the electrophilic moiety in a hydrophobic, toxic substrate (Mannervik and Danielson, 1988). The resulting glutathione-conjugate is more water soluble and can be exported from cells by an ATP-dependent glutathione *S*-conjugate export pump (Ishikawa, 1992) followed by metabolism via the mercapturate pathway (Habig et al., 1974) and eventual elimination. In addition to their catalytic activity, GSTs may function as intracellular transporters of various non-substrate hydrophobic compounds, where binding often results in inhibition of the enzymes catalytic activity (Wilce and Parker, 1994). The cytosolic/soluble GSTs have been classified into several species independent gene classes based on primary to quaternary structural similarity (Dirr et al., 1994b; Sheehan et al., 2001): Alpha, Mu, Pi (Mannervik et al., 1985), Sigma (Ji et al., 1995), Theta (Meyer et al., 1991), Kappa (Pemble et al., 1996), Omega (Board et al., 2000) and Zeta (Board et al., 1997) each existing as either homo- or heterodimers. However, the heterodimers only occur between subunits of the same enzyme class. A nomenclature system has been proposed (Mannervik et al., 1992) such that rGST M1-1 refers to rat GST from Mu class composed of two type 1 subunits. All of the GSH transferases catalyse the nucleophilic addition of GSH to an electrophilic centre (RX) as illustrated below:

$$RX + GSH \leftrightarrow GSR + XH \qquad (5)$$

Class Mu GSTs are more specific for nucleophilic aromatic substitution reactions and have a preference for epoxides as substrates (Armstrong, 1991; Wilce and Parker, 1994).

1.3.1 Structural features of GST M1-1

The crystal structure of GST M1-1 from rat liver, in complex with GSH has been solved at 2.2 Å (Ji et al., 1992) (Figure 1). Each subunit contains four β-strands and eight α-helices. These subunits are divided into two domains separated by a short linker, a smaller α/β domain (domain I/N-terminal domain) and a larger α domain (domain II/C-terminal domain). The major secondary structural elements of domain I are arranged in a βαβαββα motif. This motif is characteristic of the thioredoxin fold (Reinemer et al., 1991), and accordingly the protein is classified under the thioredoxin superfamily. The two subunits are related by a noncrystallographic 2-fold axis and contact one another primarily by interactions between domain I of one subunit and domain II of the adjacent subunit. Hydrogen bonds and electrostatic interactions appear to play an important role in stabilising the relative positions of the two domains (Ji et al., 1992). The primary function of domain I is to provide a binding site for the physiological substrate GSH referred to as the G-site (Figure 1). Domain II provides structural elements for the recognition of xenobiotic substrates and helps to define the substrate selectivities of the various isoenzymes referred to as the H-site (Armstrong, 1997). The active sites of the two subunits which compose the dimer are some distance from one another e.g., the sulphur atoms of the two bound GSH molecules are 21.6 Å apart suggesting the active sites probably behave independently in most respects (Armstrong et al., 1993). Despite the similar overall topologies of GSTs, the structures differ. Class Pi, Alpha, and Theta enzymes all contain a short helix near the GSH binding site (α2-helix) that replaces the mu-loop found in class Mu enzymes (McCallum et al., 2000). The mu-loop (Figure 1) is adjacent to the GSH binding site and causes a more constricted active site. The carboxy terminus of the class Pi enzyme is shorter than that found in class Mu enzymes. In class Alpha and Theta enzymes, the carboxy terminus forms an alpha helix that covers the active site. Structural topologies of the class Mu, Alpha, and Theta enzymes indicate that some degree of conformational mobility is required for substrate binding and product release. The mu-loop samples different conformational states in both liganded and unliganded enzymes on the microsecond to nanosecond time scale (McCallum et al., 2000). The time scale for the mobility of the mu-loop suggests that this conformational change may be involved in gating the access of substrates to and the release of products from the active site (McCallum et al., 2000). In addition, these

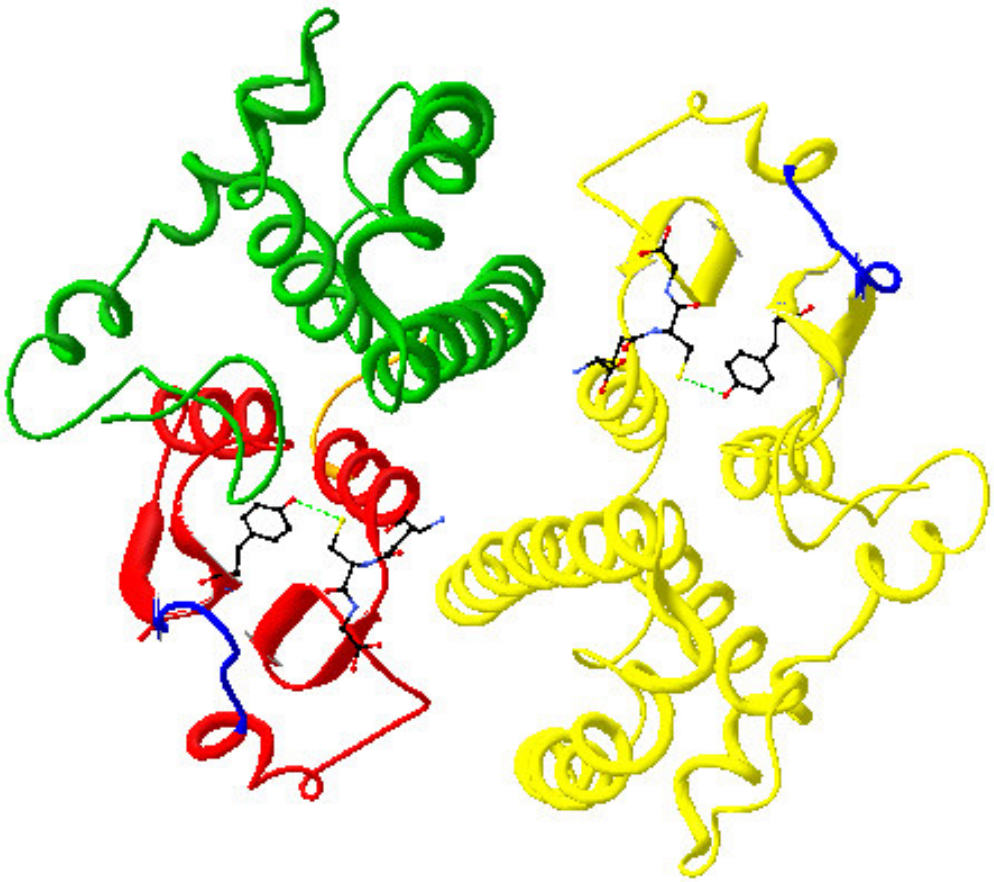

Figure 1: Ribbon representation of the structure of the rat glutathione transferase M1-1 homodimer with GSH bound viewed down the two-fold axis.

Subunit I is shown in yellow. The smaller domain 1 of the second subunit is in red and the larger domain 2 in green. The linker region between the two domains is shown in orange. GSH is bound in an extended conformation at one end of the β-sheet of domain I. Tyrosine 6 is shown in black and the hydrogen bond between this residue and glutathione is shown in bright green. The mu-loop is shown in blue. The figure was generated using the pdb code 6gst (Ji et al., 1992).

NMR measurements also show that the mu-loop assumes a more open conformation in solution, further facilitating ligand binding and product release (McCallum et al., 2000). The dynamics of the mu-loop has also been shown to be essential for the egress of product from the active site (Codreanu et al., 2002). During ligand binding, Codreanu et al. (2005) showed that the binding of GSO_3^- to the active site causes the formation of a much tighter complex (more ordered mu-loop) compared to the rGST M1-1●GSH complex.

1.3.2 The active site

1.3.2.1 Glutathione binding site

Glutathione (γ-glutamyl-cysteinyl-glycine) is bound at the active site (G-site) of rGST M1-1 in an extended conformation (Figure 1). The γ-glutamyl residue points down towards the dimer interface, the cysteinyl sulphur points towards the subunit in which it is bound and the glycyine residue is situated near the surface of the protein. The α-carboxylate group of the γ-glutamyl moiety of GSH is the major binding determinant that allows the thiol group to align properly at the reaction site and is recognised by the conserved core ββα motif (Adang et al., 1990). Correct positioning of the thiol group for conjugation by GSTs appears to be crucial. Crystal structures of class Alpha (Gu et al., 2000), Mu (Xiao et al., 1996) and Pi (Oakley et al., 1999) isoenzymes in complex with GSH reveal the presence of many conserved structural features. The presence of a conserved tyrosine residue in the active site of these enzymes (Tyr9 in class Alpha, Tyr6 in class Mu (Figure 1) and Tyr7 in class Pi) is of particular interest. The most fundamental difference among the GSH binding sites of the various enzyme classes involves the interaction of the protein with the sulphydryl moiety of the tripeptide. The class Alpha, Mu, Pi and Sigma enzymes have recruited the hydroxyl group of a tyrosyl residue, located in a slightly different position, to interact with the thiol group of GSH (Kolm et al., 1992; Kong et al., 1992; Wang et al., 1992; Ji et al., 1995). In contrast, the Theta class enzymes, appear to utilise the hydroxyl group of a serine residue located near the N-terminus of the polypeptide to interact with the sulphydryl group of bound GSH (Nishida et al., 1994). The Omega class enzymes utilise the thiol group of a cysteine residue which makes a mixed disulfide with GSH (Board et al., 2000). The absence of an equivalent residue in the

Omega class GSTs suggests that they may not catalyse the glutathione conjugation reactions typical of many GSTs and may be involved in thiol transfer reactions (Board et al., 2000).

Two schools of thought as to the actual role of the active site hydroxyl group in catalysis exist. The difference of opinion is over the position of protons in the active site, i.e., does the hydroxyl group act as an electrophilic participant (hydrogen bond donor, Equation 6) or as a general base (hydrogen bond acceptor, Equation 7) either in the binding of GSH or in the reactant state binary complex (Armstrong, 1997)?

$$\text{E-O-H} + \text{GS-H} \leftrightarrow \text{E-O-H----}^{-}\text{SG} + \text{H}^{+} \quad (6)$$

$$\text{E-O-} + \text{GS-H} \leftrightarrow \text{E-O-H----SG} \quad (7)$$

Although these two mechanisms shown are contradictory, sufficient evidence has been obtained to support Equation 6 and will be discussed further. This evidence transpires from a wide variety of experimental procedures including crystallography (Reinemer et al., 1991; Dirr et al., 1994a), natural and unnatural amino acid mutagenesis (Stenberg et al., 1991; Kolm et al., 1992; Liu et al., 1992; Parsons and Armstrong, 1996; Thorson et al., 1998) as well as ultraviolet difference spectroscopy (Graminski et al., 1989).

Reinemer (Reinemer et al., 1991) and Dirr (Dirr et al., 1994a) solved the crystallographic structure of pGST P1-1 complexed with glutathione sulphonate (GSO_3^-). Crystallographic data show evidence of a hydrogen bond between Tyr7 and one of the sulphonate oxygen atoms of GSO_3^- suggesting that Tyr7 acts as a hydrogen bond donor thereby stabilising the thiolate anion in the enzyme-substrate complex (Reinemer et al., 1991; Dirr et al., 1994a). Global incorporation of 3-fluorotyrosine (3-Ftyr) into rGST M1-1 (Parsons and Armstrong, 1996) altered the mechanism of GSH ionisation to one with characteristics of general base catalysis. The spectral properties and pH dependence of k_{cat}/K_m^{CDNB} suggest a behavioural difference between the fluorotyrosyl mutant and the wild-type enzyme, thereby indicating that the native enzyme functions by electrophilic stabilisation of the thiolate (Parsons and

Armstrong, 1996). Creation and characterisation of mutant enzymes in which the active site tyrosine was replaced with phenylalanine has revealed the important role of this residue in stabilisation and ionisation of GSH (Kong et al., 1992; Liu et al., 1992; Manoharan et al., 1992; Wang et al., 1992). Spectroscopic studies indicate that GSTs effectively lower the pK_a of the cysteine thiol of glutathione, resulting in formation of the nucleophilic thiolate anion at the active site, at physiological pH (Graminski et al., 1989). The equilibrium position of the proton shared between substrate and protein, and the free energy contained in this hydrogen bond, depend on the relative pK_a values of the active site tyrosine and the thiol of GSH (Cleland, 1992). By "matching" the pK_a values of the hydrogen bond donor and acceptor, it is possible to maximise the nucleophilicity of GSH (Cleland, 1992; Ji et al., 1992). The pK_a of the bound thiol can be determined by direct titration of the ultraviolet absorption band at 239 nm assigned to the thiolate anion (Graminski et al., 1989). Both spectroscopic evidence and the binding of anionic analogues of GSH strongly suggest that the thiolate anion is the predominant species of glutathione bound at the active site of GSH transferase at neutral pH (Graminski et al., 1989). By acting as a hydrogen bond donor to the sulphur, the active site tyrosine lowers the pK_a of the thiol in the E•GSH complex so that it is predominantly ionised at physiological pH. The reactive species in the binary complexes is the thiolate anion (E-O-H----$^-$SG), which accepts a hydrogen bond from the seryl or tyrosyl hydroxyl group (Armstrong, 1997).

In addition to the shape and size of the active site, electrostatic participation of residues is an important aspect of substrate selectivity through stabilisation of the transition state (Armstrong, 1997). GSH is anchored in the active site via electrostatic interactions (Figure 2) using nearly all the hydrogen bond donor and acceptor sites on the peptide (Armstrong, 1997). Activation of the thiol of GSH in the G-site of rGST M1-1 involves an intricate hydrogen-bonding network (Figure 2) (Xiao et al., 1996). A first-sphere interaction involves a direct interaction between the hydroxyl group of Y6 and the sulphur of GSH (Xiao et al., 1996). This direct interaction is thought to be largely responsible for lowering the pK_a of the bound GSH. Replacement of tyrosine (Y6F mutant) causes the loss of the difference absorption band at 240 nm associated with the thiolate anion of E-GS$^-$ and results in a pK_a shift of bound GSH from 6.2 in the native E•GSH complex to ~7.8 in the mutant (Liu et al., 1992). This shift corresponds to a –9.2 kJ/mol stabilisation energy provided to the thiolate by the

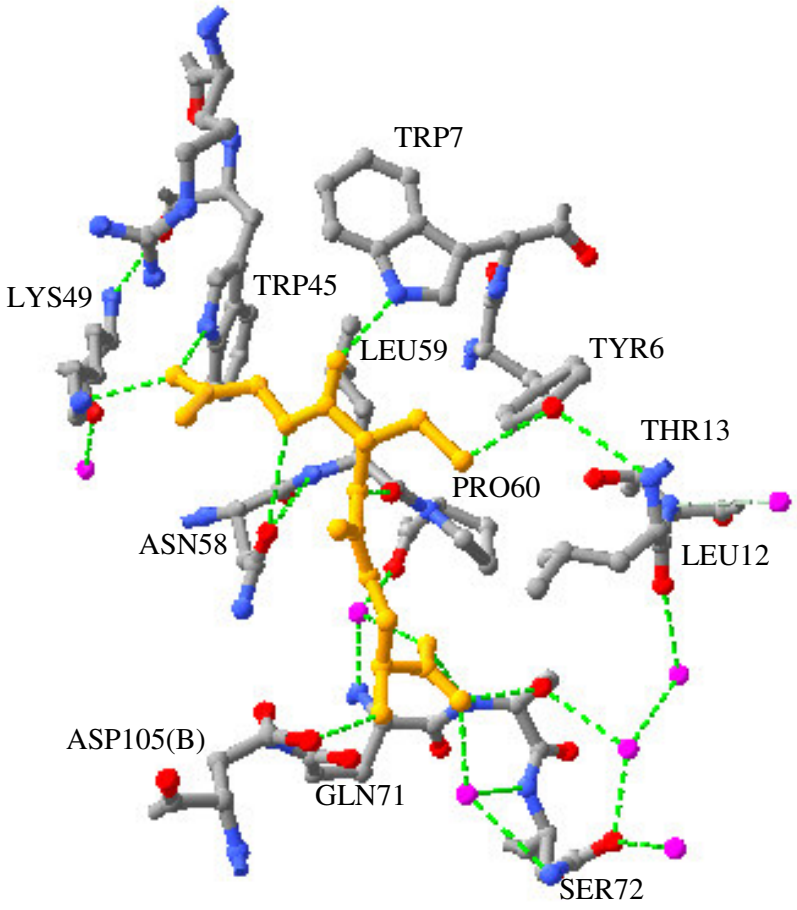

Figure 2: Three-dimensional view of the hydrogen-bonding network of the rGST M1-1•GSH complex.

GSH bound at the active site is shown in orange with the surrounding amino acids and water molecules shown in CPK colour and pink, respectively. Hydrogen bonds are shown in green. GSH hydrogen bonds with the active site amino acids directly and via water mediated interactions. All residues shown belong to subunit I except for Asp105, which belongs to the second subunit. The diagram was generated using the pdb code 6gst.

hydroxyl group of Tyr6 (Armstrong, 1997). These results implicate the hydrogen bond between Tyr6 and the sulphur in GSH in the lowering of the pK_a of GSH in the binary enzyme-substrate complex as well as stabilisation and orientation of the thiol in a manner favourable for product formation (Armstrong, 1991). Although replacement of this conserved tyrosine residue with phenylalanine (Y6F mutant) has a drastic impact on the ionisation of GSH and hence the specific activity, the binding of GSH in not compromised (Stenberg et al., 1991; Kolm et al., 1992; Kong et al., 1992; Liu et al., 1992; Manoharan et al., 1992). The refined three-dimensional structure of the Y6F mutant in complex with GSH shows no major structural perturbation of the protein other than a change in the coordination environment of the sulphur (Xiao et al., 1996). Second-sphere interactions cause an increase in the strength of the first sphere hydrogen bonding interaction or contribute to an electropositive field near the thiolate hence assisting in lowering the pK_a of the thiol and enhancing the stability of the nucleophile (Xiao et al., 1996). Second-sphere interactions involve a hydrogen bond between the main-chain amide N-H of L12 and the hydroxyl group of Y6 and an on-face hydrogen bond between the hydroxyl group of T13 and the π-electron cloud of Y6 (i.e., T13-OH---π-Y6-OH----SG) (Xiao et al., 1996) (Figure 2). Removal of the hydroxyl group Y6 (Y6F mutant) eliminates both the hydrogen-bonding interactions with the sulphur of GSH and the main-chain N-H of L12 (Xiao et al., 1996). The rGST M1-1 enzyme appears to provide for the partial desolvation of the thiolate anion in the active site (Xiao et al., 1996). One face of the sulphur atom is completely shielded from solvent being pushed up against the side chain of L12 (Xiao et al., 1996) (Figure 2). The solvent structure in the active site of rGST M1-1 in complex with GSH shows only one or two water molecules hydrogen bonded to the thiolate where at least two or three others would be expected if the anion was fully exposed to solvent (Ji et al., 1992). In the native enzyme, however, one of the water molecules is replaced by a reactive group (hydroxyl of tyrosine) which is functionally related to water (Karshikoff et al., 1993). A preliminary examination of the crystal structure of theY6F mutant in complex with GSH indicates that the geometry of the active site is essentially unchanged with respect to the native enzyme but that an additional water molecule occupies the solvation shell of the sulphur (Xiao et al., 1996). This may explain why the mutant enzyme is not as active as the native enzyme at high pH (Xiao et al., 1996).

Mechanism of GSH binding

The mechanism of GSH binding to GSTs has been a focal point of research in the recent past. Spectroscopic evidence reveals the presence of the thiolate anion (GS^-) in the active site of these GSTs, suggesting the existence of a positively charged electrostatic field in the active site of the enzyme that functions to destabilise the thiol of the enzyme-bound GSH (Graminski et al., 1989), i.e., deprotonation of the bound GSH prior to its conjugation with the relevant electrophilic substrates. This reaction can be represented by the following:

$$GSH + E \rightarrow E{\bullet}GSH \rightarrow E{\bullet}GS^- + H^+ \qquad (8)$$

where E represents the wild-type enzyme. The resulting thiolate anion has been reported to be up to 10^9 times more reactive than its conjugate acid, hence enhancing the rate of nucleophilic attack 200-300 fold (Armstrong, 1991).

The enzyme utilises some of the energy for binding GSH (binding energy, ΔG_b) to destabilise the thiol (Figure 3A). The fraction of the binding energy of GSH utilised to destabilise the bound thiol, ΔG_d, is given by $\Delta G_d = R\mathrm{T}\ln(K_a^{E\bullet GSH}/K_a^{GSH}) = 3.3$ kcal/mol (Armstrong, 1991). A good structural mimic of GS^-, that is, a peptide that has a stabilised anionic group replacing the side chain of cysteine (e.g. GSO_3^-), should bind to the active site with much higher affinity than does GSH since some of the binding energy normally used to destabilise the thiol should be translated into observed binding energy (as illustrated in Figure 3B) (Armstrong, 1991). The rather pronounced affinity of the enzyme for the side-chain anion (GSO_3^-) is an obvious indication of a positively charged electrostatic field in the active site of the enzyme, the function of which is to lower the pK_a of the thiol (Armstrong, 1991). The rest of the complementary surfaces of the enzyme and peptide presumably function to position the thiol in that electrostatic field (Armstrong, 1991). Another role of the active site of the enzyme may be to shield the thiolate anion from solvent and enhance its reactivity (Armstrong, 1991).

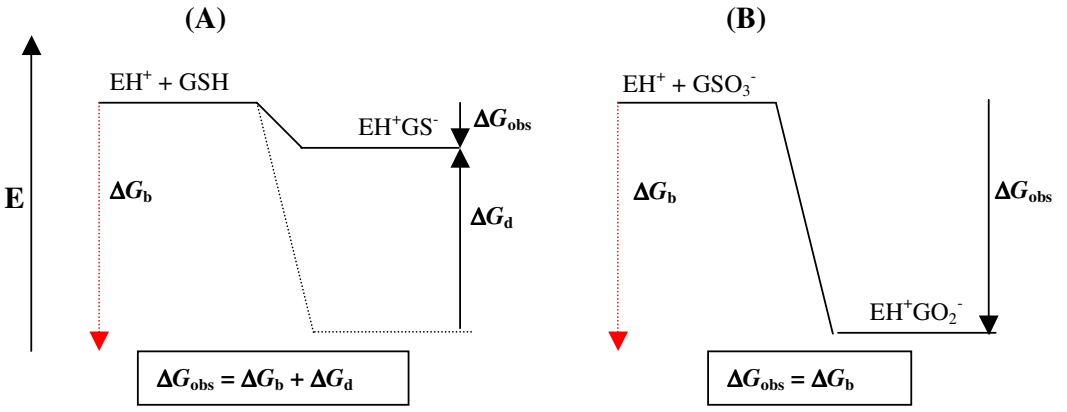

Figure 3: (A) Utilisation of binding energy (ΔG_{be}) for deprotonation of GSH in the active site of the enzyme and (B) realisation of ΔG_{be} as observed binding energy for the resonance-stabilised carboxylate analogues of GSH.

The observed binding energy for the protonated tripeptide (ΔG_{obs}) is smaller than ΔG_{be} by the energy required to destabilise the thiol, ΔG_d. The figure was adapted from Armstrong (Armstrong, 1991).

Thermodynamic analysis of the Y6F mutant of *Schistosoma japonicum* GST binding GSH showed negative co-operativity at a pH of 6.5, justified by the postulation of a conformational change during binding (Yassin et al., 2003). GSH binding to GSTs has also been shown to be enthalpically driven where the enthalpy change of binding is not strongly temperature dependent, arising from a small negative heat capacity change of binding, suggesting only moderate changes in the apolar surfaces accessible to solvent (Ortiz-Salmeron et al., 2001). The enthalpy change for binding to SjGST Y7F mutant is more negative than for binding to the wild-type and the change in entropy is larger (Andujar-Sanchez et al., 2003). Crystallographic studies on this enzyme show that the sulphur in GSH is in the thiolate form and hydrogen bonds to the Tyr7 hydroxyl group (Andujar-Sanchez et al., 2003). This hydrogen bond is not present in the mutant, therefore the enthalpy change is less negative for the GSH●mutant complex than for the GSH●wild-type complex. In unliganded SjGST, a water molecule forms a hydrogen bond with Tyr7 that is displaced upon the formation of the SjGST●GSH complex (Andujar-Sanchez et al., 2003). This water molecule would not be present in the Y7F mutant. The balance between the number of hydrogen bonds before and after substrate binding would account for the more

favourable enthalpy change of binding for the Y7F mutant (Andujar-Sanchez et al., 2003). This more negative enthalpy change, together with the more favourable entropy change, is responsible for the higher negative value of ΔG_b and would explain the enhanced affinity of the substrate GSH to the SjGST mutant (Andujar-Sanchez et al., 2003). The more negative value of ΔC_p obtained for the mutant suggests a higher and significant hydrophobic contribution to the SjGST●Y7F●GSH interaction (Andujar-Sanchez et al., 2003). Binding of GSH to rGST A1-1 as studied using isothermal titration calorimetry (ITC) shows that overall, ligand binding is driven by a combination of entropy and enthalpy (Nieslanik et al., 2001). However, there is a dramatic difference in the contribution of entropy or enthalpy to the individual steps of the binding reaction (Nieslanik et al., 2001). An entropically favourable and enthalpically unfavourable ligand docking step suggests that the active site and C-terminus are highly solvated in the apoenzyme (Nieslanik et al., 2001). The displacement of structured water and the burial of hydrophobic groups upon ligand docking apparently overcome the negative entropy resulting from losses of translational, rotational, and vibrational degrees of freedom upon complexation of the enzyme and ligand (Nieslanik et al., 2001). The second step of the binding reaction, the transition of the C-terminal helix to its localised, well-packed position over the active site, comprises the favourable enthalpic component of binding energy in rGST A1-1 and is entropicallly unfavourable (Nieslanik et al., 2001). Therefore, the C-terminus of rGST A1-1 is required for the favourable entropic contribution to binding, and desolvation precedes the transition of the C-terminus to its final localised state (Nieslanik et al., 2001).

Up to now, it has been established that the thiol of GSH is activated via proton release affording the more catalytically active thiolate anion. The question that remains is the fate of that released proton. Is the proton released into the environment in which the protein finds itself, or does a residue within the active site environment accept the proton? Widersten (Widersten et al., 1996) identified the α-carboxylate of the γ-glutamyl portion of GSH as a possible proton acceptor. It has been suggested that GSH itself promotes the deprotonation of its cysteinyl thiol prior to protonation at its glutamyl carboxylate (Widersten et al., 1996). The existence of an unbalanced negative charge on the glutamyl carboxylate provides further evidence for this theory (Widersten et al., 1996). Contrary to these results, Caccuri et al (1998, 1999)

performed potentiometric experiments on hGST P1-1 (Caccuri et al., 1998) , hGST A1-1 and hGST M2-2 (Caccuri et al., 1999) and the results showed that approximately 0.5 proton per monomer was released at pH 6.5 upon formation of the GSH thiolate at the G-site (Caccuri et al., 1999). Thermodynamic analysis of GSH binding to GST from *Schistosoma japonicum* revealed the release of approximately 0.3 proton into solution upon complex formation (Andujar-Sanchez et al., 2003). The negative number of protons exchanged at pH below 7 agrees with the loss of a proton from the thiol group of GSH (Andujar-Sanchez et al., 2003).

1.3.2.2 The hydrophobic binding site

The hydrophobic binding site (H-site) is located at the domain interface and is composed of structural components from both domain I and II. It is defined by the active site loop connecting β1 and α1, one face of the α4 helix and the C-terminal loop (Figure 4). It contains clusters of nonpolar amino acid side-chains that serve to provide a hydrophobic surface that is accessible to solvent in the apoenzyme (Sinning et al., 1993; Dirr et al., 1994). Whereas the G-site displays a high specificity for GSH, the H-site has evolved to accommodate a much broader array of substrates. This is attributed to the fact that substrate recognition is mediated primarily by hydrophobic interactions thus allowing the site to accommodate a range of structurally different hydrophobic compounds (Dirr et al., 1994). Sequence variability is higher in domain II (Zhang et al., 1992) thereby contributing to the variability between the different GST classes. The major variability among the different classes is localised to the C-terminal region. In class Alpha, the additional C-terminal α9-helix forms a "lid" over the H-site, providing an additional H-site wall (Hoesch and Boyer, 1989; Board and Mannervik, 1991). In the Sigma class, the C-terminal tail is much shorter which results in a more open active site. The crystal structure of rGST M1-1 in complex with (9*S*,10*S*)-9-(*S*-glutathionyl)-10-hydroxy-9-10-dihrophenathrene, a conjugation product, has revealed the H-site in rGST M1-1 and the particular residues involved in ligand binding at this site: Y6, W7, L12, V9, I111, Y115, S209. The dihydrophenanthryl group is in van der Waals contact with side chains contributed by domain II, namely I111 of the α4 helix and S209 of the C-terminal tail (Figure 4).

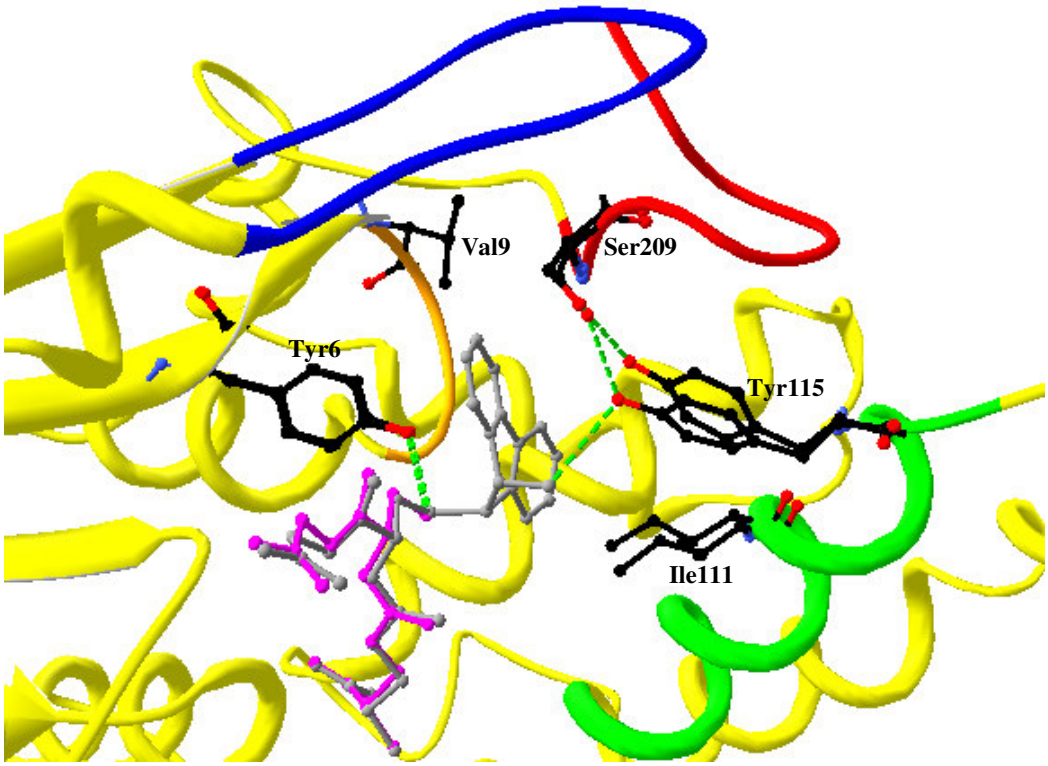

Figure 4: H-site in subunit A of rGST M1-1 in complex with GSH and (9*S*,10*S*)-9-(*S*-glutathionyl)-10-hydroxy-9-10-dihydrophenathrene.

GSH is shown in pink and the 9*S*,10*S* diastereomeric product is shown in grey. Hydrogen bonding interactions with Y6 and Y115 are shown as green dashed lines. Structural elements that make up the active site are also shown: the mu-loop (blue), the short peptide segment forming the floor of the site (orange), the D-helix (green) and the carboxy-terminal loop (red). The figure was generated using pdb codes 6gst (Ji et al., 1992) and 2gst (Ji et al., 1994).

The side chain of V9 is also in contact with the product. The direct hydrogen bond between Y115 and the 10*S*-hydroxyl group of the ring-opened product suggests that the hydroxyl group of Y115 my be proximal to the epoxide oxygen in the encounter complex between the enzyme and substrate and therefore could assist in stabilising the incipient oxyanion by donating a hydrogen bond or transferring a proton in the transition state for the reaction (Armstrong et al., 1993). It is also suggested that the hydrogen-bonding interactions between the hydroxyl groups of Y115 and S209 help tie together the α4-helix and the C-terminal tail of the protein and in so doing, decrease the segmental motion of the protein and inhibit product release (Ji et al., 1994). Currently, there is no X-ray structure of a ligand free class Mu GST. Therefore, the question remains as to whether the class Mu C-terminus is disordered in the absence of ligand (McCallum et al., 1999). The conformational flexibility of the C-terminus may enhance the breadth of substrate specificity by providing a mechanism of generating different H-sites from the same primary sequence (McCallum et al., 1999). The C-terminus in Mu class isozymes is found to be over the active site (Figure 4), and sterically hinders ligand binding and product release (McCallum et al., 1999). In Mu class enzymes, the hydrophobic binding site is composed of four structural elements (McCallum et al., 2000). The α-β domain provides an extended loop (the mu-loop) that forms one wall of this site. A short peptide segment forms the floor of the hydrophobic binding site, the α-helical domain contributes the carboxy terminus of the fourth helix (D-helix) and the 10-residue carboxy-terminal loop to the hydrophobic binding site (Figure 4) (McCallum et al., 2000).

1.3.3 The ligandin binding site

Not only do GSTs function as catalysts, they also function as intracellular transporters of various hydrophobic non-substrate compounds such as bilirubin, haem, steroids, bile salts, drugs etc. Ligandin binding characteristics of GSTs were first realised when protein from rat liver, later identified to be GST, showed high binding affinities towards lipophilic anionic ligands (Litwack et al., 1971). GSTs have also been shown to have a broad specificity for the binding of nonsubstrate ligands (Ketley et al., 1975). This function is believed to be associated with drug resistance as suggested from the binding of antischistosomal drug, praziquantel, to SjGST (McTigue et al.,

1995). This ligandin function has evoked the interest of many and in addition to the G- and H-sites, it is suggested that there may exist one or more non-substrate ligand binding sites/L-sites, distinctly distant from the active site. Techniques employed to elucidate the position and stoichiometry of the L-site include fluorescence resonance energy transfer (Sluis-Cremer et al., 1996; Sluis-Cremer et al., 1998), isothermal titration calorimetry (Sayed et al., 2002; Kolobe et al., 2004; Yassin et al., 2004; Dirr et al., 2005), affinity labelling (Barycki and Colman, 1997) and co-crystallisation of GSTs with non-substrate ligands (McTigue et al., 1995; Ji et al., 1996; Oakley et al., 1999). The crystal structure of class Sigma SjGST revealed the L-site to be located at the dimer interface (Figure 1). The crystal structure of class Pi showed this site is located at the promiscuous H-site (Oakley et al., 1999). The L-site may still be occupied when the substrate binding sites are occupied (Ji et al., 1996) and its affinity may even be affected by G-site occupancy (Dirr and Wallace, 1999).

2 OBJECTIVES

Although a large amount of information exists regarding ligand binding to GSTs at both the G- and H-sites, knowledge regarding the forces driving these processes is modest. It is well-established that the catalytic functioning of GSTs is dependent on the binding and ionisation of GSH at the G-site. It is also known that ligand binding to rGST M1-1 causes changes in the dynamics of the mu-loop, situated at the 'entrance' to the active site (McCallum et al., 2000; Codreanu et al., 2005). ITC was employed in order to investigate the effect of temperature as well as buffer ionisation on the rGST M1-1●ligand interaction. These studies serve to generate knowledge with regard to forces driving the binding of ligands to rGST M1-1 and to obtain a clearer understanding of the effect of the dynamics of the mu-loop on ligand binding.

In addition to their catalytic activity, GSTs also function to transport a wide variety of non-substrate ligands (ligandin function). Due to the lack of structural data, the location of the ANS binding site in rGST M1-1 is unknown. Fluorescence-resonance energy transfer has identified the intersubunit cleft as the binding site for ANS and aflatoxin B1 in hGST A1-1, accommodating one molecule of non-substrate ligand per dimer (Sluis-Cremer et al., 1996). ITC studies suggest that hGST A1-1 binds one molecule of ANS per monomer at or near the H-site with the process being enthalpically driven and characterised by a negative heat capacity change (Sayed et al., 2002). ITC studies were undertaken in order to determine the stoichiometry of ANS binding to rGST M1-1 and the forces driving this interaction. Displacement and molecular docking studies were utilised in an attempt to gain more insight into the possible location of the non-substrate binding site using ANS as a probe.

3 EXPERIMENTAL PROCEDURES

3.1 Materials

ANS, ethacrynic acid, glutathione sulphonate, reduced glutathione, *S*-hexylglutathione and 1-chloro-2,4-dinitrobenzene (CDNB) were purchased from Sigma. Isopropylthiogalactoside (IPTG) and SDS-PAGE markers were purchased from Fermentas. The pET-20b(+) plasmid containing the rGST M1-1 cDNA insert was kindly supplied by Prof. R.N. Armstrong (Vanderbilt University, Nashville). All other chemicals were of analytical grade.

3.2 Expression and purification of rGST M1-1 protein

An overnight culture of *Escherichia coli* BL21(DE3)pLys*S* cells transformed with the pET-20b(+) plasmid containing the rGST M1-1 cDNA insert was diluted 10-fold into fresh LB medium containing 100 µg/ml ampicillin and 100 µg/ml chloramphenicol. The cells were grown at 37 ºC until mid-log phase where the OD_{600} ~ 1.0. Over-expression of rGST M1-1 was induced via the addition of 0.7 mM IPTG (final concentration) and grown overnight with vigorous shaking. These cells were harvested by centrifugation for 30 minutes at 6000 x*g*. Pelleted cells were resuspended in 10 mM Tris-HCl, 200 mM NaCl, 1 mM EDTA, 0.02% sodium azide, pH 7.8 (buffer A). The cell suspension was aliquoted into eppendorfs and frozen at –20 ºC to promote cell lysis. The cells were lysed by sonication at 4 ºC and centrifuged at 13000 rpm for 30 minutes in a microcentrifuge at 4 ºC. The rGST M1-1 protein was purified using *S*-hexylglutathione affinity chromatography (Zhang and Armstrong, 1990). The resultant protein-containing supernatant was loaded onto a *S*-hexylglutahione affinity matrix pre-equilibrated with buffer A. The column was then washed with buffer A in order to remove non-specific proteins. rGST M1-1 was eluted from the column with 50 mM glycine-NaOH buffer, pH 10 (Cameron et al., 1995). Protein was detected by measuring the absorbance at 280 nm. Fractions containing rGST M1-1 protein were added to 500 mM Mes-NaOH buffer, pH 6.5 and pooled only after assessment using SDS-PAGE. In order to ensure the removal of any excess ligand, purified protein was applied to a Sephadex G-25 gel filtration column.

3.3 Protein concentration determination

The protein concentration was estimated using the molar extinction coefficient, ε, at 280 nm calculated by the method detailed in Perkins (Perkins, 1986):

$$\varepsilon(M^{-1}.cm^{-1}) = 5550(\text{no.Trp}) + 1340(\text{no.Tyr}) + 150(\text{no. Cys}) \quad (9)$$

where no. denotes the number of the specific residues within the protein and 5500, 1340 and 150, the extinction coefficients of tryptophan, tyrosine and cysteine respectively, in $M^{-1}.cm^{-1}$. The concentration of the protein was then determined using the absorbance value obtained at A_{280}, the extinction coefficient of the rGST M1-1 dimer (81 480 $M^{-1}cm^{-1}$) and the Beer-Lambert relationship:

$$A_{280} = \varepsilon cl \quad (10)$$

where l is the pathlength of light through a cuvette, measured in cm.

3.4 Investigation of the structural and functional properties of rGST M1-1

3.4.1 SDS-PAGE

Purity and homogeneity of the purified rGST M1-1 protein was assessed by SDS-PAGE according to the method of Laemmli (Laemmli, 1970), on a 15% polyacrylamide gel. Molecular weight marker proteins [β-galactosidase (116.0 kDa), bovine serum albumin (66.2 kDa), ovalbumin (45.0 kDa), lactate dehydrogenase (35.0 kDa), restriction endonuclease Bsp981 (25.0 kDa), β-lactoglobulin (18.4 kDa) and lysozyme (14.4 kDa)] were used to construct a standard curve.

3.4.2 SEC-HPLC

SEC-HPLC was performed on a TSK G2000 SWXL size exclusion column equilibrated with 0.1 M sodium phosphate, 0.1 M sodium sulphate and 0.05% sodium azide, pH 6.5. The buffer was filtered and degassed before use. An LKB 2150 pump

(Pharmica) was used to maintain the flow rate at 0.5 ml/min. Molecular weight marker proteins [thyroglobulin (670 kDa), bovine γ-globulin (158 kDa), chicken ovalbumin (44 kDa), equine myoglobulin (17 kDa)] were used to construct a standard curve.

3.4.3 Specific activity

The catalytic activity of rGST M1-1 was determined spectrophotometrically at 340 nm in 0.1 M sodium phosphate, 1 mM EDTA and 0.02% sodium azide, pH 6.5 using the general CDNB-conjugating assay (Habig and Jakoby, 1981). The assay contained final concentrations of 1 mM reduced glutathione and 1 mM 1-chloro-2,4-dinitrobenzene (CDNB) in 3% (v/v) ethanol and 47 nM protein. Formation of 1-(*S*-glutahionyl)-2,4-dinitrobenzene (extinction coefficient of 9 600 $M^{-1}cm^{-1}$) was monitored as linear progress curves over a period of 60 seconds at 20 ºC on a Hewlett Packard model 8452A-diode array spectrophotometer interfaced with a Vectra CS computer. All reaction rates were corrected for the non-enzymatic reaction rates.

3.5 Spectral analysis of rGST M1-1

3.5.1 Intrinsic fluorescence spectroscopy

The spectroscopic signature of rGST M1-1 was measured at a protein concentration of 2 μM. The intrinsic fluorescence emission spectra of tryptophan (excitation at 295 nm) were measured using a Hitachi model 850-fluorescence spectrofluorimeter. Excitation and emission bandwidths were set at 5 nm and emission spectra were collected at a scan rate of 60 nm/minute.

3.5.2 Far-UV circular dichroism

Far-UV CD spectral analysis was performed on 2 μM rGST M1-1 using a Jasco J-810 spectrapolarimeter with a 2 mm pathlength. The data from 20 runs was collected from 250 nm to 200 nm and averaged.

3.6 ANS displacement studies

The fluorescence intensity of ANS is enhanced when it binds to hydrophobic groups on proteins. Utilisation of this property allows for investigation of its interactions with proteins. In order to determine the ligand concentration that results in a 50% decrease in ANS fluorescence, 2 μM rGST M1-1 was incubated with 200 μM ANS (final concentration) for 1 hour at 20 ºC prior to titration with incrementing ligand. Ligands used in ANS displacement studies were GSH, GSO_3^-, *S*-hexylglutathione and ethacrynic acid. All experiments were carried out in 20 mM sodium phosphate, 150 mM NaCl, 1 mM EDTA, 1 mM TCEP and 0.02% sodium azide, pH 6.5 using a Hitachi model 850-fluorescence spectrofluorimeter. ANS was excited at 390 nm and emission was monitored between 400 and 500 nm with emission maxima occurring at 483 nm. Excitation and emission band widths were set at 5 nm and 10 nm, respectively and data were collected at a scan rate of 60 nm/minute. Final volumes of added ligand did not exceed 10% of the initial sample volume. Concentrations of ligand stock solutions used were 5 mM GSH, 1.5 mM GSO_3^-, 12 mM *S*-hexylglutathione and 6 mM ethacrynic acid. Controls for experiments conducted were prepared similarly in the absence of enzyme. IC_{50} values were obtained from non-linear regression analysis of the data. All data were corrected as follows:

Corrections for controls: $F_1 = F_{obs} - F_{control}$ (11)

Correction for dilution effects: $F_2 = F_1 \times V_f/V_i$ (12)

where V_f and V_i represent the final and initial reaction volumes, respectively.

3.7 Isothermal titration calorimetry

3.7.1 Thermodynamics of ligand binding to rGST M1-1

The energetics of ligand binding to rGST M1-1 was investigated using a VP-ITC Microcalorimeter from Microcal Incorporated. Purified rGST M1-1 was dialysed against 20 mM sodium phosphate, 150 mM NaCl, 1 mM EDTA, 1 mM TCEP and 0.02% sodium azide, pH 6.5 using dialysis tubing with a molecular weight cut-off of 3 500 Da. The dialysis buffer was changed three times after no less than 6 hours and the final dialysate buffer was used in the following experiments. Certificates of

analysis from the suppliers indicated that the ligands used in this study were chemically pure. Therefore, no further purification of the ligands was needed. Ligands were prepared in the final dialysate buffer and filtered using a 0.22 μm filter. Protein and ligand samples were centrifuged in a microcentrifuge at 13 000 rpm for 30 minutes at 4 ºC in order to remove any aggregate matter. The protein concentration was estimated spectrophotometrically at 280 nm using the extinction coefficients reported earlier. The protein concentration was corrected for light scattering effects (Winder and Gent, 1971). Protein spectra were obtained between 240 and 370 nm. Absorbance values were taken between 320 and 370 nm at 6 nm intervals. The resulting absorbance values were plotted against wavelength in order to obtain a linear fit with the equation: $y = ax + c$, where a and c are obtained from the linear regression curve fit. By substituting $x = 280$ nm into the above equation, the value of y is found. This value represents the contribution of light scattering effects to the protein sample. Subtraction of this value from the absorbance obtained at 280 nm yields the true absorbance in the absence of light scattering effects. rGST M1-1 was loaded into the sample cell and the respective ligand loaded into the syringe. The system was then allowed to equilibrate and a stable base line was obtained prior to automatic initiation of the titrations. The reference power was set to 15 μcal/sec and the initial delay was 60 seconds for all interactions investigated. The stirring speed was kept constant at 310 rpm. To correct for heats of dilution effects, the averaged heat of the post-saturation injections was subtracted from each injection.

3.7.1.1 Energetics of GSH binding to rGST M1-1

The energetics of the rGST M1-1● GSH interaction were investigated using monomer concentrations of protein of 0.25 mM and a GSH stock solution of 5 mM. The initial titration of GSH was 2 μl followed by seventy-nine 3 μl injections. Between each injection, the base line was allowed to stabilise for 6 minutes.

3.7.1.2 Energetics of GSO_3^- binding to rGST M1-1

The energetics of the rGST M1-1●GSO_3^- interaction were investigated using monomer concentrations of protein of 0.07 mM and a GSO_3^- stock solution of 1.5 mM. The initial titration of GSO_3^- was 2 μl followed by thirty to forty 3 μl injections. Between each injection, the base line was allowed to stabilise for 4 minutes.

3.7.1.3 Energetics of *S*-hexylglutathione binding to rGST M1-1

The energetics of the rGST M1-1●*S*-hexylglutathione interaction were investigated using monomer concentrations of protein of 0.038 mM and *S*-hexylglutathione stock solution of 0.5 mM. The initial titration of *S*-hexylglutathione was 2 µl followed by fifty to sixty 3 µl injections. Between each injection, the base line was allowed to stabilise for 4 minutes.

3.7.1.4 Energetics of ANS binding to rGST M1-1

The energetics of the rGST M1-1●ANS interaction was investigated using monomer concentrations of protein between 0.07 mM and an ANS stock solution of 3.3 mM. The ANS concentration was measured spectrophotometrically using a molar extinction coefficient (at 350 nm) of 4 950 M^{-1} cm^{-1}. An ANS absorbance spectrum was obtained between 300 nm and 550 nm. Contribution due to light-scattering effect was measured from 550 nm to 455 nm and the ANS concentration was corrected as described earlier (Section 6.6.1). The initial titration of ANS was 2 µl followed by fifty-nine 3 µl injections. Between each injection, the base line was allowed to stabilise for 4 minutes.

3.7.2 Temperature dependence of thermodynamic parameters

In order to investigate the effect of temperature on thermodynamic parameters, identical experiments were performed at varying temperatures in the range of 5-30 ºC for GSH, *S*-hexylglutathione and ANS binding and 10-25 ºC for GSO_3^- binding. Experiments were carried out in 20 mM sodium phosphate, 150 mM NaCl, 1 mM EDTA, 1 mM TCEP and 0.02% sodium azide, pH 6.5. ΔC_p was obtained as the slope of the linear plot of ΔH_{obs} versus temperature in kelvin for GSO_3^- binding. For GSH and *S*-hexylglutathione binding the data was fitted to a second order polynomial and ΔC_p values were obtained at each individual temperature as the tangent to each datum point.

3.7.3 Protonation/deprotonation events linked to binding enthalpy

The binding enthalpy obtained from ITC experiments often includes contributions from proton linkage effects (see Section 5.1). To evaluate whether the binding of GSH and GSO_3^- to rGST M1-1 is coupled to any protonation effects, ITC experiments were performed at 25ºC in different buffers with different ionisation enthalpies (Baker and Murphy, 1996). The buffers used were: Phosphate (ΔH_{ion} = 5.12 kJ/mol), PIPES (ΔH_{ion} = 11.45 kJ/mol), MES (ΔH_{ion} = 15.53 kJ/mol), HEPES (ΔH_{ion} = 21.01 kJ/mol) and Imidazole (ΔH_{ion} = 36.59 kJ/mol) (Fukada and Takahashi, 1998). The true binding enthalpy and the number of protons exchanged between the rGST M1-1●GSH and the rGST M1-1●GSO_3^- complex and the buffer were obtained as the y-intercept and the slope of a plot of ΔH_{obs} versus ΔH_{ion},.

3.8 Software for data analysis and molecular graphics

Unless stated otherwise, all least-squares data fitting was performed using the programme SigmaPlot (ver. 5.0) (Jandel Corporation). All raw data obtained from calorimetric experiments were integrated using the ORIGIN (version 5.0) software package supplied with the VP-ITC calorimeter. Where necessary, the baseline was adjusted manually before correcting the raw data.

All three-dimensional structures were viewed using the molecular graphics package Swiss PDB Viewer (ver. 3.7) (Guex and Peitsch, 1997). Calculation of possible hydrogen bonding and inter-atomic distances were also performed using the Swiss PDB Viewer.

The change in accessible surface area upon complex formation, ΔASA, was estimated as:

$$\Delta ASA = ASA_{\text{dimer-ligand}} - ASA_{\text{dimer}} - ASA_{\text{ligand}} \qquad (13)$$

The *ASA* values were calculated using the NACCESS computer programme (Designed by S.J. Hubbard and J.M. Thornton (1993), Department of Biochemistry and Molecular Biology, University College London, London, U.K.). The ΔASA values were used to calculate the expected ΔC_p upon complex formation as (Makhatadze and Privalov, 1995; Brokx et al., 2001):

$$\Delta C_{p,calc} = 2.14(\Delta ASA_{ali}) + 1.55(\Delta ASA_{arm}) - 1.81(\Delta ASA_{bb}) - 0.88(\Delta ASA_{pol}) \quad (14)$$

where $\Delta C_{p,calc}$ is the calculated change in heat capacity on complex formation, ΔASA is the change in accessible surface area on complex formation, the subscripts ali, arm, bb and pol represent aliphatic, aromatic, backbone and polar surfaces, and the four numerical coefficients are expressed in kJ/mol/K per $Å^2$. The algorithm used to calculate the ΔASA values from the data obtained from NACCESS was designed by M. Fernandes and Y. Sayed.

Molecular docking simulations were undertaken using the Internet-based programme PatchDock (http://bioinfo3d.cs.tau.ac.il/PatchDock/) (Duhovny et al., 2002; Schneidman-Duhovny et al., 2003). Two molecules (protein and ligand) are entered into the algorithm with a clustering RMSD of 1.5 Å used for protein-small molecule docking. The output is a list of potential complexes that are sorted by shape complementarity criteria. Three major stages of the algorithm exist: molecular shape representation, surface patch matching and filtering and scoring. Results obtained were viewed using Swiss PDB Viewer (ver. 3.7) (Guex and Peitsch, 1997).

4 RESULTS

4.1 Characterisation of rGST M1-1

The rGST M1-1 cDNA insert within the pET-20b plasmid was verified via DNA sequencing using the T7 promoter by Inqaba Biotech (Pretoria, South Africa). The resultant sequence showed 100% identity to wild-type rGST M1-1 sequence. Recombinant rGST M1-1 was expressed in *Escherichia coli* BL21(DE3)pLys*S* cells and purified using *S*-hexylglutathione affinity chromatography. The purity and homogeneity of the protein was assessed by SDS-PAGE and SEC-HPLC. Analysis on SDS-PAGE (Figure 5) showed that the protein migrated as a single band with an apparent subunit molecular mass of 27 kDa. Analysis by SEC-HPLC (Figure 6) indicates that the protein eluted as a single peak with an apparent homodimeric molecular mass of 47 kDa. The specific activity of the enzyme (at 20 ºC) using a standard enzyme assay with GSH and CDNB as substrates was determined as 4.3 ± 1.2 μmol/min/mg (Figure 7). The tryptophan fluorescence emission spectrum (excitation at 295 nm) is shown in Figure 8A. This spectrum shows a maximum fluorescence intensity at 348 nm. This confirms crystallographic evidence (Ji et al., 1992) regarding the positions of the four tryptophan residues of each subunit (Trp7, Trp45, Trp146 and Trp214) as being partially buried in a hydrophobic environment. The far-UV CD spectrum of rGST M1-1 with minima at 208 nm and 222 nm is typical for predominantly α-helical proteins (Figure 8B).

4.2 Ligand binding to the active site of rGST M1-1

The binding energetics of glutathione, GSO_3^- and *S*-hexylglutathione to rGST M1-1 were investigated using ITC. Glutathione is the physiological substrate for GSTs whereas glutathione sulphonate and *S*-hexylglutathione are competitive inhibitors of GSTs. GSO_3^- is a substrate analogue, whereas *S*-hexylglutathione is a substrate-product analogue. ITC experiments were designed to satisfy a c-value between 1 and 1000 (Wiseman et al., 1989). The c-value is defined as the product of the association constant and the macromolecule concentration. The K_d for the interaction between rGST M1-1 and GSH was previously determined to be 20 μM (Ji et al., 1992).

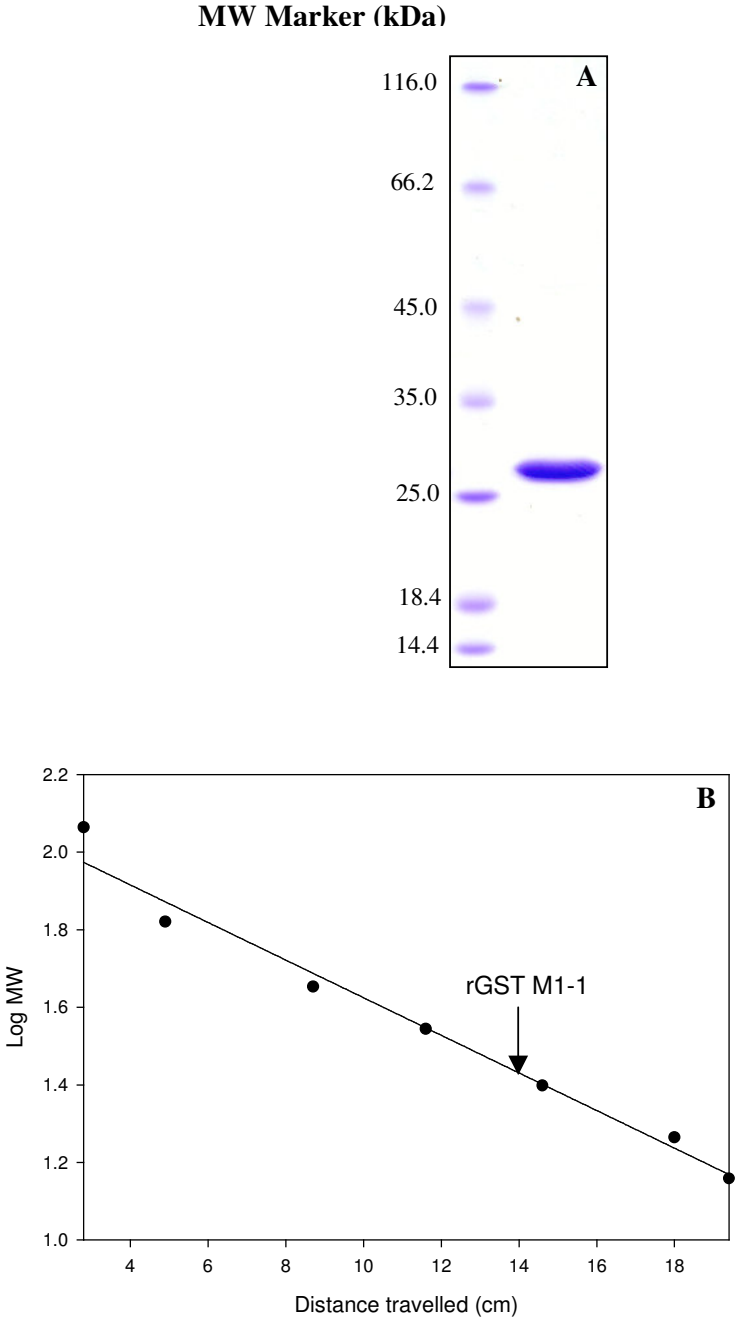

Figure 5: Determination of the subunit molecular mass from SDS-PAGE.

A: lane 1 (left) represents the molecular weight standards: β-galactosidase (116.0 kDa), bovine serum albumin (66.2 kDa), obalbumin (45.0 kDa), lactate dehydrogenase (35.0 kDa), restriction endonuclease Bsp981 (25.0 kDa), β-lactoglobulin (18.4 kDa) and lysozyme (14.4 kDa). Lane 2 (right) contains rGST M1-1 purified using *S*-hexylglutathione affinity chromatography. B: Calibration curve for SDS-PAGE molecular weight markers. The subunit molecular weight was calculated as 27 kDa. The correlation coefficient is 0.98.

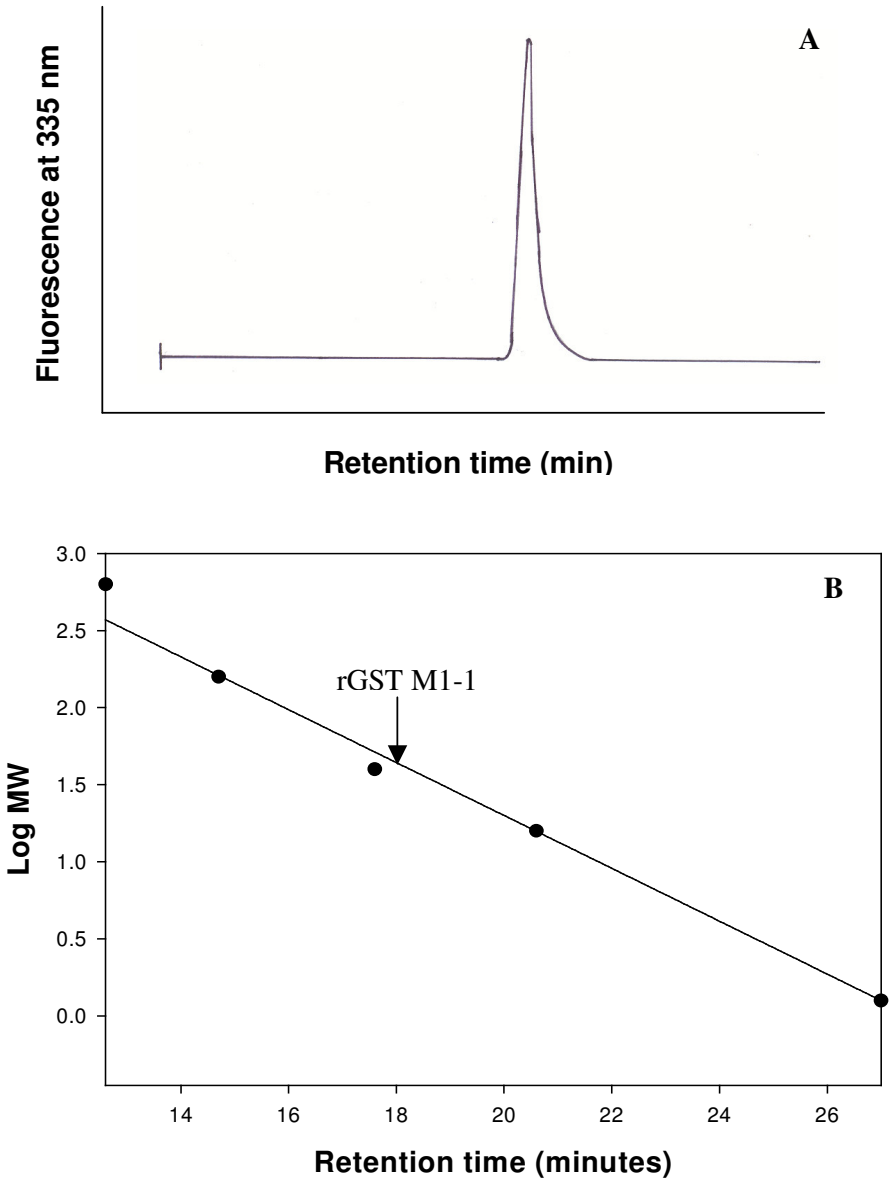

Figure 6: SEC-HPLC elution profile for rGST M1-1.

A: rGST M1-1 elution profile with a single peak indicating no detectable presence of contaminants. B: calibration curve for the SEC-HPLC standards: thyroglobulin (670 kDa), bovine gammaglobulin (158 kDa), chicken ovalbumin (44 kDa) and equine myoglobin (17 kDa). The homodimeric molecular weight of homodimeric rGST M1-1 was calculated as 47 kDa. The correlation coefficient is 0.99.

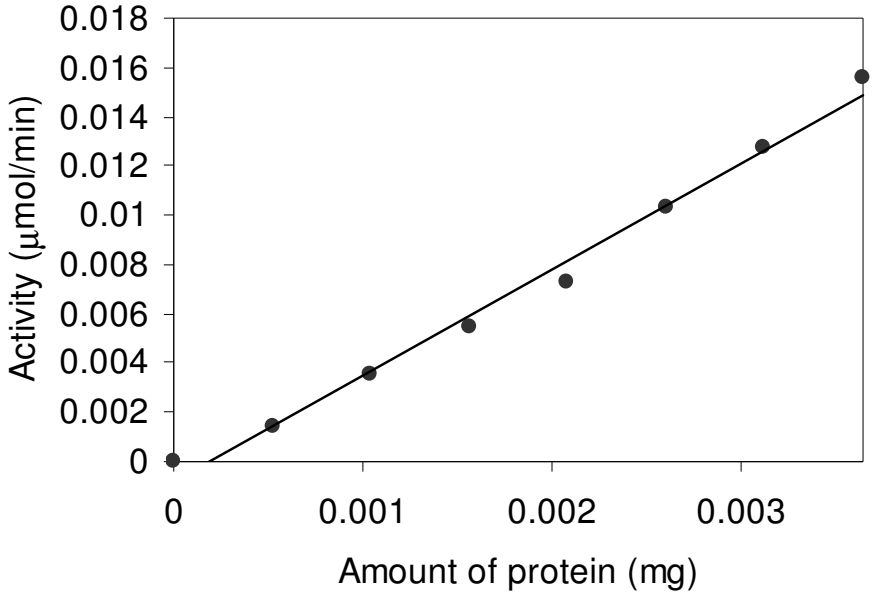

Figure 7: Specific activity determination for rGST M1-1.

The standard assay system involving the conjugation between reduced glutathione and CDNB was used to determine the specific activity of the enzyme. The solid line through the data represents a linear fit with a correlation coefficient of 0.99. The specific activity of rGST M1-1 was determined from the slope of the fit.

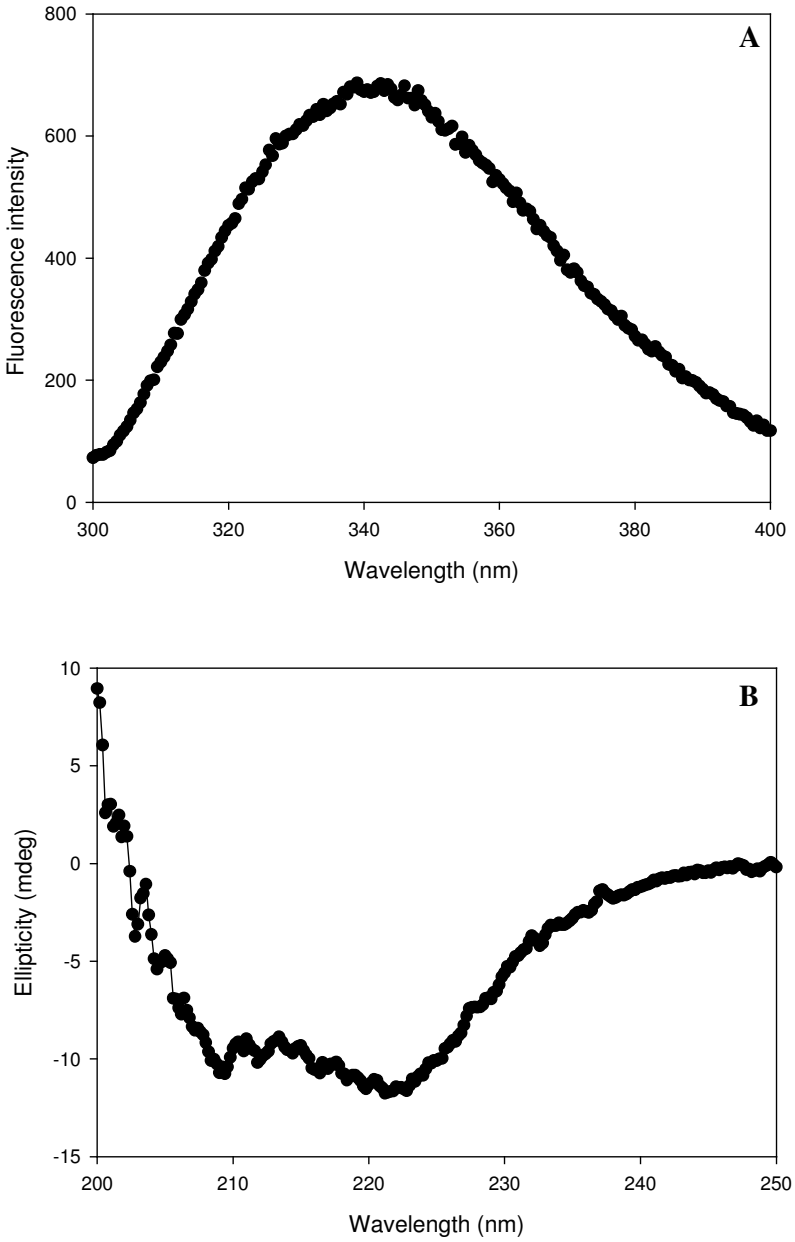

Figure 8: (A) Tryptophan emission spectrum and (B) far-UV circular dichroism of rGST M1-1.

(A) Tryptophan residues were selectively excited at 295 nm and the emission wavelength monitored. The emission maximum for rGST M1-1 occurs at 348 nm. Excitation and emission band widths were set at 5 nm. (B) The data from 20 runs were collected from 250 nm to 200 nm and averaged. Both experiments were performed in a 20 mM sodium phosphate buffer containing 100 mM NaCl, 1 mM EDTA and 0.02% sodium azide, pH 6.5, at 20 ºC.

The K_d for the association of GSO_3^- (4 μM) and *S*-hexylglutathione (2 μM) with pGST P1-1 (Erhardt and Dirr, 1996) were used as reference points for experimental design so as to satisfy a c-value of 27 for GSO_3^- and 190 for *S*-hexylglutathione. Figure 9, Figure 10 and Figure 11 show typical calorimetric titrations of rGST M1-1 with GSH, GSO_3^- and *S*-hexylglutathione, respectively, in sodium phosphate buffer, pH 6.5 at 25 ºC. Each peak in the top panel represents the binding of ligand to the protein and as the binding reaction progresses, the area under each peak decreases due to increased occupancy of binding sites on rGST M1-1. Control reactions in which ligand was titrated into buffer represented the heat due to dilution effects. The heat of dilution was very similar to that seen at the end of a titration experiment (shown in the top panel in Figure 9, Figure 10 and Figure 11). In order to correct for any heat of dilution effects, post-saturation heats were averaged and subtracted from the raw data. Post-saturation peaks shows that no more binding sites are available for occupancy by the respective ligand. Association of all three ligands with rGST M1-1 is characterised by successive exothermic heats representative of a favourable change in enthalpy (ΔH). The bottom panel in each figure shows the isotherm obtained by integrating the heats obtained after each injection as a function of ligand concentration per protein monomer, corrected for heats of dilution. All data from each experiment fit well to a single-site binding model (i.e., one independent binding site per monomer). The binding isotherms are best described as monophasic with a sigmoidal fit to the data representing the decrease in available binding sites on the protein.

Thermodynamic parameters obtained from the data fitting are shown in Table 1. The stoichiometry of binding ranges from 0.7 to 1.2 and is interpreted as one molecule of each ligand bound per monomer of rGST M1-1. There is no evidence of cooperativity between the binding sites in this study. This is the typical mode of ligand binding to GSTs as shown for GSH binding to rGST M1-1 in the crystal structure in complex with GSH (Ji et al., 1992), the crystal structure of pGST P1-1 with GSO_3^- (Reinemer et al., 1991), hGST P1-1 in complex with *S*-hexylglutathione (Reinemer et al., 1992), *S*-alkylglutathione conjugates bound to GSTs from different gene classes (Ortiz-Salmeron et al., 2001; Ortiz-Salmeron et al., 2003; Kuhnert et al., 2005), with no evidence of cooperativity between the binding sites (Kuhnert et al., 2005).

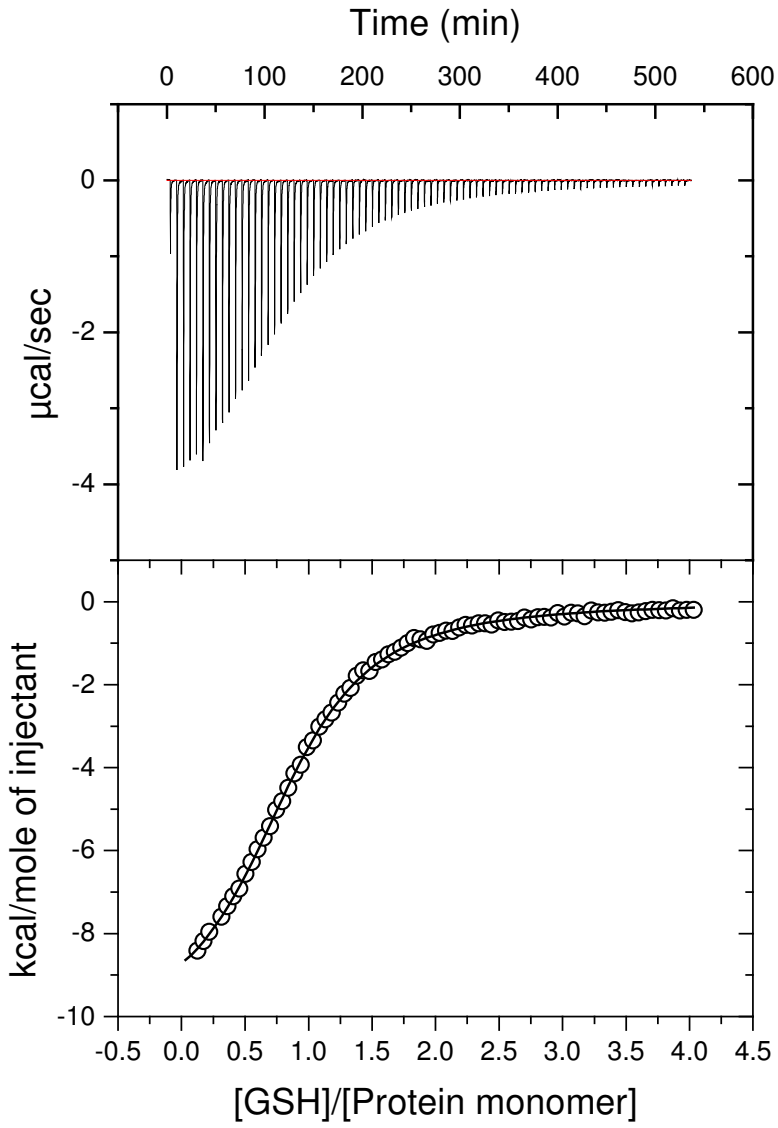

Figure 9: A representative calorimetric profile of the titration of rGST M1-1 with GSH.

The experiment was performed in a 20 mM sodium phosphate buffer containing 100 mM NaCl, 1 mM EDTA, 1.3 mM TCEP and 0.02% sodium azide, pH 6.5, at 25 ºC. The monomer protein concentration was 0.2 mM and the GSH stock concentration was 5 mM. The top panel shows the raw exothermic heats generated upon each injection of GSH into rGST M1-1 (corrected for heats of dilution). The bottom panel shows the integrated heats for peaks in the top panel versus the molar ratio of ligand to protein monomer. The solid line through the data represents the best non-linear least squares fit to the experimental data using a one-site binding model.

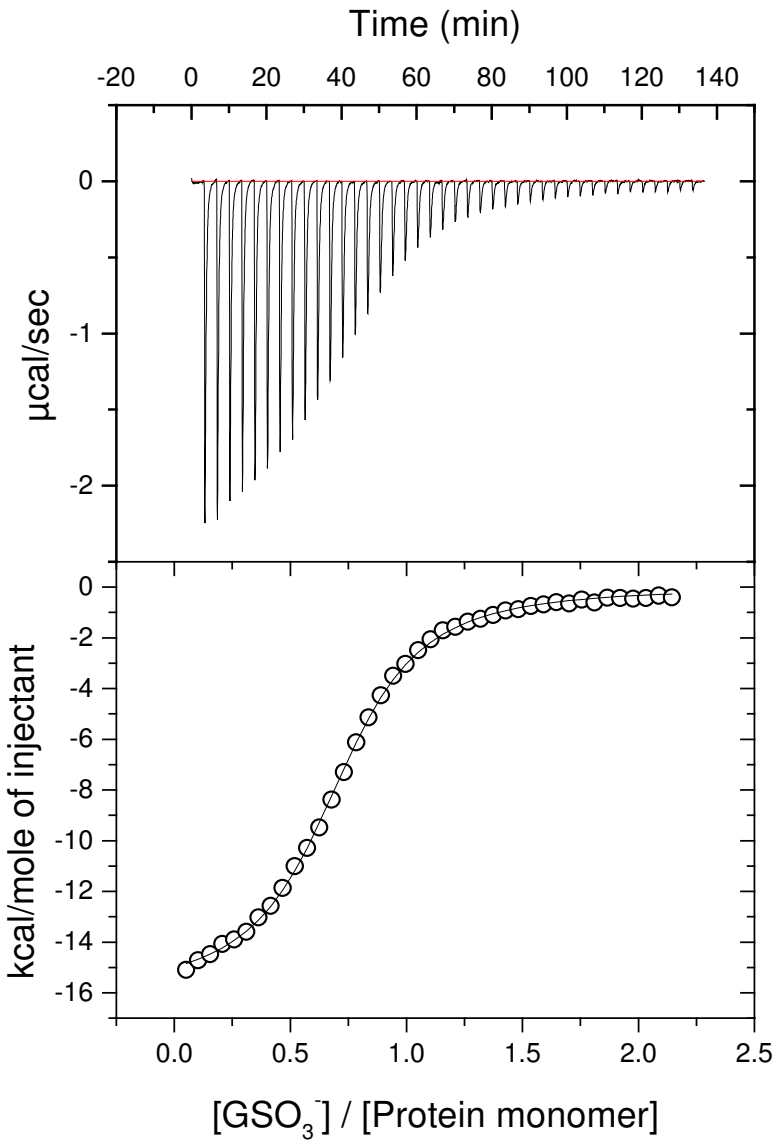

Figure 10: A representative calorimetric profile of the titration of rGST M1-1 with GSO_3^-.

The experiment was performed in a 20 mM sodium phosphate buffer containing 100 mM NaCl, 1 mM EDTA, 1.3 mM TCEP and 0.02% sodium azide, pH 6.5, at 25 ºC. The monomer protein concentration was 0.07 mM and GSO_3^- stock concentration was 1.5 mM. The top panel shows the raw exothermic heats generated upon each injection of GSO_3^- into rGST M1-1 (corrected for heats of dilution). The bottom panel shows the integrated heats for peaks in the top panel versus the molar ratio of ligand to protein monomer. The solid line through the data represents the best non-linear least squares fit to the experimental data using a one-site binding model.

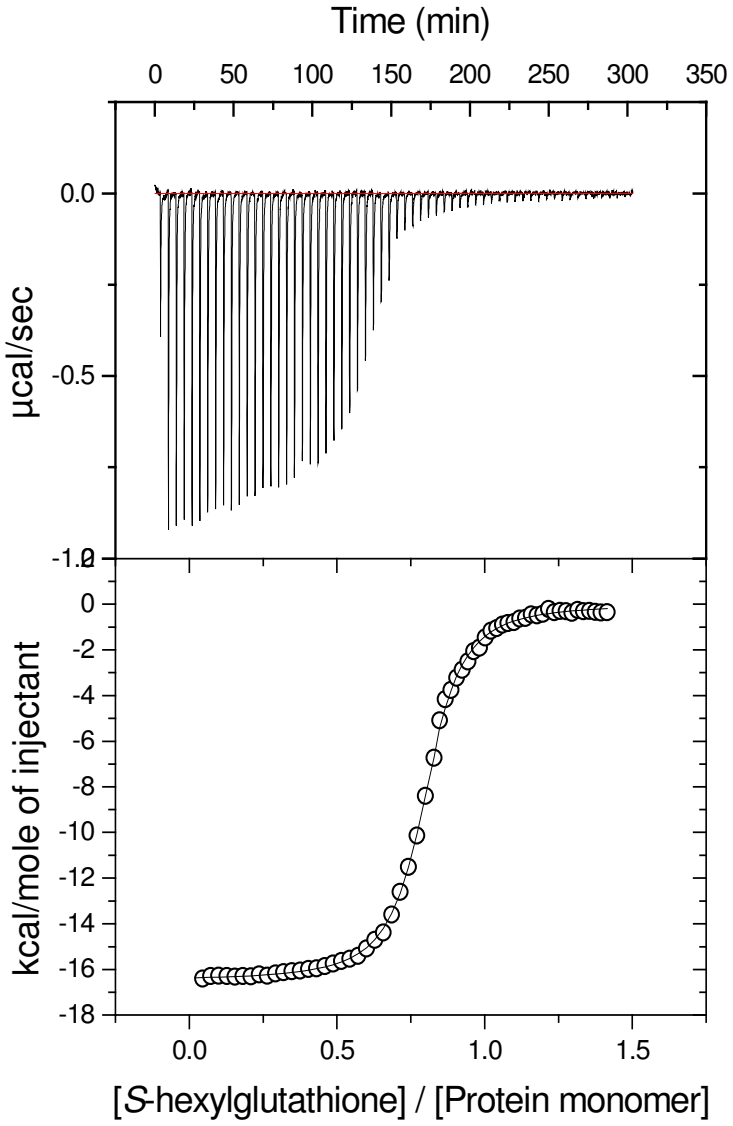

Figure 11: A representative calorimetric profile of the titration of rGST M1-1 with *S*-hexylglutathione.

The experiment was performed in a 20 mM sodium phosphate buffer containing 100 mM NaCl, 1 mM EDTA, 1.3 mM TCEP and 0.02% sodium azide, pH 6.5, at 25 ºC. The monomer protein concentration was 0.038 mM and *S*-hexylglutathione stock concentration was 0.5 mM. The top panel shows the raw exothermic heats generated upon each injection of *S*-hexylglutathione into rGST M1-1 (corrected for heats of dilution). The bottom panel shows the integrated heats for peaks in the top panel versus the molar ratio of ligand to protein monomer. The solid line through the data represents the best non-linear least squares fit to the experimental data using a one-site binding model.

4.2.1 Temperature dependence of the thermodynamic parameters

In order to better comprehend the thermodynamics of the binding interaction, a temperature dependent study was conducted. ITC experiments were undertaken over the temperature range of 5-30 ºC under identical pH and buffer conditions. Results for these titrations are summarised in Table 1. The stoichiometry remains constant over the temperature range i.e., one molecule of ligand bound per protein monomer. The association between rGST M1-1 and GSH decreases as the temperature increases while remaining constant for GSO_3^- and *S*-hexylglutathione. The enthalpy and entropy values change with temperature for all three ligands and all show the same trend: an increase in temperature leads to a decrease in enthalpy (more negative) and a decrease in entropy (more negative) i.e., enthalpy becomes more favourable whereas entropy becomes less favourable. It can therefore, be stated that enthalpy and entropy for the interaction are temperature dependent (Figure 12 Figure 13 and Figure 14). Table 1 shows that the Gibbs free energy of binding for all three ligands remains constant at all temperatures. This is an example of enthalpy-entropy compensation, a phenomenon observed for many interactions, attributed to bond formation that overcomes the unfavourable entropy change (Lumry and Rajender, 1970). Compensation, which occurs broadly throughout biochemistry means that the enthalpy is not independent of the entropy (Dill, 1997). This explains the consistency in the overall favourable Gibbs free energy change of binding observed for ligand binding over the temperature range. It can be clearly stated that binding to rGST M1-1 is enthalpically driven. It is evident from the results presented that overall, ΔG is more favourable for inhibitor binding than for GSH binding. The relationship between ΔH_{obs} and temperature is linear for GSO_3^- binding to rGST M1-1 (Figure 13). The heat capacity determined as the slope to the linear regression fit to the data was –1.86 kJ/mol/K. However, this relationship is different for glutathione and *S*-hexylglutathione binding to the enzyme and data are not well described by a straight line. For these two ligands' binding, the data was best fit to a second order polynomial (Figure 12 and Figure 14). Accordingly, heat capacity changes at each individual temperature were determined as the tangent to the datum point at that specific temperature. The ΔC_p at 25 ˚C is –2.69 kJ/mol/K and –3.68 kJ/mol/K for glutathione and *S*-hexylglutathione binding, respectively. The negative ΔC_p is a good indicator of the changes in hydrophobic interactions occurring during binding and is

Table 1: Temperature dependence of the thermodynamic parameters obtained for the association of rGST M1-1 with GSH, GSO_3^- and *S*-hexylglutathione.

Data were obtained from one to three isotherms per temperature. The standard errors represent the deviation of experimental data from the fit.

Temperature (°C)	*N*	K_d (μM)	ΔH_{obs} (kJ/mol)	$T\Delta S$ (kJ/mol)	ΔG (kJ/mol)
GSH binding					
5	1.2 ± 0.01	15.5 ± 0.9	-19.1 ± 0.05	6.5	-25.6
10	1.1 ± 0.01	19.8 ± 0.1	-26.4 ± 0.1	-0.9	-25.5
15	1.1 ± 0.01	20.6 ± 0.8	-29.2 ± 0.1	-3.4	-25.8
20	1.1 ± 0.01	33.7 ± 0.2	-34.9 ± 0.2	-9.8	-25.1
25	0.9 ± 0.001	38.5 ± 0.2	-49.1 ± 0.3	-23.9	-25.2
30	0.9 ± 0.001	47.2 ± 0.2	-63.0 ± 0.6	-37.9	-25.1
GSO_3^- binding					
5	0.7 ± 0.001	1.6 ± 0.3	-27.9 ± 0.05	2.9	-30.8
10	0.8 ± 0.003	1.1 ± 0.3	-44.4 ± 0.2	-12.1	-32.3
15	0.7 ± 0.003	1.6 ± 0.4	-52.2 ± 0.3	-20.4	-31.8
20	0.7 ± 0.003	1.6 ± 0.2	-55.1 ± 0.3	-22.6	-32.5
25	0.7 ± 0.005	2.6 ± 0.1	-64.1 ± 0.6	-32.2	-31.9
***S*-hexylglutathione binding**					
5	0.7 ± 0.001	0.2 ± 0.003	-39.3 ± 0.1	-3.0	-36.3
10	0.8 ± 0.001	0.2 ± 0.007	-44.4 ± 0.1	-7.6	-36.8
15	0.8 ± 0.001	0.2 ± 0.005	-50.5 ± 0.1	-13.3	-37.2
20	0.8 ± 0.001	0.1 ± 0.006	-58.4 ± 0.1	-20.0	-38.4
25	0.8 ± 0.001	0.2 ± 0.005	-69.0 ± 0.1	-30.9	-38.1
30	0.8 ± 0.001	0.3 ± 0.02	-88.2 ± 0.1	-50.5	-37.7

Representative calorimetric profiles for each ligand binding to rGST M1-1 at the respective temperature are shown in the appendix (Figure 21, Figure 22 and Figure 23).

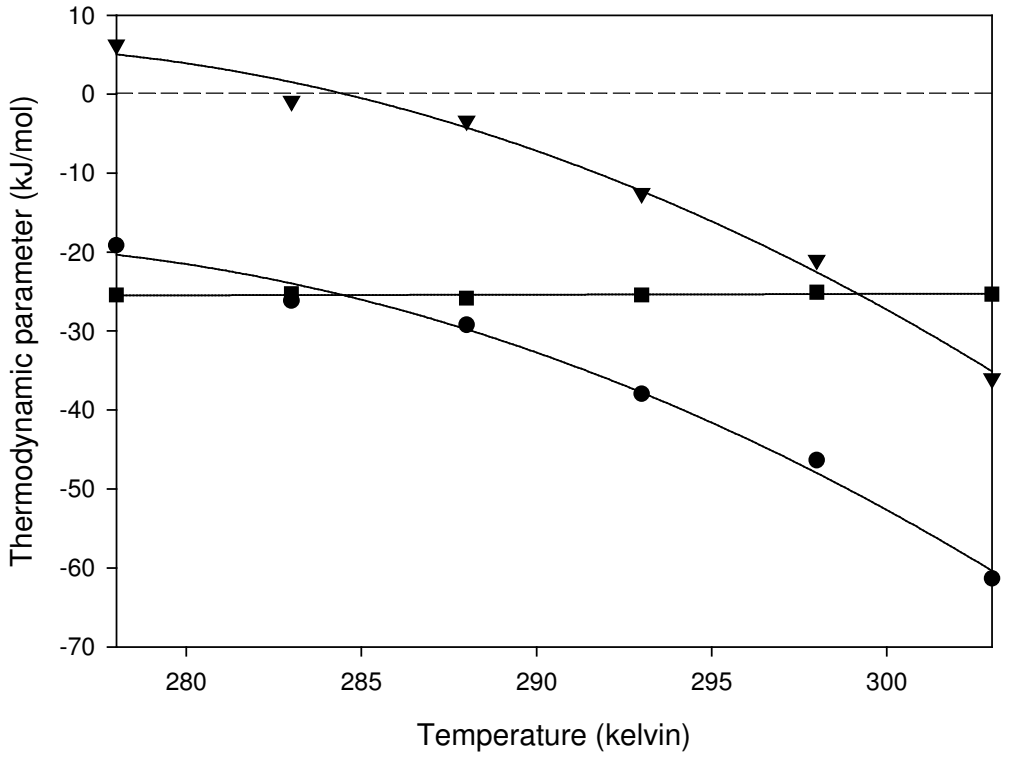

Figure 12: Temperature dependence of the thermodynamic parameters for the binding of GSH to rGST M1-1.

All experiments were performed in a 20 mM sodium phosphate buffer containing 100 mM NaCl, 1 mM EDTA, 1.3 mM TCEP and 0.02% sodium azide, pH 6.5. Solid lines represent second order polynomial fits to the data, ΔH_{obs} (●), $T\Delta S$ (▼) and ΔG (■). The heat capacity change associated with the binding was determined at each temperature as the tangent to each datum point from the polynomial fit to the plot of ΔH_{obs} versus temperature.

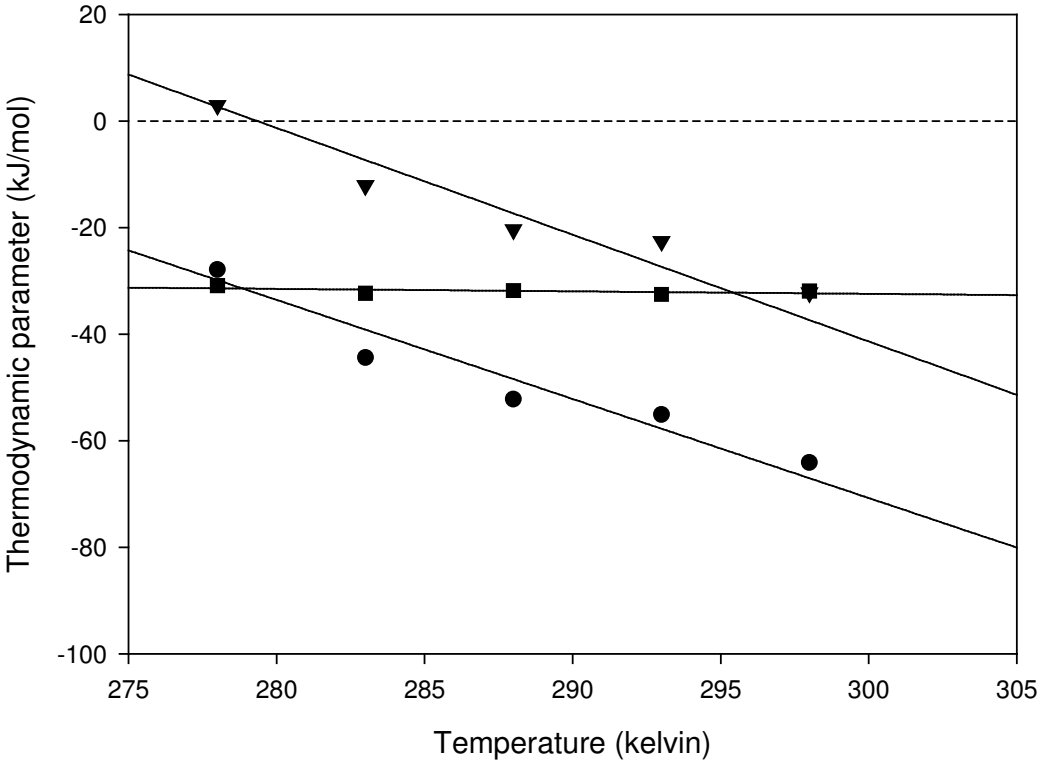

Figure 13: Temperature dependence of the thermodynamic parameters for the binding of GSO_3^- to rGST M1-1.

All experiments were performed in a 20 mM sodium phosphate buffer containing 100 mM NaCl, 1 mM EDTA, 1.3 mM TCEP and 0.02% sodium azide, pH 6.5. The solid lines represent linear fits to the experimental data, ΔH_{obs} (●), $T\Delta S$ (▼) and ΔG (■). The heat capacity change associated with the binding was determined as the slope from the linear regression fit to the plot of ΔH_{obs} versus temperature.

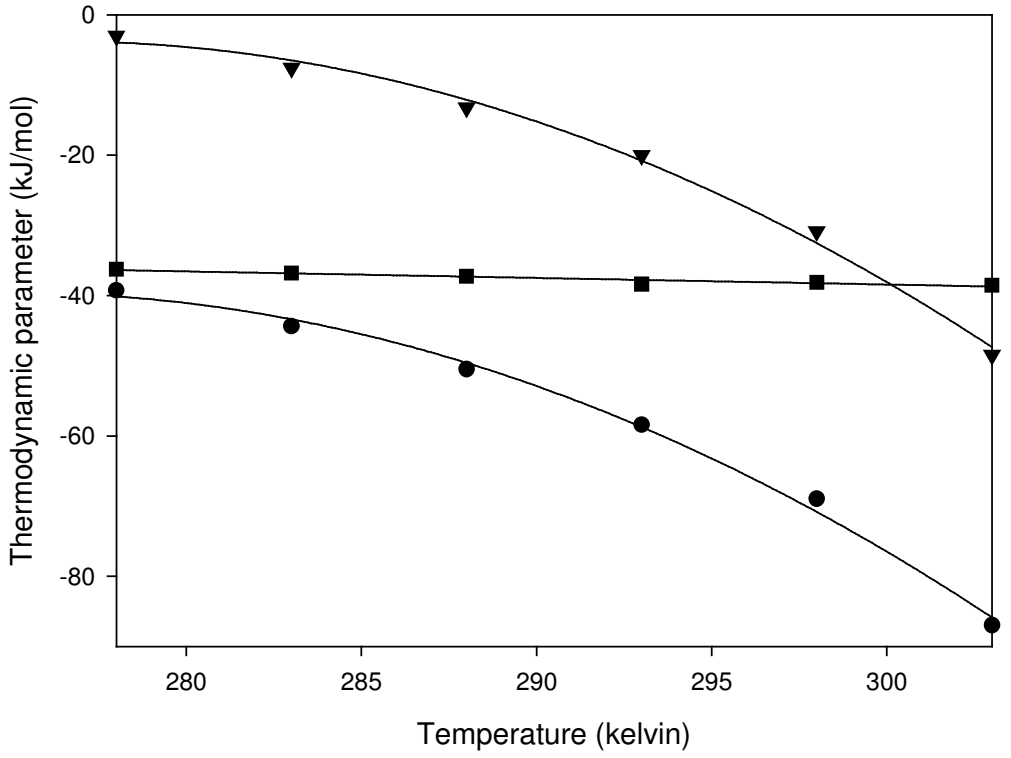

Figure 14: Temperature dependence of the thermodynamic parameters for the binding of *S*-hexylglutathione to rGST M1-1.

All experiments were performed in a 20 mM sodium phosphate buffer containing 100 mM NaCl, 1 mM EDTA, 1.3 mM TCEP and 0.02% sodium azide, pH 6.5. The solid lines represent second order polynomial fits to the experimental data, ΔH_{obs} (●), $T\Delta S$ (▼) and ΔG (■). The heat capacity change associated with the binding was determined at each temperature as the tangent to each datum point from the polynomial fit to the plot of ΔH_{obs} versus temperature.

characteristic of a specific interface irrespective of the overall stability of the complex formed (Ladbury et al., 1994). If hydrophobic bonds are formed the value is negative and if these bonds are broken the value is positive (Luque et al., 1998). The change in heat capacity observed for ligand binding processes is related to the change in protein and ligand solvation (Sturtevant, 1977; Eftink et al., 1983). The interaction between rGST M1-1 and glutathione, GSO_3^- and *S*-hexylglutathione is characteristic, therefore, of a binding process driven by enthalpy, associated with the burial of solvent accessible-hydrophobic surface area.

4.2.2 Proton linkage effects

When one obtains experimental values for ΔH, these values may contain contributions linked to enthalpy associated with the exchange of protons between the protein-ligand complex and the buffer system (Baker and Murphy, 1996). In order to investigate the observed binding enthalpy, the relationship between binding enthalpy and buffer ionisation enthalpy was investigated for the binding of glutathione and GSO_3^- to rGST M1-1. Table 2 shows the binding enthalpies obtained for glutathione and GSO_3^- binding to rGST M1-1. It is evident from the table that the binding enthalpy for glutathione is dependent on the buffer system whereas that for GSO_3^- binding is independent. Figure 15 shows the relationship between enthalpy for ligand binding and the ionisation enthalpy of the buffer. The slope of the linear regression analysis (Figure 15) of the data in Table 2 yields the number of protons released (negative value) or taken up (positive value) upon binding of GSH to rGST M1-1. The value obtained shows 0.5 proton is released into the buffer system upon glutathione binding and 0.07 proton is taken up from the buffer system for GSO_3^- binding. The intercept on the y-axis gives the binding enthalpy (ΔH_{bind}) corrected for ionisation enthalpy of the buffer, which was determined as -47.1 kJ/mol for glutathione binding and –52.9 kJ/mol for GSO_3^- binding. These results clearly show the coupling of proton linkage effects to the binding of GSH to rGST M1-1 and hence the experimentally determined enthalpy is not the actual enthalpy of binding. Figure 15 also shows that there are no protonation changes occurring during the binding of GSO_3^- to rGST M1-1 and therefore, the enthalpy observed for the binding interaction is the actual enthalpy of binding, i.e., $\Delta H_{obs} = \Delta H_{bind}$.

Table 2: Observed enthalpy associated with the rGST M1-1●GSH and rGST M1-1●GSO_3^- interaction in different buffer systems at pH 6.5 and 25 °C.

The data were obtained from two to three experiments per temperature with the standard errors representing deviation from the fitting.

Buffer	ΔH_{ion} (kJ/mol)	ΔH_{obs} (kJ/mol) GSH binding	ΔH_{obs} (kJ/mol) GSO_3^- binding
1. Phosphate	5.12	-49.1 ± 0.3	-66.9 ± 0.3
2. PIPES	11.45	-54.0 ± 0.7	-51.9 ± 0.6
3. MES	15.53	-54.2 ± 0.8	-45.5 ± 0.4
4. HEPES	21.01	-56.8 ± 0.5	-47.6 ± 0.7
5. Imidazole	36.59	-65.1 ± 0.5	-55.6 ± 0.8

Representative calorimetric profiles are shown in the appendix (Figure 25 and Figure 26).

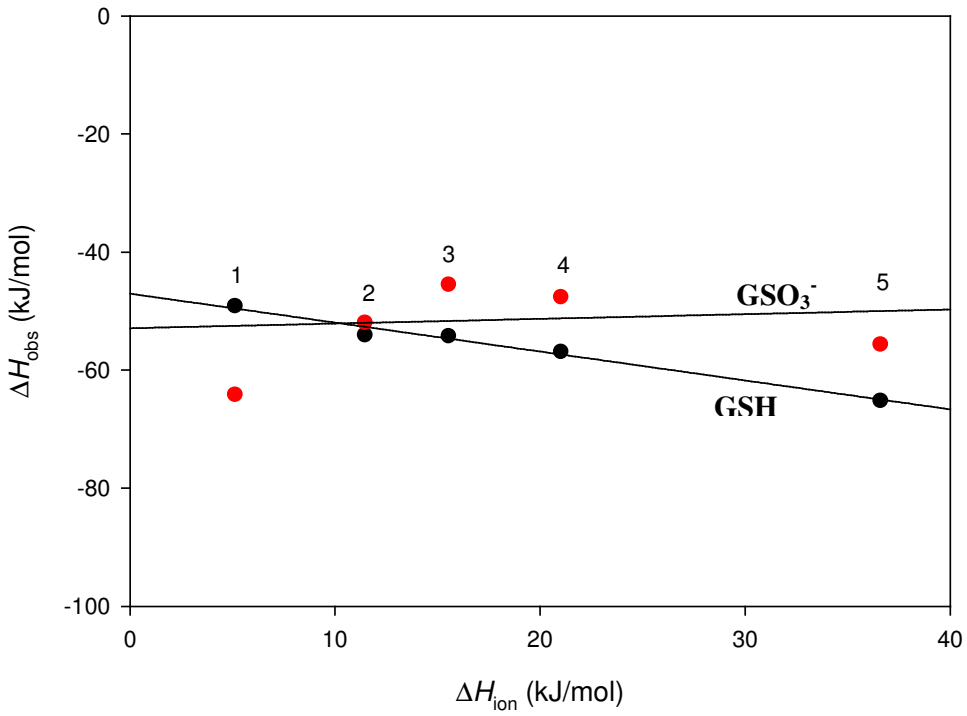

Figure 15: The dependence of the observed enthalpy for the interaction between rGST M1-1 and GSH or GSO_3^- on ionisation enthalpies of different buffers at pH 6.5, at 25 ºC.

The solid lines represent a linear fit to the experimental data. The numbers 1-5 denote the different buffers used as shown in Table 2. The slope of the fit yields the number of protons taken up or released upon complex formation. The Y-intercept yields the binding enthalpy corrected for ionisation enthalpy of the buffer. The correlation co-efficient is 0.98 for GSH binding.

4.3 Non-substrate binding to rGST M1-1

GSTs have also been implicated in the binding of lipophilic ligands such as haemin, bilirubin, bile salts, thyroid hormones, fatty acids and drugs. ANS is a much utilised fluorescent "hydrophobic probe" for examining the nonpolar character of proteins and membranes (Matulis and Lovrien, 1998). ANS is amphiphilic in nature possessing both a charged and a hydrophobic moiety. In all work undertaken concerning ANS, the sulphonate group (SO_3^-) was viewed as a solubilising group for what would otherwise be a nearly water-insoluble anilino-naphthalene moiety (Matulis and Lovrien, 1998). In the present study, the binding of the non-substrate ligand 8-anilino-1-naphthalene sulphonate (ANS) was investigated via ITC as well as fluorescence displacement studies.

4.3.1 Thermodynamics of ANS binding to rGST M1-1

The binding energetics of ANS to rGST M1-1 was investigated using ITC. Figure 16 shows a typical calorimetric titration of rGST M1-1 with ANS in sodium phosphate buffer, pH 6.5 at 25 ºC. The binding isotherm was obtained by titrating ANS into a solution of rGST M1-1 Figure 16. The association of ANS with rGST M1-1 is characterised by successive heats representative of a favourable change in enthalpy. Correction for heats of dilution were carried out as per section 7.2. The bottom panel in Figure 16 shows the isotherm obtained by integrating the heats obtained after each injection as a function of ligand concentration per protein monomer concentration corrected for heats of dilution. These integrations represent the enthalpy change (ΔH). The binding isotherm is best described as monophasic with a sigmoidal fit representing a model assuming one independent binding site per monomer. Thermodynamic parameters obtained from the fit are shown in Table 3. The stoichiometry of binding ranges from 1.1 to 1.4, which is interpreted as one molecule of ANS bound per monomer of rGST M1-1. The stoichiometry of ANS binding to hGST A1-1 and SjGST is one ANS molecule per monomer (Sayed et al., 2002; Yassin et al., 2004). As can be seen in Figure 17 the free energy remains constant throughout the temperature range due to enthalpy-entropy compensation (Lumry and Rajender, 1970); a process that is characteristic of weak interactions found between proteins and their ligands (Dunitz, 1994).

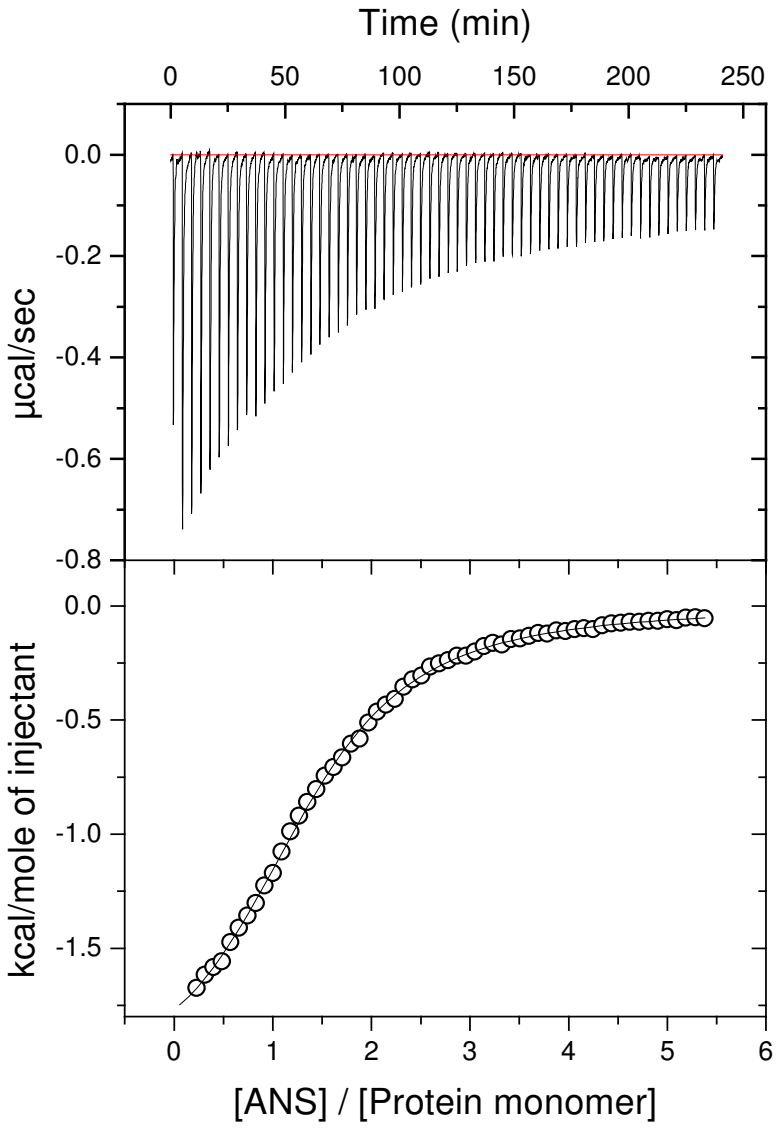

Figure 16: A representative calorimetric profile of the titration of rGST M1-1 with ANS.

The experiment was performed in a 20 mM sodium phosphate buffer containing 100 mM NaCl, 1 mM EDTA, 1.3 mM TCEP and 0.02% sodium azide, pH 6.5, at 25 ºC. The monomer protein concentration was 0.07 mM and ANS stock concentration was 3.3 mM. The top panel in each figure shows the raw exothermic heats generated upon each injection of ligand into rGST M1-1 (corrected for heats of dilution). The bottom panel shows the integrated heats for peaks in the top panel versus the molar ratio of ligand to protein monomer. The solid line through the data represents the best non-linear least squares fit to the experimental data using a one-site binding model.

Table 3: Temperature dependence of the binding parameters for the association of rGST M1-1 with ANS.

Data were obtained from one experiment per isotherm. The standard errors represent the deviation of experimental data from the fit.

Temperature (°C)	*N*	K_d (μM)	ΔH_{obs} (kJ/mol)	TΔS (kJ/mol)	ΔG (kJ/mol)
5	1.1 ± 0.01	20.0 ± 0.6	-2.2 ± 0.03	22.8	-25.0
10	1.2 ± 0.01	33.0 ± 1.3	-4.7 ± 0.06	19.6	-24.3
15	1.2 ± 0.07	35.3 ± 2.2	-6.8 ± 0.05	17.8	-24.6
20	1.1 ± 0.01	40.8 ± 2.0	-10.2 ± 0.1	14.4	-24.6
25	1.4 ± 0.01	27.2 ± 1.2	-9.2 ± 0.08	16.9	-26.1
30	1.3 ± 0.08	20.6 ± 1.0	-10.1 ± 0.08	17.1	-27.2

Representative calorimetric profiles are shown in Figure 24 (appendix).

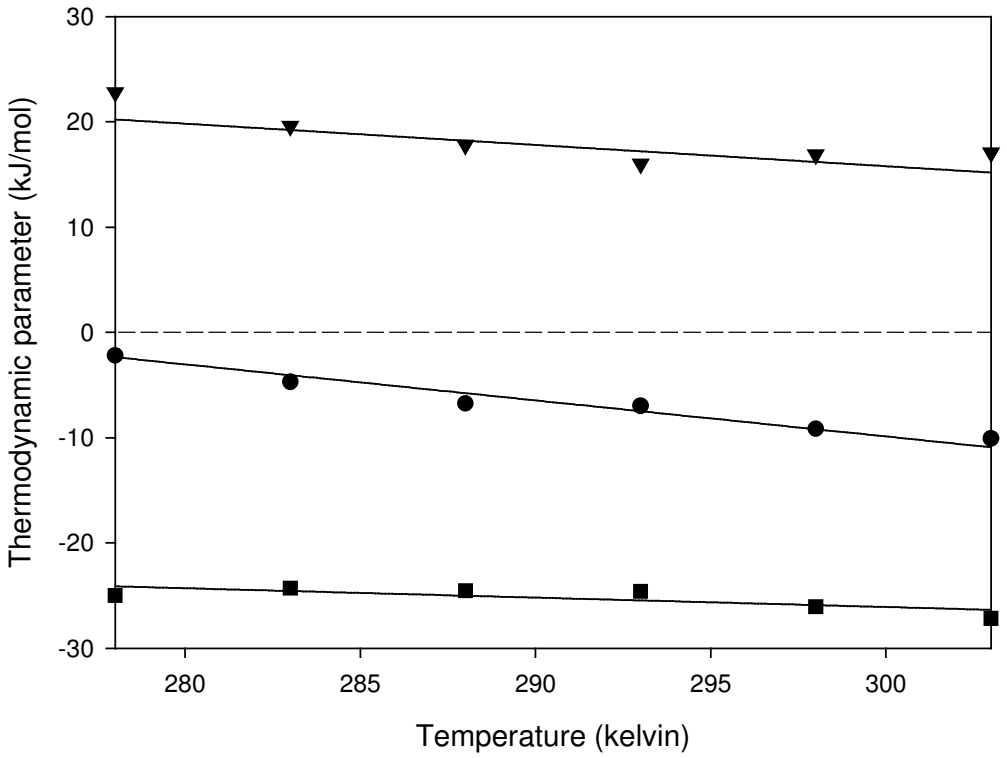

Figure 17: Temperature dependence of the thermodynamic parameters for the binding of ANS to rGST M1-1.

All experiments were performed in a 20 mM sodium phosphate buffer containing 100 mM NaCl, 1 mM EDTA, 1.3 mM TCEP and 0.02% sodium azide, pH 6.5. The solid lines represent linear fits to the experimental data, ΔH (●), $T\Delta S$ (▼) and ΔG (■). The heat capacity change associated with the binding was determined as the slope from the plot of ΔH_{obs} versus temperature.

This phenomenon is a common occurrence found for ANS binding to proteins (Kirk et al., 1996; Ory and Banaszak, 1999; Sayed et al., 2002; Dirr et al., 2005). In order to better understand the binding interaction, a temperature dependent study was conducted as per section 4.2.1. The strength of ANS binding decreases as temperature rises from 5 to 20 ºC. At 25 ºC the strength the interaction begins to increase until the affinity at 30 ºC equals that at 5 ºC. It is interesting to note that although the entropy decreases with increasing temperature, the value remains positive (favourable) Figure 17. Due to enthalpy-entropy compensation, no significant changes in ΔG were observed with increasing temperature. The heat capacity change associated with the binding reaction is estimated from the slope of the linear fit to enthalpy. The ΔC_p is –0.34 kJ/mol/K.

4.3.2 ANS displacement studies

The fluorescence of ANS has been shown to be dramatically sensitive to the presence of water which has been interpreted in terms of a specific solute-solvent interaction (Kirk et al., 1996). There have been other interpretations, however, which have been based on the classical model of an increased dipole moment of the excited state over the ground state of ANS, leading to increasing red shift with solvent polarity (Kirk et al., 1996). ANS has accordingly been used widely as a probe for putative hydrophobic binding sites in proteins and even applied as a diagnostic test for such sites in protein "molten globules", the assumption being that ANS binding to proteins is primarily via hydrophobic interactions mediated through its two aromatic moieties (Kirk et al., 1996). ANS has been shown to bind the active site of class Alpha (Dirr and Wallace, 1999; Kolobe et al., 2004; Dirr et al., 2005) and Pi (Bico et al., 1995; Sluis-Cremer et al., 1996) and was therefore used to probe the active site of rGST M1-1. Using fluorescence spectroscopy, the effect of GSH, GSO_3^-, *S*-hexylglutathione and ethacrynic acid on ANS binding was assessed by exploiting the fluorescence properties of ANS. Addition of GSH to ANS-saturated rGST M1-1 showed no change in the intensity of ANS fluorescence (Figure 18A). However, binding of the other three ligands showed a marked effect on ANS fluorescence. When ANS binds to protein, the fluorescence intensity is enhanced. When ANS is displaced from protein, the fluorescence intensity is decreased due to the change in

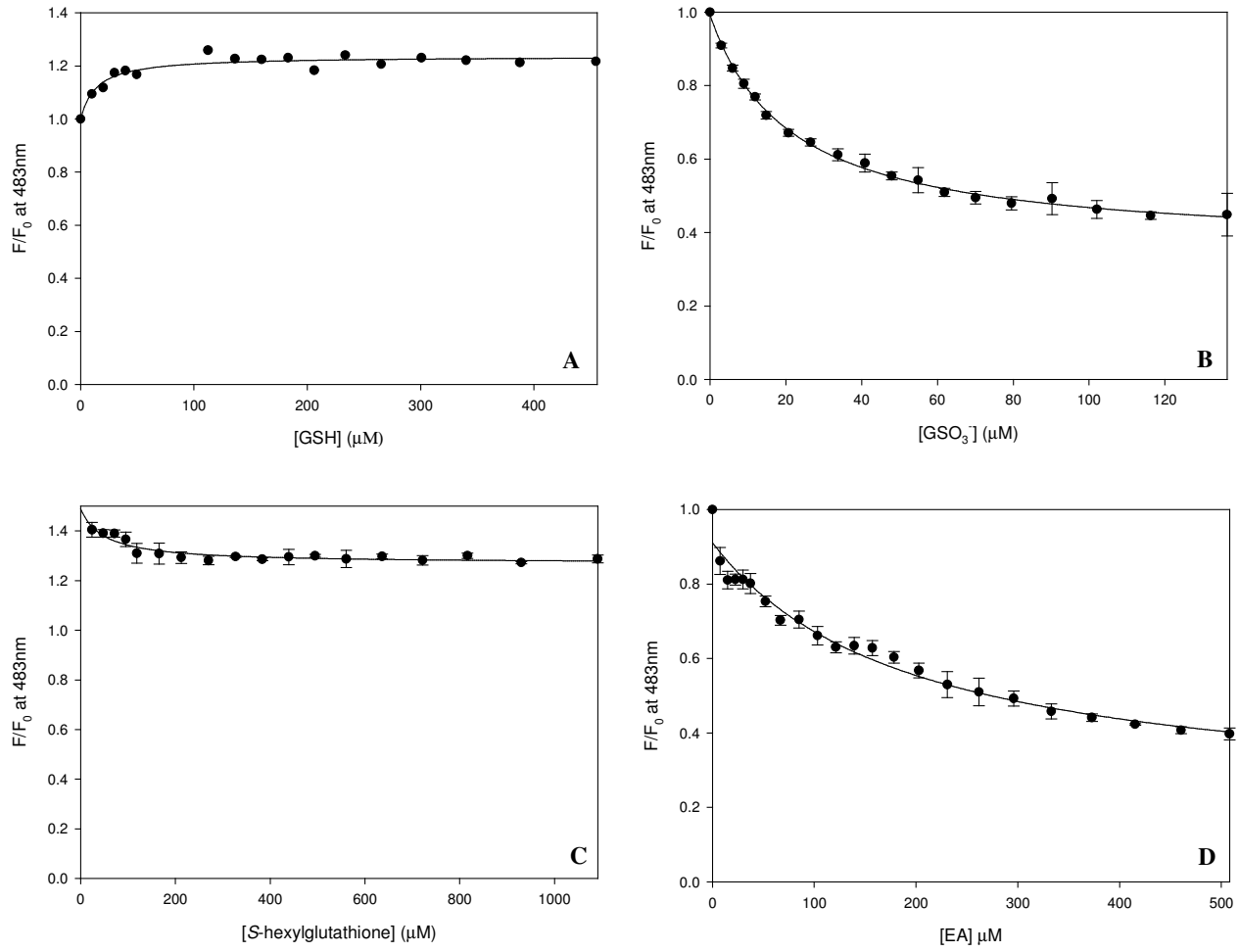

Figure 18: Displacement of ANS by (A) GSH, (B) GSO_3^- (C) *S*-hexylglutathione and (D) ethacrynic acid.

The solid line through the data represents the non-linear regression fit. IC_{50} values were obtained from the fit to the datum points. Experiments were carried out in 20 mM sodium phosphate, 150 mM NaCl, 1 mM EDTA, 1 mM TCEP and 0.02% sodium azide, pH 6.5. Samples consisting of 200 μM ANS and 2 μM rGST M1-1, were titrated with active-site ligands and the fluorescence of bound ANS was followed at 483 nm (excitation at 390 nm). Excitation and emission band widths were set at 5 nm and 10 nm, respectively.

the environment from hydrophobic to polar. Figure 18B-D shows displacement of ANS by GSO_3^-, S-hexylglutathione and ethacrynic acid, respectively. Displacement of ANS is best represented by a hyperbolic decay: as the amount of each ligand added increases, more ANS is displaced until finally all ANS is displaced from the binding site and replaced by the respective ligand. The concentration of GSO_3^-, *S*-hexylglutathione and ethacrynic acid that resulted in displacement of 50% of ANS from rGST M1-1 (IC_{50}) was determined as 21.2 μM, 49.9 μM and 194.2 μM, respectively, from non-linear regression analysis of the data.

4.3.3 Docking of ANS to rGST M1-1

Docking simulations were undertaken in order to locate the ANS binding site on rGST M1-1 using the Internet based algorithm PatchDock (Duhovny et al., 2002; Schneidman-Duhovny et al., 2003). ANS was docked to subunit A of the rGST M1-1 dimer with and without glutathione present. The top 10 results for each simulation were collected and entered into Table 4 in order of decreasing score. It should be noted that the algorithm is solely based on molecular complementarity and factors such as electrostatics are not taken into account during docking simulations. Figure 19 shows the results obtained for docking ANS to the rGST M1-1 monomer in the absence of GSH. The GSH molecule seen in this figure was inserted after docking simulations were undertaken. ANS molecules from solution 3, 5, 7, 8 and 10 clash with glutathione at the G-site (Figure 19A). Since glutathione does not displace ANS, observed in displacement studies (Section 4.3.2), one can exclude these solutions as possible modes of ANS binding. Figure 19B shows solution 2, 4 and 9 docked at the dimer interface. Although the dimer interface has previously been reported as a possible ligandin binding site (see Section 1.3.3) the mere fact that ANS is displaced by H-site ligands (Section 4.3.2) suggests the possible exclusion of these solutions. However, one can clearly see in Figure 18 that ligands that displace ANS (GSO_3^-, *S*-hexylglutathione and ethacrynic acid) do not completely displace all ANS bound to the protein (F/F_0 does not tend toward zero), thus suggesting that the H-site is able to accommodate more than one ligand. This theory is further supported by ITC results in Table 3 showing that only one ANS molecule is bound per protein monomer. This excludes solutions showing ANS docked at the dimer interface and hence, only one

Table 4: Results obtained for ANS docking to rGST M1-1

Solution Number[a]	Residues within 4Å of ANS
Monomer + ANS	
1	**Y6, W7, V9, G11, M34, R42, I111, Y115, S209, L211**
2	D105 → K133, Y166, F169, Q213
3	Y6, W7, L12, L59, I111, Y115, F208, S209
4	D105 → K133, Y166, F169, Q213
5	Y6, W7, M34, R42, N58, L59, I111, Y115, F208, S209, L211
6	Y6, W7, L12, R42, W45, N58, L59, S209
7	Y6, W7, M34, R42, W45, L49, N58, L59, S209
8	Y6, W7, L12, R42, Y45, L49, N58, L59, Q71
9	Q109, M112, L113, N116, Q122, F126, T129, L133
10	Y6, W7, M34, R42, N58, L59, Y115, S209
Monomer + ANS (GSH present)	
1	Y6, G11, L12, M108, I111, Y115, Y115, F208, S209
2	Y6, M34, R42, I111, Y115, S209, L211
3	Y6, W7, M34, I111, Y115, F208, S209, L211
4	Y6, W7, G11, M34, R42, I111, Y115, F208, S209
5	Y6, W7, G11, M34, Y115, F208, S209, L211
6	Y6, V9, M34, I111, Y115, F208, S209
7	Y6, W7, M34, R42, Y115, F208, S209
8	Y6, W7, M34, I111, Y115, S209, L211
9	Y6, W7, V9, L12, M34, I111, Y115, S209, L211
10	Y6, W7, M34, Y115, F208, S209

[a]Entered in order of decreasing score

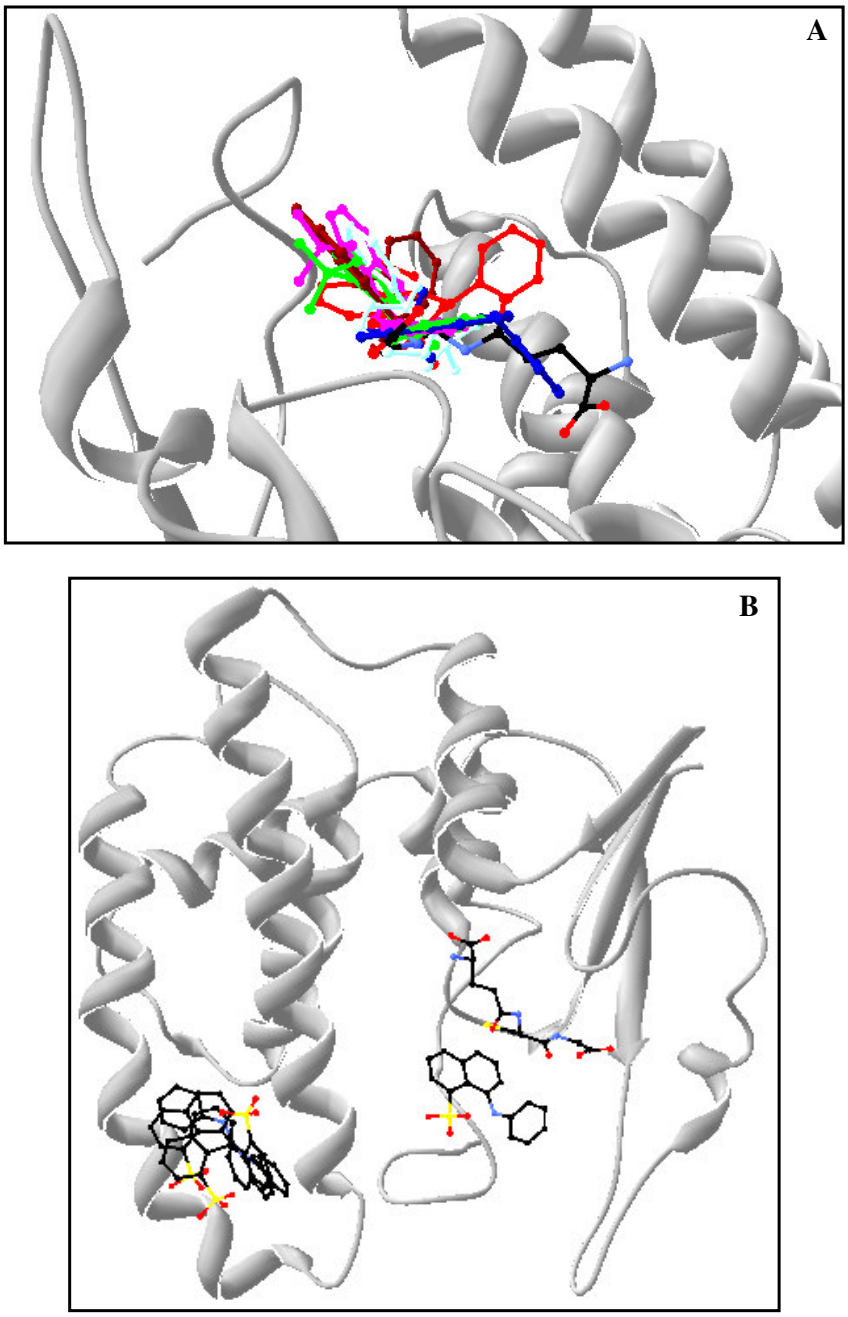

Figure 19: Molecular docking between ANS and rGST M1-1 in the absence of GSH.

Glutathione was inserted after docking simulations and is shown in black in both A and B. **(A)** Solutions 3, 5, 6, 7, 8 and 10 are shown in red, brown, light blue, green, dark blue and pink, respectively, and collide with GSH at the G-site. **(B)** Solutions 2, 4 and 9 are shown in black at the dimer interface. Solution 1 is shown in black at the H-site of rGST M1-1.

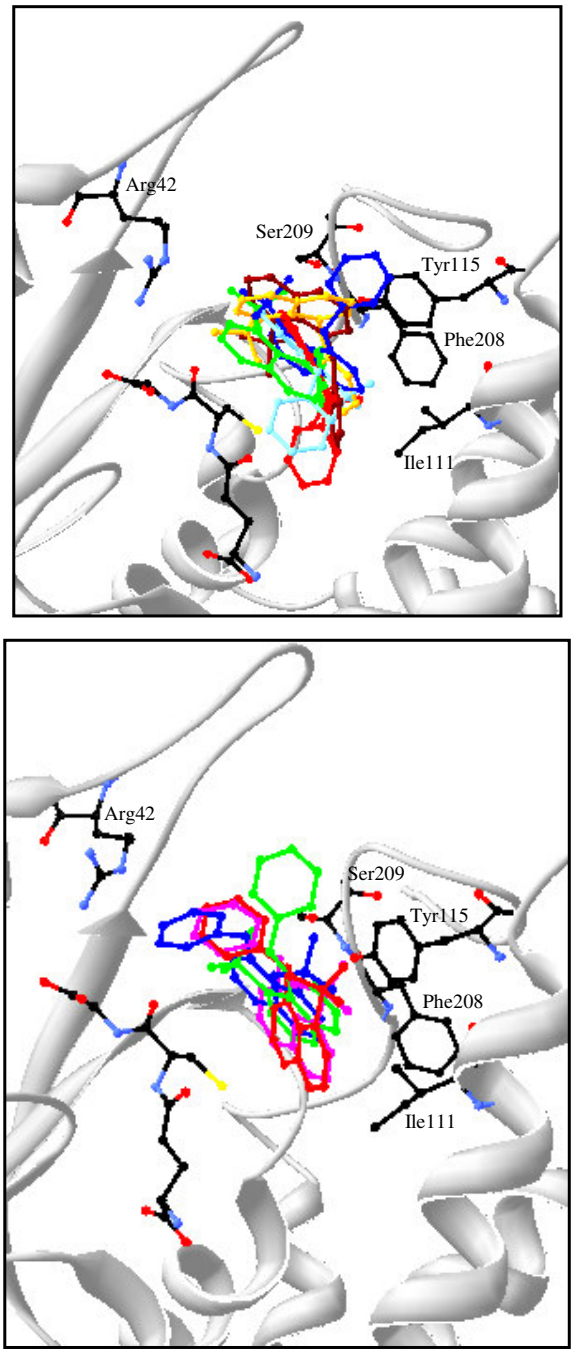

Figure 20: Molecular docking between ANS and rGST M1-1 in the presence of GSH.

GSH is shown in black in both figures. **(A)** Solutions 1 (red), 4 (orange), 5 (green), 6 (light blue), 8 (dark blue), 9 (brown) and 10 (pink) are shown at the H-site with the SO_3^- moiety pointing into the active site. **(B)** Solutions 2 (red), 3 (green) and 7 (blue) are shown at the H-site with the SO_3^- moiety pointing out of the active site toward the surrounding solvent. Solution 1 obtained from docking in the absence of GSH is shown in pink.

docking solution is possible for the docking of ANS to rGST M1-1 in the absence of GSH, solution 1 (Figure 19B). Residues within 4 Å of this ANS molecule is highlighted in Table 4. Figure 20 shows the results obtained for docking ANS to rGST M1-1 in the presence of GSH. All ten solutions place ANS at the H-site in various modes. The majority of solutions place ANS with the SO_3^- group pointing into the active sight toward GSH (Figure 20A). Only three of the solutions place ANS with its SO_3^- group pointing out of the active site toward the surrounding solvent (Figure 20B). Solution 1 obtained from ANS docking in the absence of GSH corresponds to Solution 2 obtained from ANS docking in the presence of GSH.

5 DISCUSSION

5.1 Forces driving ligand binding to the active site

The binding of glutathione, GSO_3^- and *S*-hexylglutathione to rGST M1-1 was investigated using ITC in order to attain a clearer understanding of the forces driving these interactions.

Affinity

Energetic contributions to binding affinity are not simply localised to the direct interactions between the molecules, but contain contributions from structural and dynamic changes propagated throughout the protein, and from counter ions and hydrating water molecules located at the binding site (Ladbury and Williams, 2004). Very high affinity can only be achieved if both enthalpy and entropy contribute favourably to the Gibbs free energy of binding. The binding of glutathione (K_d = 38.5 μM), GSO_3^- (K_d = 2.1 μM) and *S*-hexylglutathione (K_d = 0.2 μM) is seen to be hierarchical with *S*-hexylglutathione having the highest affinity and GSH the lowest affinity for rGST M1-1. It has previously been shown that glutathione analogues with a stable anion replacing the uncharged thiol group, such as glutathione sulphonate, bind the G-site more tightly than reduced glutathione (Graminski et al., 1989). Generally, there are four types of interactions between glutathione and the binding site of GSTs: stabilisation and orientation of the γ-glutamate of glutathione; alignment of the glutathione peptide backbone; stabilisation of the terminal carboxylate of glycine and interaction with the sulphydryl of cysteine for enzymatic activation. The interaction of GSH with the active site of rGST M1-1 involves up to 15 hydrogen bond or salt-bridge contacts to residues within the active site (Ji et al., 1992) (Figure 2). Glutathione is bound to rGST M1-1 in an extended conformation with its backbone facing the cavity between the two subunits and the sulphur pointing toward the subunit to which it is bound. In pGST P1-1, glutathione sulphonate occupies the G-site (Reinemer et al., 1991) and is accessible to solvent and orientated at the G-site with its γ-glutamyl arm pointing downward in the direction of the dimer's large cavity, and the glycine part pointing away from domain II and in the direction of bulk solvent. The sulphonate group of the inhibitor interacts with the side chain of Tyr7 (Tyr6 is the equivalent residue in rGST M1-1). The amide nitrogen of glutathione sulphonate does not interact with protein as it points into the bulk solvent.

The presence of the α-carboxyl group of the γ-glutamyl moiety exerts a stabilising effect (Reinemer et al., 1991). The conformation of the peptide backbone of bound *S*-hexylglutathione is similar to the conformation of glutathione sulphonate bound to pGST P1-1 (Reinemer et al., 1992). The glutathione peptide of the enzyme-bound inhibitor has the γ-Glu moiety pointing down to the internal cavity while the Gly moiety is oriented up to bulk solvent (Reinemer et al., 1992). The hexyl group points towards bulk solvent. Recognition and binding of the glutathione moiety of *S*-hexylglutathione which involves several side- and main-chain polar interactions, is essentially identical to that of glutathione sulphonate as expected from the common conformations they adopt at the active site (Reinemer et al., 1992). The hexyl-group's interactions with the protein are not as intimate and specific as for the glutathione peptide allowing more conformational freedom (Reinemer et al., 1992). The crystal structure of hGST A1-1 with *S*-hexylglutathione bound at the active site indicates that there is enough room in the H-site to allow multiple conformations of the hexyl group and an absence of specific interactions allows for these multiple conformations (Le Trong et al., 2002). ITC studies previously undertaken have reported K_d values of 0.07 μM, 1.23 μM and 1.6 μM for *S*-hexylglutathione binding to hGST A1-1 (Kuhnert et al., 2005), hGST P1-1 (Ortiz-Salmeron et al., 2003) and SjGST (Andujar-Sanchez et al., 2005), respectively, at 25 °C. The K_d value for the hGST A1-1●*S*-hexylglutathione complex is comparable to that of the rGST M1-1●*S*-hexylglutathione complex. The higher affinity in hGST A1-1 has been attributed to additional van der Waals contacts formed at the interface between the localised C-terminal region and *S*-hexylglutathione bound at the active site (Kuhnert et al., 2005). This would apply to the *S*-hexylglutathione●rGST M1-1 interaction with regards to additional contacts between the mu-loop and *S*-hexylglutathione at the active site.

Enthalpy

The enthalpic term (ΔH) reflects the energetic contribution of many individual interactions (hydrogen bonds (Ross and Subramanian, 1981), van der Waals, electrostatic, polar and dipolar interactions etc.) between the two binding molecules, considering the interactions with the solvent as a reference and, therefore, it reflects also the solvation enthalpy (Velazquez-Campoy and Freire, 2005). It is negative (favourable) if the interactions between the binding molecules overcompensate the interactions of the individual molecules with the solvent; otherwise, it will be positive (unfavourable, as for hydrophobic interactions). The interaction of all three ligands

with rGST M1-1 is seen to be enthalpically favourable (Table 1) with *S*-hexylglutathione having the most favourable enthalpy and GSH the least favourable enthalpy. It can, therefore, be concluded that there are more interactions/bond formations between *S*-hexylglutathione and rGST M1-1 compared to the other two ligands and that the exclusion of water upon complex formation plays an important role i.e., interactions between the three ligands and specific residues at the binding site overcompensate their individual interactions with surrounding solvent molecules.

The individual contributions of the enthalpy term to the Gibbs free energy for binding of all three ligands suggest that in all three cases, the binding process is enthalpically driven. The majority of energy, therefore, stems from hydrogen bonding and van der Waals interactions. The role of the hydrogen bond is recognised as being of fundamental importance in determining the structures of proteins as well as their complexes with ligands (Connelly et al., 1994). Table 1 shows the overall Gibbs free energy of ligand binding to rGST M1-1. It is evident that the overall ΔG is more favourable for GSO_3^- and *S*-hexylglutathione binding than for GSH binding to the enzyme. This observation may be explained in terms of the binding energy and the ionisation of GSH. Glutathione sulphonate and *S*-hexylglutathione differ from reduced glutathione by the replacement of the thiol moiety by a negatively charged sulphonate group and a hexyl group, respectively. Reduced glutathione is predominantly bound in its thiolate form (GS^-), whereas, GSO_3^- is already in a state of ionisation prior to the binding reaction. This implies that upon binding, the enzyme would utilise some of its intrinsic binding energy to remove the proton from the uncharged GSH in order to generate the thiolate anion (Figure 3). In order to understand the source of the ionisation energy, the difference in the Gibbs free energy ($\Delta\Delta G$) between glutathione and glutathione sulphonate was calculated as 6.8 kJ/mol. This implies that 6.8 kJ/mol is utilised for ionisation and stabilisation of the thiolate anion (GS^-) in the binary complex at the active site of rGST M1-1. Liu *et al*. (1992) have suggested that the hydroxyl group of tyrosine 6 in the rat isoenzyme 3-3 contributes $\geq$ 5.9 kJ/mol toward the stabilisation of GS^- in the wild type enzyme. For the interaction with GSO_3^- and *S*-hexylglutathione the majority of the binding energy is utilised in the actual binding interaction. In the pGST P1-1●*S*-hexylglutathione complex (K_d = 2 μM), non-specific apolar contacts with the hexyl moiety at the adjacent H-site provide additional binding energy resulting in tighter binding (Erhardt and Dirr, 1996). The stabilised anionic side chain of glutatione sulphonate (K_d = 4 μM) interacts more tightly with Tyr7 than does the thiol moiety of reduced

glutathione (K_d = 200 μM) (Erhardt and Dirr, 1996). A possible explanation for the observed destabilising effect that glutathione exerts on the conformation of pGSTP1-1 when compared with glutathione sulphonate, is that some binding energy is lost to stabilisation against urea as a result of it being required for the activation of the thiol group of glutathione (Erhardt and Dirr, 1996).

Proton linkage effects

Values of ΔH_{obs} obtained from ITC experiments often include the contribution from the enthalpy associated with the exchange of protons between the protein-ligand complex and the buffer system (Baker and Murphy, 1996). Coupling of proton exchange to a binding event is a consequence of the change in the protonation state of groups on the protein and/or ligand upon complex formation (Brokx et al., 2001). The relationship between these enthalpies is expressed by the following equation:

$$\Delta H_{obs} = \Delta H_{bind} + N_{H^+}\Delta H_{ion} \qquad (15)$$

where ΔH_{bind} is the binding enthalpy without any buffer contributions, N_{H^+} is the number of protons taken up or released upon complex formation and ΔH_{ion} is the enthalpy of buffer ionisation (Gomez and Freire, 1995; Baker and Murphy, 1996). The protonation changes upon rGST M1-1●GSH complex formation can be viewed as arising in a shift in the pK_a of one or more groups during complex formation. The difference in the observed (ΔH_{obs}) and actual ΔH (ΔH_{bind}) for the binding of GSH to rGST M1-1 is 2 kJ/mol. This implies that 2 kJ/mol of energy is utilised for proton release. For GSH binding to SjGST, 0.31 proton is released at 25 °C (Ortiz-Salmeron et al., 2001). It has previously been reported that GSH interacts with GST P1-1 via a multi-step binding process and that, after thiolate formation at the active site, approximately 0.5 proton is released from the thiol of GSH into solution, at pH 6.5 (Caccuri et al., 1998). It has also been reported that A1-1 and M2-2 isoenzymes release approximately 0.5 proton from the thiol of the substrate when the binary complex is formed (Caccuri et al., 1999).

Entropy

The change in entropy (ΔS) is composed of various contributions so that:

$$\Delta S = \Delta S_{solv} + \Delta S_{conf} + \Delta S_{mix} \quad (16)$$

where ΔS_{solv} represents the gain in degrees of freedom of the water molecules that, prior to the binding, are localised in the surface of the binding molecules and are released to bulk solvent upon binding (Murphy, 1999; Velazquez-Campoy and Freire, 2005), ΔS_{conf} is the ΔS arising from changes in the conformational degrees of freedom of the backbone and side chain groups of the protein and the ligand, and ΔS_{mix} is the ΔS arising from changes in translational, rotational, and vibrational degrees of freedom upon binding (Murphy, 1999). The ΔS due to loss of conformational degrees of freedom of amino acid side chains (represented by a negative value) comes from the fact that side chains on the surface of proteins can sample different rotameric states whereas buried side chains, either in the protein interior or at an interface, are usually fixed in a single rotamer (Murphy, 1999).

When GSH, GSO_3^- or *S*-hexylglutathione bind to the active site of rGST M1-1, the interacting residues as well as the ligand itself lose their rotational degrees of freedom thus resulting in a loss in conformational entropy. As can be seen in Table 1, the change in entropy becomes more unfavourable as the temperature increases. Binding reactions that are characterised by a less favourable entropy contribution with increasing temperature, have been previously described by Sturtevant (1977) as well as Ross and Subramanian (1981). These authors suggest that at low temperature, the solvent structure around nonpolar groups of the protein and ligand is enhanced such that when the molecules interact, the positive contribution towards ΔS_{solv} is increased. At high temperatures, the solvent structure is minimised, as a result upon complex formation, the positive contribution to ΔS_{solv} is diminished. Due to enthalpy-entropy compensation, the enthalpy contribution dominates at high temperature to compensate for the decrease in entropic contribution. Sturtevant further attributed this pattern to the vibrational contribution that becomes more negative with increasing temperature. This suggests that at high temperatures, both the protein and ligand have more kinetic energy and thus upon complex formation, the vibrational contribution to the binding entropy becomes more negative, and thus less favourable compared to lower temperatures (Ross and Subrimanian, 1981). Due to lack of structural data of the rGST M1-1●GSO_3^- and rGST M1-1●*S*-hexylglutathione complex, the reduction in the entropy contribution at high temperatures cannot be attributed to the vibrational contribution (in accord with Stutervant, 1977) because at this point it is not clear whether the reduction is due to ΔS_{conf} , ΔS_{mix} or both.

Figure 12 and Figure 14 show that the dependence of entropy on temperature for GSH and *S*-hexylglutathione binding to rGST M1-1 is described by a non-linear fit whereas Figure 13 shows a linear fit for the dependence of entropy on temperature for GSO_3^- binding. Although rotational degrees of freedom are lost upon ligand binding, the non-linear fit to the data suggests that a region of the protein remains mobile after the ligand is bound. This is supported by data recently obtained by Codreanu et al., (2005) where a 30% reduction in the rate constant for H/D exchange in the E●GSO_3^- complex compared to that of the E●GS^- complex suggests that GSO_3^- forms a tighter complex that more effectively limits fluctuations in conformations at the active site. These conformational fluctuations are attributed to the mu-loop of rGST M1-1. The temperature dependence implies that at higher temperatures the loop is able to sample more conformations than at low temperatures due to an increase in the kinetic energy of residues composing the loop as well as the ligand itself. This temperature dependence of structural conformation has been shown in GST P1-1. In GST P1-1 the α2-helix replaces the mu-loop found in class Mu enzymes. NMR studies of the unliganded hGST P1-1 enzyme and the GSH and *S*-hexylglutathione complexes show that a single conformation dominates due to the presence of ligand or a reduction in temperature below 17 °C (Hitchens et al., 2001). The ligand-induced folding of the α2-helix in hGST P1-1 (Hitchens et al., 2001) most likely contributes to the unfavourable change in entropy. Earlier studies using time-resolved fluorescence spectroscopy on GST P1-1 showed that in the absence of GSH the enzyme exists in at least two different families of conformational states, one polar and the other apolar (Stella et al., 1998). In the presence of GSH, the equilibrium of these states shifted toward an apolar component with the polar conformers increasing their distributions showing a slight increase in rigidity (Stella et al., 1998). The highly unfavourable entropy of ligand binding at temperatures above 5 °C to rGST M1-1 reflects ligand immobilisation at the active site thereby causing a decrease in ligand flexibility and hence increasing its rigidity at the active site. Given the large number of rotatable bonds compared to the total number of non-hydrogen atoms in a molecule of *S*-hexylglutathione, the free inhibitor is not conformationally constrained (Kuhnert et al., 2005). The entropy term ($T\Delta S$) for *S*-hexylglutathione binding to wild-type hGST A1-1 is –21 kJ/mol (Kuhnert et al., 2005). It is interesting to note that the rigid-body interaction between SjGST and *S*-alkylglutathione conjugates yields $T\Delta S$ values of about –11 kJ/mol (Ortiz-Salmeron et al., 2001; Andujar-Sanchez et al., 2005). The interaction between hGST P1-1 and *S*-hexylglutathione is about –34 kJ/mol (Ortiz-

Salmeron et al., 2003). The small entropic advantage for hGST A1-1 upon complex formation is most likely due to greater desolvation of its active-site on localisation of the C-terminal region (Kuhnert et al., 2005).

The entropy of solvation is usually positive (favourable) and very large, since most ligands have a greater percentage of non-polar than polar surface area buried upon binding (Velazquez-Campoy and Freire, 2005). Solvation entropy is a consequence of the burial of hydrophobic groups and release of constrained water molecules at the interface of interacting molecules into the bulk solvent (Sturtevant, 1977; Ross and Subramanian, 1981). In order for the overall entropy change to contribute favourably to the binding, the liberation of solvent molecules bound to the surface of the ligand and/or the binding site of the macromolecule must occur to an extent sufficiently high to overcome the entropy changes for the ligand and the macromolecule (Sigurskjold et al., 1991). It is possible that solvent displacement occurs upon ligand binding to rGST M1-1 but not to an extent sufficiently high enough to overcome the unfavourable entropy changes of conformation. Figure 2 represents the active site structure of rGST M1-1 in complex with GSH and reveals the location of the active site water molecules. A well-defined network of water molecules in the active site of mouse GST P1-1 has also been observed and the formation of GST P1-1●GSH complex resulted in the displacement of one of the water molecules and a second water molecule was displaced when the electrophilic binding site was occupied (Parraga et al., 1998). The crystal structure data also showed that the thiolate anion is stabilised by the presence of three water molecules as well as the tyrosyl hydroxyl group at the active site. The tyrosine 7 hydroxyl group is not ionised in the free or in the GSH complex at physiological pH. The authors also suggested that one of these water molecules might be responsible in assisting the release of the proton from the GSH thiol group. The favourable entropy observed at 5 °C for GSH and GSO_3^- is possibly a result of a positive contribution from solvation entropy (ΔS_{solv}), which more than offsets other unfavourable entropy contributions at this temperature.

Heat Capacity

The change in heat capacity of a system on going from one state of equilibrium to another (ΔC_p) originates primarily from the changes in the hydration of non-polar and polar molecular surface areas (Freire, 1997). A correlation between non-polar and polar surface area has made the parameterisation of ΔC_p in terms of solvent-accessible surface areas (*ASA*) possible (Spolar and Record, 1994; Makhatadze and Privalov,

1995; Luque and Freire, 1998). A negative ΔC_p is thought to arise from burial of nonpolar groups (having a major effect on the parameter) whereas a positive ΔC_p is associated with burial of polar groups (having a smaller effect) (Sturtevant, 1977; Gomez and Freire, 1995; Loladze et al., 2001). A large negative ΔC_p also signifies the formation of a specific interface (Ladbury et al., 1994). A negative ΔC_p has been shown to be a common occurrence in many binding studies (e.g., (Ladbury et al., 1994; Gomez and Freire, 1995; Sayed et al., 2002; Kuhnert et al., 2005). The changes in heat capacity upon binding of *S*-hexylglutathione to rGST M1-1 are more negative than that for the binding of GSO_3^- and GSH (Table 5) indicating that *S*-hexylglutathione shows a greater reduction in hydrophobic surface area compared to the other two ligands. This is to be expected as *S*-hexylglutathione occupies both the G- and H-sites whereas GSH and GSO_3^- occupy only the G-site thus implying that a larger amount of non-polar surface area is buried due to surface area covered by *S*-hexylglutathione and due to the fact that the H-site contains more hydrophobic residues than the G-site. When inspecting the empirical relationship between non-polar surface covered in binding and the heat capacity for rGST M1-1●ligand formation, the magnitude of the predicted heat capacity is substantially smaller than that observed (Table 5). The ΔH vs. temperature plots for most binding interactions appear to be linear i.e., the ΔC_p of binding is constant. Biomolecules, however, are not rigid bodies, but populate and exchange between many structural equilibria (Ladbury and Williams, 2004). These equilibria will have different heat capacities and, because their populations change with temperature, the changes in heat capacity of the binding partners and the complex will create curvature of the plot of ΔH vs. temperature (Ladbury and Williams, 2004) (Figure 12 and Figure 14). When a protein folds upon binding its ligand, the significant change in biomolecular surface hydration may give rise to a much more readily observable curvature (Ladbury and Williams, 2004). In a study of the association of the DNA binding domain with the 13 base pair target DNA duplex, the reaction was shown to exhibit a large negative heat capacity change which was temperature-dependent and could not be accounted for by the amount of polar and nonpolar surface buried at the complex interface, as would be the case for a rigid body type of association (Milev et al., 2003). ΔC_p of association between integrase Tn916 and its target DNA is temperature dependent and is significantly larger than the structure-based estimate of this value (Milev et al., 2003a). This peculiar behaviour of ΔC_p is due to restricted thermal motions of the

Table 5: Calculated and observed heat capacity changes on formation of GSH, GSO_3^- and *S*-hexylglutathione●GST complexes

Complex	$\Delta C_{p,obs}$ (kJ/mol/K)	$\Delta C_{p,calc}$ [a] (kJ/mol/K)
rGST M1-1●GSH	-2.69[b]	-0.17[c]
hGST A1-1●GSH[d]	-0.44	-0.60
SjGST●GSH[e]	-1.0	-0.11
hGST P1-1●GSH[f]	-1.23	-0.37
rGST M1-1●GSO_3^-	-1.86	-
hGST A1-1●GSO_3^- [d]	-0.47	-
SjGST●GSO_3^- [g]		-0.12
hGST P1-1●GSO_3^- [f]	-0.67	-0.38
rGST M1-1●*S*-hexylglutathione	-3.68[b]	-
hGST A1-1●*S*-hexylglutathione [h]	-1.71	-1.79
SjGST●*S*-alkylglutathione [i]		-1.37, -1.00, -0.83

[a] See Experimental Procedures for details.

[b] Observed values at 25 °C

[c] The PDB structure 6GST was used for the calculations

[d] Sayed (2001), unpublished data

[e] Ortiz-Salmeron et al., (2001)

[f] J. Hornby and R. Vather, unpublished data

[g] The PDB structure 1M99 was used for the calculations

[h] Kuhnert et al., (2005)

[I] Ortiz-Salmeron et al., (2001). Values for *S*-methylglutathione, *S*-butylglutathione and *S*-octylglutathione, respectively

protein and the DNA in the complex and, possibly, the presence of water-filled cavities at the complex interface (Milev et al., 2003a). Ladbury, et al. (1994) invoked the idea that the answer to the discrepancy lies in a failure to realise the complete extent to which the specific interface of the complex restricts the degrees of freedom of the complementary polar, hydrated surfaces. For a delocalised region that is disordered, the amount of surface area that would become buried on complex formation, coupled to the localisation of the region, would be more extensive, resulting in a much larger negative $\Delta C_{p,obs}$. This phenomenon has also been interpreted by the fact that experimentally calculated enthalpy is the association enthalpy change of the molecules in their real conformational state, including thermal fluctuations, conformational changes, and perhaps even partial unfolding (Milev et al., 2003a). Differences between calculated and observed heat capacity can be explained by dividing the association reaction into two steps: 1. transition of protein and ligand from the free to the binding-competent conformations, and, 2. the association of the binding-competent molecules to the complex (Milev et al., 2003a). Binding is accompanied by a number of structural rearrangements that are system specific and difficult to account for. This conformational adaptation is typical for macromolecular recognition and adaptation occurs at the cost of introducing conformational disorder in parts of a binding domain. Currently, there is no X-ray structure of a ligand free class Mu GST. Therefore, the question remains as to whether the class Mu C-terminus is disordered in the absence of ligand (McCallum et al., 1999). The conformational flexibility of the C-terminus may enhance the breadth of substrate specificity by providing a mechanism of generating different H-sites from the same primary sequence (McCallum et al., 1999). The C-terminus in Mu class isozymes is found to be over the active site, and sterically hinders ligand binding and product release (McCallum et al., 1999). Regions of GST M2-2 that are likely to adopt different conformations have been previously identified on the basis of high crystallographic temperature factors – these regions are the mu-loop, the carboxy terminus and the top of the D-helix (McCallum et al., 2000). The residual dipolar coupling measurements show that neither the carboxy terminus nor the D-helix experiences motion on the microsecond to nanosecond time scale (McCallum et al., 2000). In contrast residual N-H dipolar couplings suggest that the mu-loop samples different conformational states in both liganded and unliganded enzymes on the microsecond to nanosecond time scale (McCallum et al., 2000). The time scale for the mobility of the mu-loop suggests that this conformational change may be involved

in gating the access of substrates to and the release of products from the active site. In addition, these measurements also show that the mu-loop assumes a more open conformation in solution, further facilitating ligand binding and release (McCallum et al., 2000). Amide hydrogen exchange studies show that ligand binding reduces the number of conformational states sampled by the protein but does not cause the formation of only one conformational state upon ligand binding (McCallum et al., 2000). This dampening of motion may be important for generating an optimal configuration for the nucleophilic substitution reaction as well as for providing a favourable entropic contribution to the free energy of product release (McCallum et al., 2000). As mentioned earlier, it has been demonstrated that the addition of GSO_3^- to rGST M1-1 results in a much tighter complex compared to the formation of the rGST M1-1●GSH complex and effectively limits conformational fluctuations at the active site (Codreanu et al., 2005). It can reasonably be stated that the 'peculiar' behaviour of the heat capacity function for GSH and *S*-hexylglutathione binding to rGST M1-1 could be attributed to the fluctuations of the mu-loop that seem to continue, although to a lesser extent compared to the native enzyme, even after ligand is bound. The ΔC_p values obtained for the binding of both GSH and GSO_3^- to hGST P1-1 are shown in Table 5. One can clearly see a similar trend with regard to the differences in the GSH and GSO_3^- complexes. For this enzyme the observed and calculated heat capacity change for the formation of the hGST P1-1●GSO_3^- are not far off from one another. However, those observed for the GSH complex are definitely different. As mentioned earlier, the α2-helix of GST P1-1 samples different conformational states before and after GSH or *S*-hexylglutathione is bound. Table 5 also shows the observed and calculated heat capacity changes for *S*-hexylglutathione binding to hGST A1-1. This interaction shows a different trend in that these values correspond. This is attributed to the stabilisation of the α9 helix upon ligand binding (Kuhnert et al., 2005). The values obtained for SjGST●*S*-alkylglutathione conjugates correlate with those obtained for the hGST A1-1●*S*-hexylglutathione complex (Table 5) supporting the formation of a stable complex upon binding of these ligands. Since stabilisation of structural elements involved in ligand binding lead to a correlation between the observed and calculated heat capacity for an interaction, and it is known that the mu-loop samples multiple conformations after ligand binding, one can conclude that the mu-loop of rGST M1-1 is not stabilised upon GSH and *S*-hexylglutathione binding; thereby, leading to a large discrepancy in the calculated and observed change in heat capacity.

5.2 ANS as a probe of the active site

Although no experimentally determined structures of an ANS-GST complex exist, molecular docking and ligand displacement studies provide evidence that the amphipathic dye binds to both the H-site and dimer interface of rGST M1-1, albeit in different modes in the absence and presense of GSH. Ethacrynic acid, another H-site ligand, has also been shown to bind hGST A1-1 in different modes (Cameron et al., 1995). The major difference between the modes of binding with regard to the H-site involves the position of the SO_3^- group on ANS. This group either points into the H-site with the nonpolar rings exposed to solvent or it points out of the H-site toward the surrounding solvent. Residues within 4 Å of the ANS molecule at the active site, as well as the dimer interface, have been tabulated in Table 4. Residues I111, Y115, F208 and S209 are within this distance for the majority of solutions obtained (Figure 20). These amino acid residues are also found within van der Waals distance of (9*S*,10*S*)-9-(*S*-glutathionyl)-10-hydroxy-9-10-dihydrophenathrene bound to the H-site of rGST M1-1 (Ji et al., 1994) (Figure 4). The predominantly nonpolar character of the binding site for the aromatic moieties of ANS is consistent with those of other ANS-binding proteins (Ory and Banaszak, 1999; Schonbrunn et al., 2000; Lartigue et al., 2003).

A loss in fluorescence of ANS represents displacement of ANS from a hydrophobic environment. Because the ligands under study (GSO_3^-, *S*-hexylglutathione and ethacrynic acid) displace ANS and knowing how these ligands bind, one can reasonably speculate that the ANS resides in the H-site of rGST M1-1. In the crystal structure of hGST P1-1 with ethacrynic acid and its glutathione conjugate, the ethacrynic acid portion of the conjugate is found in a similar position to that of the hexyl moiety of the *S*-hexylglutathione complex crystal structure, i.e., bound at the H-site (Oakley et al., 1997). Ethacrynic acid has also been shown to bind the H-site in hGST A1-1 (Cameron et al., 1995). Dirr et al. (2005) have also shown via ligand-displacement studies and molecular docking that ANS binds to the H-site of hGST A1-1 and a high affinity-binding site for ANS at or near the promiscuous H-site of hGST P1-1 has been reported (Ralat and Colman, 2003, 2004). Although one would expect no displacement of ANS by GSO_3^- the results show the contrary. Although this inhibitor binds to the G-site of GSTs in much the same way as GSH does, its negatively charged sulphonate group has been seen to occupy a similar position to

that of ANS bound to the H-site of hGST A1-1 (Dirr et al., 2005). In docking studies presented here, in some instances the sulphonate moiety does occupy a similar position to the sulphonate moiety of GSO_3^-, however, in other instances, the anilino and naphthyl rings are in this position. One can therefore conclude that displacement of ANS by GSO_3^- is either due to the overlapping binding sites for their respective sulphonate groups at the interface of adjacent G- and H-sites, or due to steric interference by ANS. Due to the lack of displacement of ANS by GSH, one can clearly conclude that there is no competition for binding space and hence, ANS does not bind to the G-site of rGST M1-1 and hGST A1-1. Figure 18 shows the results of the displacement studies. It is obvious that ANS is not strongly displaced by the ligands under study. Very weak displacement is seen for *S*-hexylglutathione. This implies the possibility of a second ANS binding site on the protein, as a large amount of ANS still remains bound after displacement by the relative ligand. Docking studies placing ANS at the dimer interface can therefore not be excluded as possibilities. This theory is, however, not supported by the ITC studies presented here and by others (Sayed et al., 2002; Yassin et al., 2004; Dirr et al., 2005) showing a stoichiometry of one ANS molecule per protein monomer. One can therefore conclude that the H-site is able to accommodate more than one ligand.

ITC was used to investigate the forces driving non-substrate binding to rGST M1-1 and to obtain a clearer understanding of the ligandin function of this enzyme. Table 3 shows that the K_d values are temperature dependent with ANS binding to rGST M1-1 ~2-fold tighter at 5 °C than at 20 °C. This phenomenon has also been observed for ANS binding to hGST A1-1 (Sayed et al., 2002). The free energy remains constant throughout the temperature range, a process characteristic of weak interactions found between proteins and their ligands (Dunitz, 1994).

Enthalpy

The ΔH obtained is exothermic at each temperature studied and becomes more negative/favourable as the temperature increases. The favourable enthalpic event may be attributed to hydrogen bonding and van der Waals interactions. Given the amphipathic nature of ANS, its interaction with proteins cannot be strictly hydrophobic, as often assumed, but will involve van der Waals and electrostatic forces (Dirr et al., 2005). The importance of van der Waals interactions has been demonstrated for the enthalpically driven formation of the hGST A1-1●ANS complex

(Sayed et al., 2002), consistent with the putative van der Waals contacts between the aromatic ring systems of ANS and the H-site, and for the formation of other protein-ANS complexes (Kirk et al., 1996; Ory and Banaszak, 1999).

Entropy

Favourable entropic contributions are observed throughout the temperature range investigated (Table 3) but is seen to decrease with increasing temperature. These positive changes in entropy attenuate the favourable enthalpy of binding. The positive $T\Delta S$ reflects a net favourable entropy change of solvation in that restrained water molecules that solvate the nonpolar surface of the aromatic ring systems and negatively charged sulphonate group of free ANS are released to bulk solvent on complex formation (Sturtevant, 1977). The $T\Delta S$ is reduced by a smaller, unfavourable change in conformational entropy due to a loss of degrees of freedom at the interface between ANS and protein (Sayed et al., 2002). The conformational freedom of ANS in solution can be described by two dihedral angles; the rotation about the N-Cl' bond between the anilino and naphthyl rings defining the angle between the plane of these rings, and the angle defined by Cl'-N-Cl-C2 (Ory and Banaszak, 1999). Unbound ANS is intrinsically flexible and its docking onto the protein would be penalised by conformational entropy (Sayed et al., 2002). Since the ordering of ANS does not cause this observed favourable entropy, the dynamics of the mu-loop is the probable contributor to the favourable entropy change. Since entropy remains favourable throughout the temperature range studied, desolvation of the interacting surfaces compensates for losses in conformational entropy (Dirr et al., 2005).

Heat capacity

The linear dependence of enthalpy indicates that the heat capacity change of rGST M1-1●ANS complex formation is not coupled to other structural equilibria with significant enthalpies. Binding of ANS to GSTs is not accompanied by any major protein conformational changes (Bico et al., 1995; Wallace and Dirr, 1999). The presence of electrostatic interactions between the sulphonate group of ANS and the guanidinium group of an arginine residue has been shown to play an important role for ANS binding to a variety of protein●ANS complexes (Ory and Banaszak, 1999; Schonbrunn et al., 2000; Lartigue et al., 2003), supporting the important role that the ion pair plays in determining binding affinity for these complexes (Dirr et al., 2005). The experimentally obtained ΔC_p for ANS binding to rGST M1-1 is –0.34 kJ/mol.

Since the change in heat capacity originates primarily from the changes in the hydration of nonpolar and polar molecular surface areas (Freire, 1997), formation of the bimolecular interface between protein and ligand results in the removal of groups from solvent (and thus dehydration of their surfaces), and the packing of these groups within the protein. Electrostatic interactions have been reported to generate positive heat capacity changes (Sturtevant, 1977; Makhatadze, 1990), hence ruling out the possibility of strong electrostatic interactions of ANS with charged groups within the H-site. The presence of Arg45 at the H-site and within 4 Å of the majority of ANS molecules docked to rGST M1-1 suggests a possible electrostatic contribution to the binding. However, as seen in Figure 20, this residue is only able to bond to a small percentage of the sulphonate group of the ANS molecules docked at the active site. In fact, this residue is seen be in close proximity of the anilino or naphthyl rings in the majority of the solutions. This would imply weak electrostatic interactions or none at all with ANS at the H-site. Electrostatic interactions have, however, been shown to drive the binding of ANS to bovine serum albumin (Celej et al., 2005) and the importance of taking these interactions into account for ANS binding to proteins have been reiterated by other authors (Kirk et al., 1996; Matulis and Lovrien, 1998). The heat capacity reported here is less negative than those previously reported for the binding of ANS to I-FABP (Kirk et al., 1996), A-LABP (Ory and Banaszak, 1999) and hGST A1-1 (Sayed et al., 2002) (-1.18 kJ/mol/K, -0.92 kJ/mol/K and –0.84 kJ/mol/K, respectively). The less negative value for the rGST M1-1●ANS interaction suggests that a smaller portion of nonpolar surface area is buried. This would support docking solutions obtained for the sulphonate of ANS pointing into the H-site and the anilino and naphthyl rings pointing toward the surrounding solvent molecules (Figure 20). Hydrophobic interactions also play a key role in determining the stability of ANS complexes with A-LBP (Ory and Banaszak, 1999), I-FABP (Kirk et al., 1996), SjGST (Yassin et al., 2004) and hGST A1-1 (Sayed et al., 2002). Contrary to this are the findings of Matulis and Lovrien (Matulis and Lovrien, 1998) that the binding of ANS to proteins is primarily dependent on ion-pair formation where the sulphonate group is the major binding determinant and the anilinonaphthalene moiety of ANS only serves to reinforce binding. The ANS site in rGST M1-1 is not strictly hydrophobic, as indicated by the fluorescence emission maximum of 483 nm for ANS bound to wild-type rGST M1-1. This is compared with the emission maximum of 545 nm for ANS in water and of 454 nm for ANS bound to the highly hydrophobic site in apomyoglobin (Stryer, 1965). The changes in heat capacity may be due to a

net loss in the thermally available number of hydrogen bond states for the relatively ordered cavity waters upon their release into the bulk (Kirk et al., 1996).

6 CONCLUSION

The binding of GSH, GSO_3^- and *S*-hexylglutathione, as investigated using ITC, is enthalpically driven and involves one site per monomeric unit of rGST M1-1. The affinity for each ligand differs with *S*-hexylglutathione having the highest affinity and glutathione the lowest. This has been attributed to a greater number of molecular contacts between *S*-hexylglutathione and the protein compared to that of GSH and GSO_3^-. Enthalpy and entropy show compensation although the contributions of the two components are different for each ligand investigated. The binding of GSH to rGST M1-1 is linked to deprotonation of the thiol group of GSH. Binding of these ligands to the enzyme is characterised by a negative ΔC_p with a linear dependence of ΔH on temperature observed for GSO_3^- binding and non-linear dependence observed for GSH and *S*-hexylglutathione binding. These differences reflect differences in the mechanisms of ligand recognition by the enzyme and implies that the interaction between rGST M1-1 and GSO_3^- forms a tighter complex with a more constrained mu-loop while that for GSH and *S*-hexylglutathione results in the formation of a complex that samples different equilibria and hence the mu-loop remains relatively mobile after ligand is bound. The results obtained in this study have enhanced the understanding of the molecular basis of the rGST M1-1●ligand interaction and the forces involved in this process.

The energetics of ANS binding to rGST M1-1 were undertaken in order to obtain a clearer understanding of the ligandin function of rGST M1-1. Displacement and docking studies were undertaken in order to locate the ANS binding site on rGST M1-1. ITC studies indicate that one molecule of ANS is bound per protein monomer with a moderate affinity. Enthalpy-entropy compensation is observed with both components contributing favourably to the Gibbs free energy of binding. The change in heat capacity associated with the interaction can be attributed to the burial of the polar sulphonate group of ANS and the exposure of the anilino and naphthyl rings to solvent as well as the possibility of weak electrostatic interactions between ANS and residues at the active site. Displacement and docking studies indicate that ANS is located in the H-pocket of the active site of rGST M1-1.

7 REFERENCES

Adang, A. E. P., Brussee, J., Van der Gen, A. and Mulder, G. J. (1990) The glutathione-binding site in glutathione *S*-transferases. *Biochem. J.* **269**, 47-54.

Andujar-Sanchez, M., Clemente-Jimenez, J. M., Las Heras-Vazquez, F. J., Rodriguez-Vico, F., Camara-Artigas, A. and Jara-Perez, V. (2003) Thermodynamics of glutathione binding to the tyrosine 7 phenylalanine mutant of glutathione *S*-transferase from *Schistosoma japonicum*. *Int. J. Biol. Macromol.* **32**, 77-82.

Andujar-Sanchez, M., Smith, A. W., Clemente-Jimenez, J. M., Rodriguez-Vico, F., Las Heras-Vazquez, F. J., Jara-Perez, V. and Camara-Artigas, A. (2005) Crystallographic and Thermodynamic Analysis of the Binding of S-Octylglutathione to the Tyr 7 to Phe Mutant of Glutathione S-Transferase from *Schistosoma japonicum*. *Biochemistry* **44**, 1174-1183.

Armstrong, R. N. (1991) Glutathione *S*-Transferases: Reaction Mechanism, Structure and Function. *Chem. Res. Toxicol.* **4**, 131-140.

Armstrong, R. N. (1997) Structure, Catalytic Mechanism, and Evolution of the Glutathione Transferases. *Chem. Res. Toxicol.* **10**, 2-18.

Armstrong, R. N., Gilliland, G. L., Ji, X., Johnson, W. W. and Liu, S. (1993) Crystallographic and mechanistic studies of class *mu* glutathione S-transferases. *Proc.Int.Meet.Struct.Funct.Glutathione Transferases*, 87-99.

Baker, B. M. and Murphy, K. P. (1997) Dissecting the energetics of a protein-protein interaction: the binding of ovomucoid third domain to elastase. *J. Mol. Biol.* **268**, 557-569.

Baker, B. M. and Murphy, K. P. (1996) Evaluation of linked protonation effects in protein binding reactions using isothermal titration calorimetry. *Biophys. J.* **71**, 2049-2055.

Barlow, D. J. and Thornton, J. M. (1983) Ion-pairs in proteins. *J. Mol. Biol.* **168**, 867-885.

Barycki, J. J. and Colman, R. F. (1997) Identification of the nonsubstrate steroid binding site of rat liver glutathione S-transferase, isozyme 1-1, by the steroid affinity label, 3β-(iodoacetoxy)dehydroisoandrosterone. *Arch. Biochem. Biophys.* **345**, 16-31.

Bico, P., Erhardt, J., Kaplan, W. and Dirr, H. (1995) Porcine class pi glutathione S-transferase: anionic ligand binding and conformational analysis. *Biochim. Biophys. Acta.* **1247**, 225-230.

Board, P. G., Baker, R. T., Chelvanayagam, G. and Jermin, L. S. (1997) Zeta, a novel class of glutathione transferases in a range of species from plants to humans. *Biochem. J.* **328**, 929-935.

Board, P. G., Coggan, M., Chelvanayagam, G., Easteal, G., Jermin, L. S., Schulte, G. K., Danley, D. E., Hoth, L. R., Griffor, M. C., Kamath, A. V., Rosner, M. H., Chrunyk, B. A., Perregaux, D. E., Gabel, C. A., Geoghegan, K. F. and Pandit, J. (2000) Identification, characterization, and crystal structure of the Omega class glutathione transferases. *J. Biol. Chem.* **275**, 24798-24806.

Board, P. G. and Mannervik, B. (1991) The contribution of the C-terminal sequence to the catalytic activity of GST2, a human alpha-class glutathione transferase. *Biochem. J.* **275**, 171-174.

Brokx, R. D., Lopez, M. M., Vogel, H. J. and Makhatadze, G. I. (2001) Energetics of target peptide binding by calmodulin reveals different modes of binding. *J. Biol. Chem.* **276**, 14083-14091.

Caccuri, A. M., Antonini, G., Board, P. G., Parker, M. W., Nicotra, M., Lo Bello, M., Federici, G. and Ricci, G. (1999) Proton release on binding of glutathione to Alpha, Mu and Delta class glutathione transferases. *Biochem. J.* **344**, 419-425.

Caccuri, A. M., Lo Bello, M., Nuccetelli, M., Nicotra, M., Rossi, P., Antonini, G., Federici, G. and Ricci, G. (1998) Proton Release upon Glutathione Binding to Glutathione Transferase P1-1: Kinetic Analysis of a Multistep Glutathione Binding Process. *Biochemistry* **37**, 3028-3034.

Cameron, A. D., Sinning, I., L'Hermite, G., Olin, B., Board, P. G., Mannervik, B. and Jones, T. A. (1995) Structural analysis of human alpha-class glutathione transferase A1-1 in the apo-form and in complexes with ethacrynic acid and its glutathione conjugate. *Structure* **3**, 717-727.

Caret, R. L., Denniston, K. J. and Topping, J. J. (1993) in Principles and applications of inorganic, organic and biologicl chemistry, pp. 465-466, Wm C. Brown Communications, Inc, U.S.A.

Celej, M. S., Dassie, S. A., Freire, E., Bianconi, M. L. and Fidelio, G. D. (2005) Ligand-induced thermostability in proteins: Thermodynamic analysis of ANS-albumin interaction. *Biochim. Biophys. Acta* **1750**, 122-133.

Cleland, W. W. (1992) Low-Barrier Hydrogen Bonds and Low Fractionation Factor Bases in Enzymatic Reactions. *Biochemistry* **31**, 319-319.

Codreanu, S. G., Ladner, J. E., Xiao, G., Stourman, N. V., Hachey, D. L., Gilliland, G. L. and Armstrong, R. N. (2002) Local protein dynamics and catalysis: detection of segmental motion associated with rate-limiting product release by a glutathione transferase. *Biochemistry* **41**, 15161-15172.

Codreanu, S. G., Thompson, L. C., Hachey, D. L., Dirr, H. W. and Armstrong, R. N. (2005) Influence of the Dimer Interface on Glutathione Transferase Structure and Dynamics Revealed by Amide H/D Exchange Mass Spectrometry. *Biochemistry* **44**, 10605-10612.

Connelly, P. R., Aldape, R. A., Bruzzese, F. J., Chambers, S. P., Fitzgibbon, M. J., Fleming, M. A., Itoh, S., Livingston, D. J., Navia, M. A., Thomson, J. A. and et al. (1994) Enthalpy of hydrogen bond formation in a protein-ligand binding reaction. *Proc. Natl. Acad. Sci. U S A* **91**, 1964-1968.

Cooper, A. (1999) Thermodynamic analysis of biomolecular interactions. *Curr. Opin. Chem. Biol.* **3**, 557-563.

Creighton, T. E. (1993) in Protein structures and molecular properties, W.H. Freeman and company, USA

Dill, K. A. (1997) Additivity principles in biochemistry. *J. Biol. Chem.* **272**, 701-704.

Dill, K. A. (1990) Dominant forces in protein folding. *Biochemistry* **29**, 7133-7155.

Dirr, H., Reinemer, P. and Huber, R. (1994a) Refined Crystal Structure of Porcine Class Pi Glutathione S-Transferase (pGST P1-1) at 2.1 A Resolution. *J. Mol. Biol.* **243**, 72-92.

Dirr, H., Reinemer, P. and Huber, R. (1994b) X-ray crystal structures of cytosolic glutathione *S*-transferases. *Eur. J. Biochem.* **220**, 645-661.

Dirr, H. W., Little, T., Kuhnert, D. C. and Sayed, Y. (2005) A conserved N-capping motif contributes significantly to the stabilisation and dynamics of the C-terminal region of class alpha glutathione transferases. *J. Biol. Chem.* **280**, 19480-19487.

Dirr, H. W. and Wallace, L. A. (1999) Role of the C-terminal helix 9 in the stability and ligandin function of class alpha glutathione transferase A1-1. *Biochemistry* **38**, 15631-15640.

Doyle, M. L. (1997) Characterization of binding interactions by isothermal titration calorimetry. *Curr. Opin. Biotechnol.* **8**, 31-35.

Duhovny, D., Nussinov, R. and Wolfson, H. J. (2002) in Proceedings of the 2'nd Workshop on Algorithms in Bioinformatics (WABI) Rome, Italy, Lecture Notes in Computer Science, vol. 2452 (Gusfield, e. a., ed.), pp. 185-200, Springer Verlag, 2002.

Dunitz, J. D. (1994) The Entropic Cost of Bound Water in Crystals and Biomolecules. *Science* **264**, 670-670.

Eftink, M. R., Anusiem, A. C. and Biltonen, R. L. (1983) Enthalpy-entropy compensation and heat capacity changes for protein-ligand interactions: general

thermodynamic models and data for the binding of nucleotides to ribonuclease A. *Biochemistry* **22**, 3884-3896.

Erhardt, J. and Dirr, H. (1996) Effect of glutathione, glutathione sulphonate and S-hexylglutathione on the conformational stability of class pi glutathione S-transferase. *FEBS Lett.* **391**, 313-316.

Freire, E. (1997) Thermodynamics of protein folding and molecular recognition. *Pure App. Chem.* **69**, 2253-2261.

Freire, E., Mayorga, O. L. and Straume, M. (1990) Isothermal Titration. *Anal. Chem.* **62**, 950-959.

Fukada, H. and Takahashi, K. (1998) Enthalpy and heat capacity changes for the proton dissociation of various buffer components in 0.1 M potassium chloride. *Proteins* **33**, 159-166.

Gomez, J. and Freire, E. (1995) Thermodynamic mapping of the inhibitor site of the aspartic protease endothiapepsin. *J. Mol. Biol.* **252**, 337-350.

Graminski, G. F., Kubo, Y. and Armstrong, R. N. (1989) Spectroscopic and Kinetic Evidence for the Thiolate Anion of Glutathione at the Active Site of Glutathion *S*-Transferase. *Biochemistry* **28**, 3562-3568.

Gu, Y., Singh, S. V. and Ji, X. (2000) Residue R216 and Catalytic Efficiency of a Murine Class Alpha Glutathione *S*-Transferase toward Benzo[*a*]pyrene 7(*R*),8(*S*)-Diol 9(*S*),10(*R*)-Epoxide. *Biochemistry* **39**, 12552-12557.

Guex, N. and Peitsch, M. C. (1997) SWISS-MODEL and the SwissPdb Viewer: An environment for comparative protein modeling. *Electrophoresis* **18**, 2714-2723.

Habig, W. H. and Jakoby, W. B. (1981) Assays for differentiation of glutathione *S*-transferases. *Methods Enzymol.* **77**, 398-405.

Habig, W. H., Pabst, M. J. and Jakoby, W. B. (1974) The first enzymatic step in mercapturic acid formation. *J. Biol. Chem.* **249**, 7130-7139.

Hitchens, T. K., Mannervik, B. and Rule, G. S. (2001) Disorder-to-order transition of the active site of human class Pi glutathione transferase, GST P1-1. *Biochemistry* **40**, 11660-11669.

Hoesch, R. M. and Boyer, T. D. (1989) Localisation of a portion of the active site of two rat liver glutathione S-transferases using a photoaffinity lavel. *J. Biol. Chem.* **264**, 17712-17717.

Ishikawa, T. (1992) The ATP-dependent glutathione S-conjugate export pump. *Trends Biochem. Sci.* **17**, 463-468.

Ishima, R. and Torchia, D. A. (2000) Protein dynamics from NMR. *Nature Struct. Biol.* **7**, 740-743.

Ji, X., Johnson, W. W., Sesay, M. A., Dickert, L., Prasad, S. M., Ammon, H. L., Armstrong, R. N. and Gilliland, G. L. (1994) Structure and function of the xenobiotic substrate binding site of a glutathione S-transferase as revealed by X-ray crystallographic analysis of product complexes with the diastereomers of 9-(S-glutathionyl)-10-hydroxy-9,10-dihydrophenanthrene. *Biochemistry* **33**, 1043-1052.

Ji, X., von Rosenvinge, E. C., Johnson, W. W., Armstrong, R. N. and Gilliland, G. (1996) Location of a potential transport binding site in a sigma class glutathione transferase by x-ray crystallography. *Proc. Natl. Acad. Sci. U S A* **93**, 8208-8213.

Ji, X., von Rosenvinge, E. C., Johnson, W. W., Tomarev, S. I., Piatigorsky, J., Armstrong, R. N. and Gilliland, G. L. (1995) Three-Dimensional Structure, Catalytic Properties, and Evolution of a Sigma Class Glutathione Transferase from Squid, a Progenitor of the Lens *S*-Crystallins of Cephalopods. *Biochemistry* **34**, 5317-5328.

Ji, X., Zhang, P., Armstrong, R. N. and Gilliland, G. L. (1992) The Three-dimensional Structure of a Glutathione *S*-Transferase from the Mu Gene Class. Structural

Analysis of the Binary complex of Isoenzyme 3-3 and Glutathione at 2.2-A Resolution. *Biochemistry* **31**, 10169-10184.

Jiang, L. and Lai, L. (2002) CH...O hydrogen bonds at protein-protein interfaces. *J. Biol. Chem.* **277**, 37732-37740.

Karshikoff, A., Reinemer, P., Huber, R. and Ladenstein, R. (1993) Electrostatic evidence for the activation of the glutathione thiol by Tyr7 in pi-class glutathione transferases. *Eur. J. Biochem.* **215**, 663-670.

Kauzmann, W. (1959) Some factors in the interpretation of protein denaturation. *Adv. Prot. Chem.* **14**, 1-63.

Ketley, J. N., Habig, W. H. and Jakoby, W. B. (1975) Binding of nonsubstrate ligands to the glutathione S-transferases. *J. Biol. Chem.* **250**, 8670-8673.

Kirk, W. R., Kurian, E. and Prendergast, F. G. (1996) Characterization of the sources of protein-ligand affinity: 1-sulfonato-8-(1')anilinonaphthalene binding to intestinal fatty acid binding protein. *Biophys. J.* **70**, 69-83.

Kolm, R. H., Sroga, G. E. and Mannervik, B. (1992) Participation of the phenolic hydroxyl group of Tyr-8 in the catalytic mechanism of human glutathione transferase P1-1. *Biochem. J.* **285**, 537-540.

Kolobe, D., Sayed, Y. and Dirr, H. W. (2004) Characterization of bromosulphophthalein binding to human glutathione S-transferase A1-1: thermodynamics and inhibition kinetics. *Biochem. J.* **382**, 703-709.

Kong, K., Nishida, M., Inoue, H. and Takahashi, K. (1992) Tyrosine-7 is an essential residue for the catalytic activity of human class pi glutathion *s*-transferase: chemical modification and site-directed mutagenesis studies. *Biochem. Biophys. Res. Commun.* **182**, 1122-1129.

Koshland, D. (1994) Key-lock and induced fit theory. *Angew. Chem. Int. Ed. Engl.* **33**, 2375-2378.

Kuhnert, D. C., Sayed, Y., Mosebi, S., Sayed, M., Sewell, T. and Dirr, H. W. (2005) Tertiary Interactions Stabilise the C-terminal Region of Human Glutathione Transferase A1-1: a Crystallographic and Calorimetric Study. *J. Mol. Biol.* **349**, 825-838.

Ladbury, J. E. and Williams, M. A. (2004) The extended interface: measuring non-local effects in biomolecular interactions. *Curr. Opin. Struct. Biol.* **14**, 562-569.

Ladbury, J. E., Wright, J. G., Sturtevant, J. M. and Sigler, P. B. (1994) A thermodynamic study of the trp repressor-operator interaction. *J. Mol. Biol.* **238**, 669-681.

Laemmli, U. K. (1970) Cleavage of structural proteins during the assembly of the head of bacteriophage T4. *Nature* **227**, 680-685.

Lartigue, A., Gruez, A., Spinelli, S., Riviere, S., Brossut, R., Tegoni, M. and Cambillau, C. (2003) The Crystal Structure of a Cockroach Pheremone-binding Protein Suggests a New Ligand Binding and Release Mechanism. *J. Biol. Chem.* **278**, 30213-30218.

Le Trong, I., Stenkamp, R. E., Ibarra, C., Atkins, W. M. and Adman, E. T. (2002) 1.3-A resolution structure of human glutathione S-transferase with S-hexyl glutathione bound reveals possible extended ligandin binding site. *Proteins* **48**, 618-627.

Leavitt, S. and Freire, E. (2001) Direct measurement of protein binding energetics by isothermal titration calorimetry. *Curr. Opin. Struct. Biol.* **11**, 560-566.

Litwack, G., Ketterer, B. and Arias, I. M. (1971) Ligandin: a hepatic protein which binds steroids, bilirubin, carcinogens and a number of exogenous organic anions. *Nature* **234**, 466-467.

Liu, S., Zhang, P., Ji, X., Johnson, W. W., Gilliland, G. L. and Armstrong, R. N. (1992) Contribution of Tyrosine 6 to the Catalytic Mechanism of Isoenzyme 3-3 of Glutathione *S*-Transferase. *J. Biol. Chem.* **267**, 4296-4299.

Livingstone, J. R., Spolar, R. S. and Record, M. T., Jr. (1991) Contribution to the thermodynamics of protein folding from the reduction in water-accessible nonpolar surface area. *Biochemistry* **30**, 4237-4244.

Loladze, V. V., Ermolenko, D. N. and Makhatadze, G. I. (2001) Heat capacity changes upon burial of polar and nonpolar groups in proteins. *Protein Sci.* **10**, 1343-1352.

Lumry, R. and Rajender, S. (1970) Enthalpy-entropy compensation phenomena in water solutions of proteins and small molecules: a ubiquitous property of water. *Biopolymers* **9**, 1125-1227.

Luque, I. and Freire, E. (2000) Structural stability of binding sites: consequences for binding affinity and allosteric effects. *Proteins Suppl.* **4**, 63-71.

Luque, I. and Freire, E. (1998) Structure-based prediction of binding affinities and molecular design of peptide ligands. *Methods Enzymol.* **295**, 100-127.

Luque, I., Gomez, J., Semo, N. and Freire, E. (1998) Structure-based thermodynamic design of peptide ligands: application to peptide inhibitors of the aspartic protease endothiapepsin. *Proteins* **30**, 74-85.

Makhatadze, G. I. (1990) Heat capacity of proteins. I. Partial molar heat capacity of individual amino acid residues in aqueous solution: hydration effect. *J. Mol. Biol.* **213**, 375-384.

Makhatadze, G. I. and Privalov, P. L. (1995) Energetics of protein structure. *Adv. Prot. Chem.* **47**, 307-425.

Mannervik, B., Alin, P., Guthenberg, C., Jensson, H., Tahir, M. K., Warholm, M. and Jornvall, H. (1985) Identification of three classes of cytosolic glutathione transferase common to several mammalian species: correlation between structural data and enzymatic properties. *Proc. Natl. Acad. Sci. USA* **82**, 7202-7206.

Mannervik, B., Awasthi, Y. C., Board, P. G., Hayes, J. D., Di Ilio, C., Ketterer, B., Litowsky, I., Morgenstern, R., Muramatsu, M. and Pearson, W. R. (1992) Nomenclature for human glutathione transferases. *Biochem. J.* **282**, 305-306.

Mannervik, B. and Danielson, U. H. (1988) Glutathione Transferases - Structure and Catalytic Activity. *CRC Crit. Rev. Biochem.* **23**, 283-337.

Manoharan, T. H., Gulick, A. M., Reinemer, P., Dirr, H. W., Huber, R. and Fahl, W. E. (1992) Mutational substitution of residues implicated by crystal structure in binding the substrate glutathione to human glutathione S-transferase Pi. *J. Mol. Biol.* **226**, 319-322.

Matulis, D. and Lovrien, R. (1998) 1-Anilino-8-Napthalene Sulfonate Anion-Protein Binding Depends Primarily on Ion Pair Formation. *Biophys. J.* **74**, 422-429.

McCallum, S. A., Hitchens, T. K. and Rule, G. S. (1999) Solution structure of the carboxyl terminus of a human class Mu glutathione S-transferase: NMR assignment strategies in large proteins. *J. Mol. Biol.* **285**, 2119-2132.

McCallum, S. A., Hitchens, T. K., Torborg, C. and Rule, G. S. (2000) Ligand-induced changes in the structure and dynamics of a human class Mu glutathione S-transferase. *Biochemistry* **39**, 7343-7356.

McTigue, M. A., Williams, D. R. and Tainer, J. A. (1995) Crystal structures of a schistosomal drug and vaccine target: glutathione S-transferase from Schistosoma japonica and its complex with the leading antischistosomal drug praziquantel. *J. Mol. Biol.* **246**, 21-27.

Meyer, D. J., Coles, B., Pemble, S. E., Gilmore, K. S., Fraser, G. M. and Ketterer, B. (1991) Theta, a new class of glutathione transferases purified from rat and man. *Biochem. J.* **274**, 409-414.

Milev, S., Gorfe, A. A., Karshikoff, A., Clubb, R. T., Bosshard, H. R. and Jelesarov, I. (2003a) Energetics of sequence-specific protein-DNA association: binding of integrase Tn916 to its target DNA. *Biochemistry* **42**, 3481-3491.

Milev, S., Gorfe, A. A., Karshikoff, A., Clubb, R. T., Bosshard, H. R. and Jelesarov, I. (2003) Energetics of sequence-specific protein-DNA association: conformational stability of the DNA binding domain of integrase Tn916 and its cognate DNA duplex. *Biochemistry* **42**, 3492-3502.

Murphy, K. P. (1999) Predicting binding energetics from structure: looking beyond DeltaG degrees. *Med. Res. Rev.* **19**, 333-339.

Nieslanik, B. S., Ibarra, C. and Atkins, W. M. (2001) The C-terminus of glutathione S-transferase A1-1 is required for entropically-driven ligand binding. *Biochemistry* **40**, 3536-3543.

Nishida, M., Kong, K., Inoue, H. and Takahashi, K. (1994) Molecular cloning and site-directed mutagenesis of glutathione S-transferase from *Escherichia coli*. The conserved tyrosyl residue near the N terminus is not essential for catalysis. *J. Biol. Chem.* **289**, 32536-32541.

Oakley, A. J., Lo Bello, M., Nuccetelli, M., Mazzetti, A. P. and Parker, M. W. (1999) The Ligandin (Non-substrate) Binding Site of Human Pi Class Glutathione Transferase is Located in the Electrophile Binding Site (H-site). *J. Mol. Biol.* **291**, 913-926.

Oakley, A. J., Rossjohn, J., Lo Bello, M., Caccuri, A. M., Federici, G. and Parker, M. W. (1997) The three-dimensional structure of the human Pi class glutathione transferase P1-1 in complex with the inhibitor ethacrynic acid and its glutathione conjugate. *Biochemistry* **36**, 576-585.

Ortiz-Salmeron, E., Nuccetelli, M., Oakley, A. J., Parker, M. W., Lo Bello, M. and Garcia-Fuentes, L. (2003) Thermodynamic description of the effect of the mutation Y49F on human glutathione transferase P1-1 in binding with glutathione and the inhibitor *S*-hexylglutathione. *J. Biol. Chem.* **278**, 46938-46948.

Ortiz-Salmeron, E., Yassin, Z., Clemente-Jimenez, J. M., Las Heras-Vazquez, F. J., Rodriguez-Vico, F., Baron, C. and Garcia-Fuentes, L. (2001) Thermodynamic

analysis of the binding of glutathione to glutathione *S*-transferase over a range of temperatures. *Eur. J. Biochem.* **268**, 4307-4314.

Ortiz-Salmeron, E., Yassin, Z., Clemente-Jimenez, M. J., Las Heras-Vazquez, F. J., Rodriguez-Vico, F., Baron, C. and Garcia-Fuentes, L. (2001) A calorimetric study of the binding of S-alkylglutathiones to glutathione S-transferase. *Biochim. Biophys. Acta* **1548**, 106-113.

Ory, J. J. and Banaszak, L. J. (1999) Studies of the ligand binding reaction of adipocyte lipid binding protein using the fluorescent probe 1, 8-anilinonaphthalene-8-sulfonate. *Biophys. J.* **77**, 1107-1116.

Pace, C. N. (1992) Contribution of the hydrophobic effect to globular protein stability. *J. Mol. Biol.* **226**, 29-35.

Parraga, A., Garcia-Saez, I., Walsh, S. B., Mantle, T. J. and Coll, M. (1998) The three-dimensional structure of a class-Pi glutathione S-transferase complexed with glutathione: the active-site hydration provides insights into the reaction mechanism. *Biochem. J.* **333**, 811-816.

Parsons, J. F. and Armstrong, R. N. (1996) Proton Configuration in the Ground State and Transisiton State of a Glutathione Transferase-Catalyzed Reaction Inferred from the Properties of Tetradeca(3-fluorotyrosyl)glutathione Transferase. *J. Am. Chem. Soc.* **118**, 2295-2296.

Pemble, S. E., Wardle, A. F. and Taylor, J. B. (1996) Glutathione S-transferase class Kappa: characterisation by the cloning of rat mitochondrial GST and identification of a human homologue. *Biochem. J.* **319**, 749-754.

Perkins, S. J. (1986) Protein volumes and hydration effects. *Eur. J. Biochem.* **157**, 169-180.

Plum, G. E. and Breslauer, K. J. (1995) Calorimetry of proteins and nucleic acids. *Curr. Opin. Struct. Biol.* **5**, 682-690.

Ralat, L. A. and Colman, R. F. (2004) Glutathione *S*-Transferase Pi Has at Least Three Distinguishable Xenobiotic Substrate Sites Close to Its Glutathione-binding Site. *J. Biol. Chem.* **279**, 50204-50213.

Ralat, L. A. and Colman, R. F. (2003) Monobromobimane occupies a distinct xenobiotic substrate site in glutathione *S*-transferase pi. *Protein Sci.* **12**, 2575-2587.

Reinemer, P., Dirr, H. W., Ladenstein, R., Huber, R., Lo Bello, M., Federici, G. and Parker, M. W. (1992) Three-dimensional structure of class pi glutathione S-transferase from human placenta in complex with S-hexylglutathione at 2.8 A resolution. *J. Mol. Biol.* **227**, 214-226.

Reinemer, P., Dirr, H. W., Ladenstein, R., Schaffer, J., Gallay, O. and Huber, R. (1991) The three-dimensional structure of class pi glutathione S-transferase in complex with glutathione sulfonate at 2.3 A resolution. *EMBO. J.* **10**, 1997-2005.

Ross, P. D. and Subramanian, S. (1981) Thermodynamics of protein association reactions: forces contributing to stability. *Biochemistry* **20**, 3096-3102.

Sayed, Y. (2001) Biochemical and thermodynamic characterization of ligand-binding to human class Alpha glutathione transferase A1-1. *PhD Thesis*, University of the Witwatersrand, Johannesburg.

Sayed, Y., Hornby, J. A., Lopez, M. and Dirr, H. (2002) Thermodynamics of the ligandin function of human class Alpha glutathione transferase A1-1: energetics of organic anion ligand binding. *Biochem. J.* **363**, 341-346.

Schneidman-Duhovny, D., Inbar, Y., Polak, V., Shatsky, M., Halperin, I., Benyamini, H., Barzilai, A., Dror, O., Haspel, N., Nussinov, R. and Wolfson, H. J. (2003) Taking geometry to its edge: fast unbound rigid (and hinge-bent) docking. *Proteins* **52**, 107-112.

Schonbrunn, E., Eschenburg, S., Luger, K., Kabsh, W. and Amrhein, N. (2000) Structural basis for the interaction of the fluorescence probe 8-anilino-1-naphthalene

sulfonate (ANS) with the antibiotic target MurA. *Proc. Natl. Acad. Sci. U S A* **97**, 6345-6349.

Sheehan, D., Meade, G., Foley, V. M. and Dowd, C. A. (2001) Structure, function and evolution of glutathione transferases: implications for classification of non-mammalian members of an ancient enzyme superfamily. *Biochem. J.* **360**, 1-16.

Sigurskjold, B. W., Altman, E. and Bundle, D. R. (1991) Sensitive titration microcalorimetric study of the binding of Salmonella O-antigenic oligosaccharides by a monoclonal antibody. *Eur. J. Biochem.* **197**, 239-246.

Sinning, I., Kleywegt, G. J., Cowan, S. W., Reinemer, P., Dirr, H. W., Huber, R., Gilliland, G. L., Armstrong, R. N., Ji, X., Board, P. G. and et al. (1993) Structure determination and refinement of human alpha class glutathione transferase A1-1, and a comparison with the Mu and Pi class enzymes. *J. Mol. Biol.* **232**, 192-212.

Sluis-Cremer, N., Naidoo, N. N., Kaplan, W. H., Manoharan, T. H., Fahl, W. E. and Dirr, H. W. (1996) Determination of a binding site for a non-substrate ligand in mammalian cytosolic glutathione S-transferases by means of fluorescence-resonance energy transfer. *Eur. J. Biochem.* **241**, 484-488.

Sluis-Cremer, N., Wallace, L. A., Burke, J., Stevens, J. M. and Dirr, H. (1998) Aflatoxin B1 and sulphobromophthalein binding to the dimeric human *S*-transerase A1-1: a fluorescence spectroscopic analysis. *Eur. J. Biochem.* **257**, 434-442.

Spolar, R. S., Ha, J. and Record, M. T., Jr. (1989) Hydrophobic effect in protein folding and other noncovalent processes involving proteins. *Proc. Natl. Acad. Sci. U S A* **86**, 8382-8385.

Spolar, R. S. and Record, M. T., Jr. (1994) Coupling of local folding to site-specific binding of proteins to DNA. *Science* **263**, 777-784.

Stella, L., Caccuri, A. M., Rosato, N., Nicotra, M., Lo Bello, M., De Matteis, F., Mazzetti, A. P., Federici, G. and Ricci, G. (1998) Flexibility of Helix 2 in the Human Glutathione Transferase P1-1. *J. Biol. Chem.* **273**, 23267-23273.

Stenberg, G., Board, P. G. and Mannervik, B. (1991) Mutation of an evolutionarily conserved tyrosine residue in the active site of a human class Alpha glutathione transferase. *FEBS Lett.* **293**, 153-155.

Stryer, L. (1965) The interaction of a naphthalene dye with apomyoglobin and apohemoglobin. A fluorescent probe on non-polar binding sites. *J. Mol. Biol.* **13**, 482-495.

Sturtevant, J. M. (1977) Heat capacity and entropy changes in processes involving proteins. *Proc. Natl. Acad. Sci. U S A* **74**, 2236-2240.

Thorson, J. S., Shin, I., Chapman, E., Stenberg, G., Mannervik, B. and Schultz, P. G. (1998) Analysis of the Role of the Active Site Tyrosine in Human Glutathione Transferase A1-1 by Unnatural Amino Acid Mutagenesis. *J. Am. Chem. Soc.* **120**, 451-452.

Tsai, C., Xu, D. and Nussinov, R. (1997) Structural motifs at protein-protein interfaces: Protein cores versus two-state and three-state model complexes. *Protein Sci.* **6**, 1793-1805.

Velazquez-Campoy, A. and Freire, E. (2005) ITC in the post-genome era...? Priceless. *Biophys. Chem.* **115**, 115-124.

Velazquez-Campoy, A., Luque, I., Todd, M. J., Milutinovich, M., Kiso, Y. and Freire, E. (2000) Thermodynamic dissection of the binding energetics of KNI-272, a potent HIV-1 protease inhibitor. *Protein Sci.* **9**, 1801-1809.

Wallace, L. A. and Dirr, H. W. (1999) Folding and assembly of dimeric human glutathione transferase A1-1. *Biochemistry* **38**, 16686-16694.

Wang, R. W., Newton, D. J., Huskey, S. E., McKeever, B. M., Pickett, C. B. and Lu, A. Y. (1992) Site-directed mutagenesis of glutathione S-transferase YaYa. Important roles of tyrosine 9 and aspartic acid 101 in catalysis. *J. Biol. Chem.* **267**, 19866-19871.

Wang, R. W., Newton, D. J., Huskey, S. W., McKeever, B. M., Picket, C. B. and Lu, A. Y. H. (1992) Site-directed Mutagenesis of Glutathione *S*-Transferase YaYa. *J. Biol. Chem.* **267**, 19866-19871.

Widersten, M., Bjornestedt, R. and Mannervik, B. (1996) Involvement of the Carboxyl Groups of Glutathione in the Catalytic Mechanism of Human Glutathione Transferase A1-1. *Biochemistry* **35**, 7731-7742.

Wilce, M. C. and Parker, M. W. (1994) Structure and function of glutathione S-transferases. *Biochim. Biophys. Acta* **1205**, 1-18.

Winder, A. F. and Gent, W. L. (1971) Correction of light-scattering errors in spectrophotometric protein determinations. *Biopolymers* **10**, 1243-1251.

Wiseman, T., Williston, S., Brandts, J. F. and Lin, L. N. (1989) Rapid measurement of binding constants and heats of binding using a new titration calorimeter. *Anal. Biochem.* **179**, 131-137.

Xiao, G., Liu, S., Ji, X., Johnson, W. W., Chen, J., Parsons, J. F., Stevens, W. J., Gilliland, G. L. and Armstrong, R. N. (1996) First-Sphere and Second-Sphere Electrostatic Effects in the Active Site of a Class Mu Glutathione Transferase. *Biochemistry* **35**, 4753-4765.

Xu, D., Lin, S. L. and Nussinov, R. (1997) Protein Binding versus Protein Folding: The Role of Hydrophilic Bridges in Protein Associations. *J. Mol. Biol.* **265**, 68-84.

Yassin, Z., Ortiz-Salmeron, E., Garcia-Maroto, F., Baron, C. and Garcia-Fuentes, L. (2004) Implications of the ligandin binding site on the binding of non-substrate ligands to Schistosoma japonicum-glutathione transferase. *Biochim. Biophys. Acta* **1698**, 227-237.

Yassin, Z., Ortiz-Salmeron, E., Glemente-Jimenez, J. M., Baron, C. and Garcia-Fuentes, L. (2003) Role of mutation Y6F on the binding properties of *Schistosoma japonicum* glutathione S-transferase. *Int. J. Biol. Macromol.* **32**, 67-75.

Zhang, P., Liu, S., Shan, S., Gilliland, G. and Armstrong, R. N. (1992) Modular mutagenesis of exons 1, 2, and 8 of a glutathione S-transferase from the mu class. Mechanistic and structural consequences for chimeras of isoenzyme 3-3. *Biochemistry* **31**, 10185-10193.

Zhang, P. H. and Armstrong, R. N. (1990) Construction, expression, and preliminary characterization of chimeric class mu glutathione S-transferases with altered catalytic properties. *Biopolymers* **29**, 159-169.

8 APPENDIX

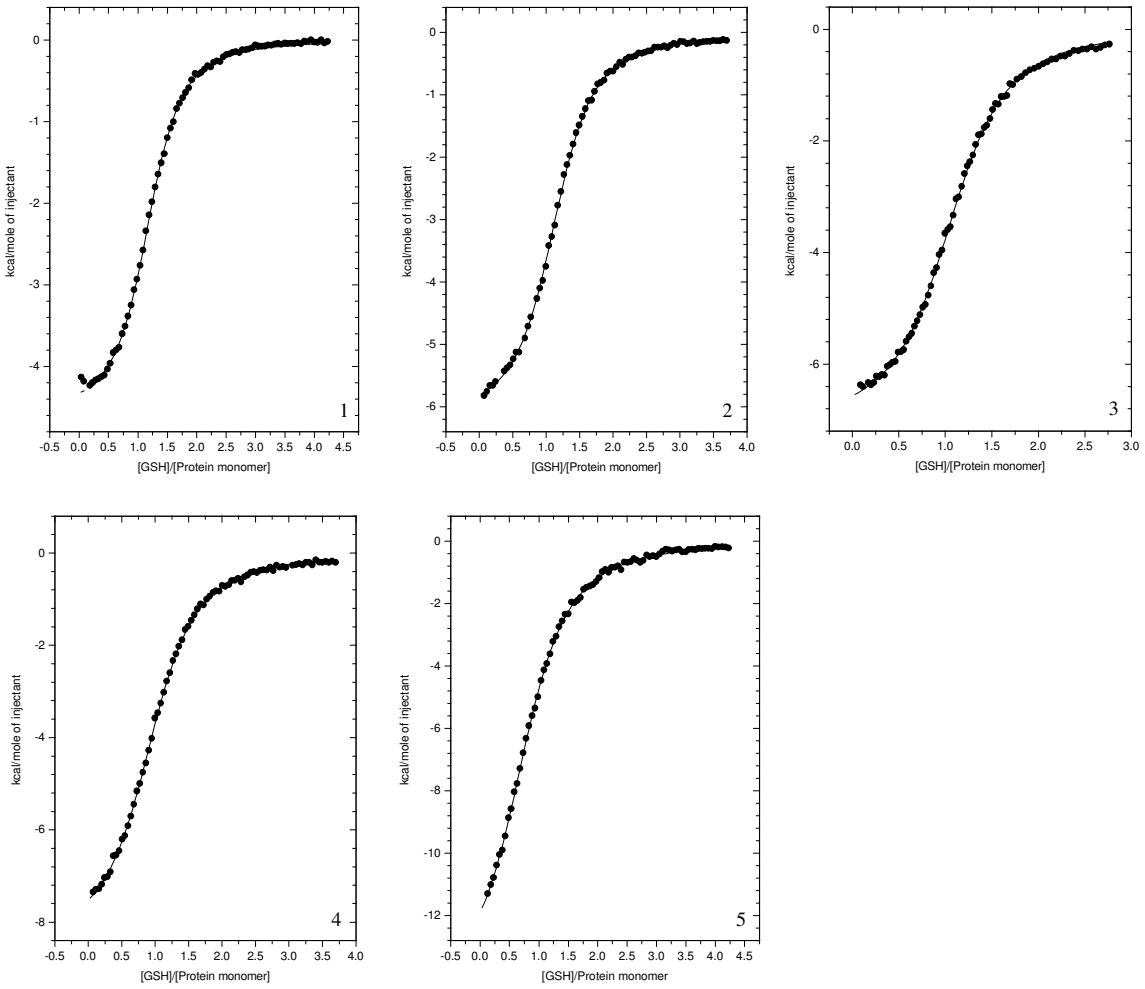

Figure 21: Temperature dependence of the binding of GSH to rGST M1-1.

Binding isotherms (1-5) were obtained at 5, 10, 15, 20 and 30 °C, respectively. Experiments were performed in a 20 mM sodium phosphate buffer containing 100 mM NaCl, 1 mM EDTA, 1.3 mM TCEP and 0.02% sodium azide, pH 6.5. Data in each panel represents the integrated exothermic heats generated upon each injection of GSH into rGST M1-1 (corrected for heats of dilution). The solid line through the data represents the best non-linear least-squares fit to the experimental data using a one-site binding model.

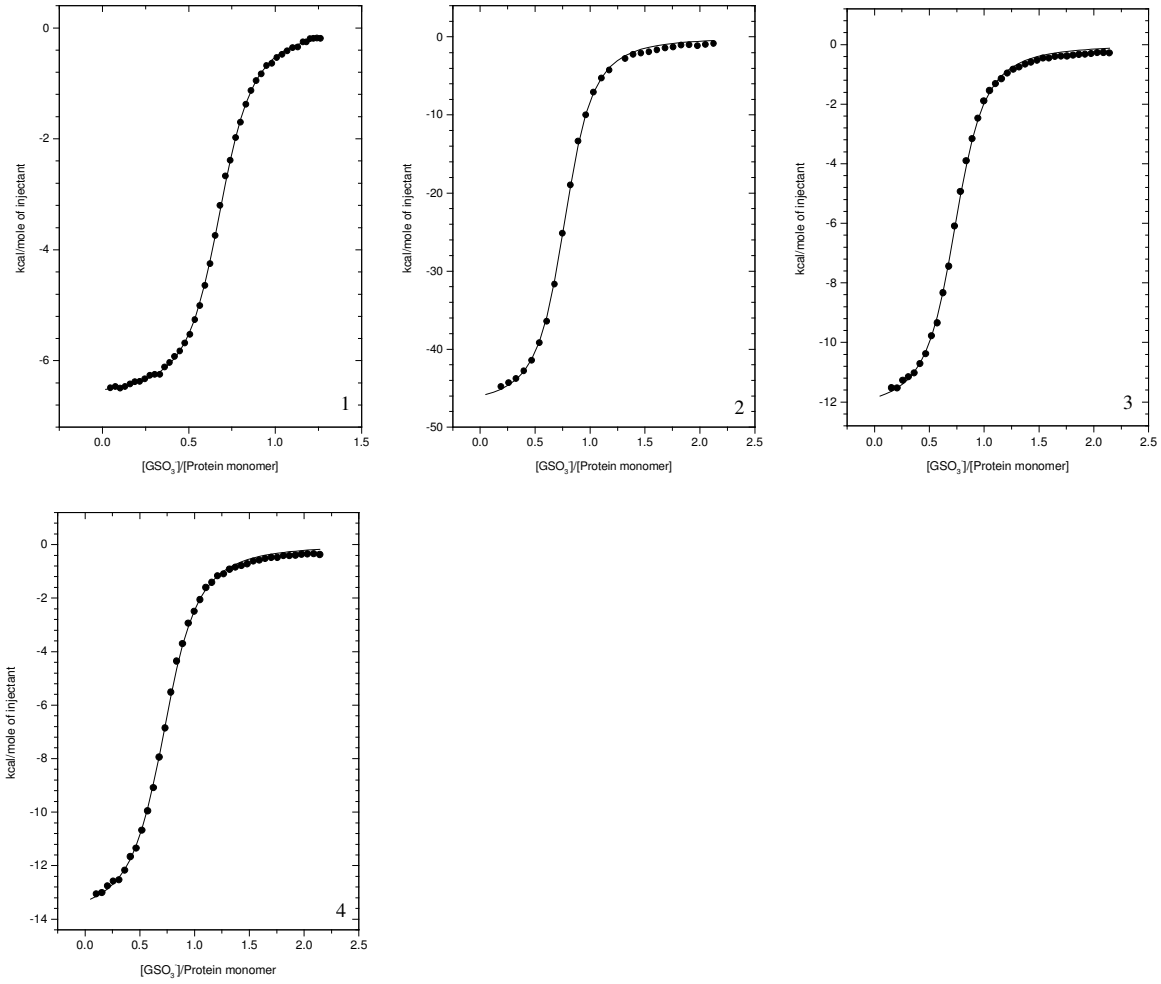

Figure 22: Temperature dependence of the binding of GSO_3^- to rGST M1-1.

Binding isotherms (1-4) were obtained at 5, 10, 15 and 20 °C, respectively. Experiments were performed in a 20 mM sodium phosphate buffer containing 100 mM NaCl, 1 mM EDTA, 1.3 mM TCEP and 0.02% sodium azide, pH 6.5. Data in each panel represents the integrated exothermic heats generated upon each injection of GSO_3^- into rGST M1-1 (corrected for heats of dilution). The solid line through the data represents the best non-linear least-squares fit to the experimental data using a one-site binding model.

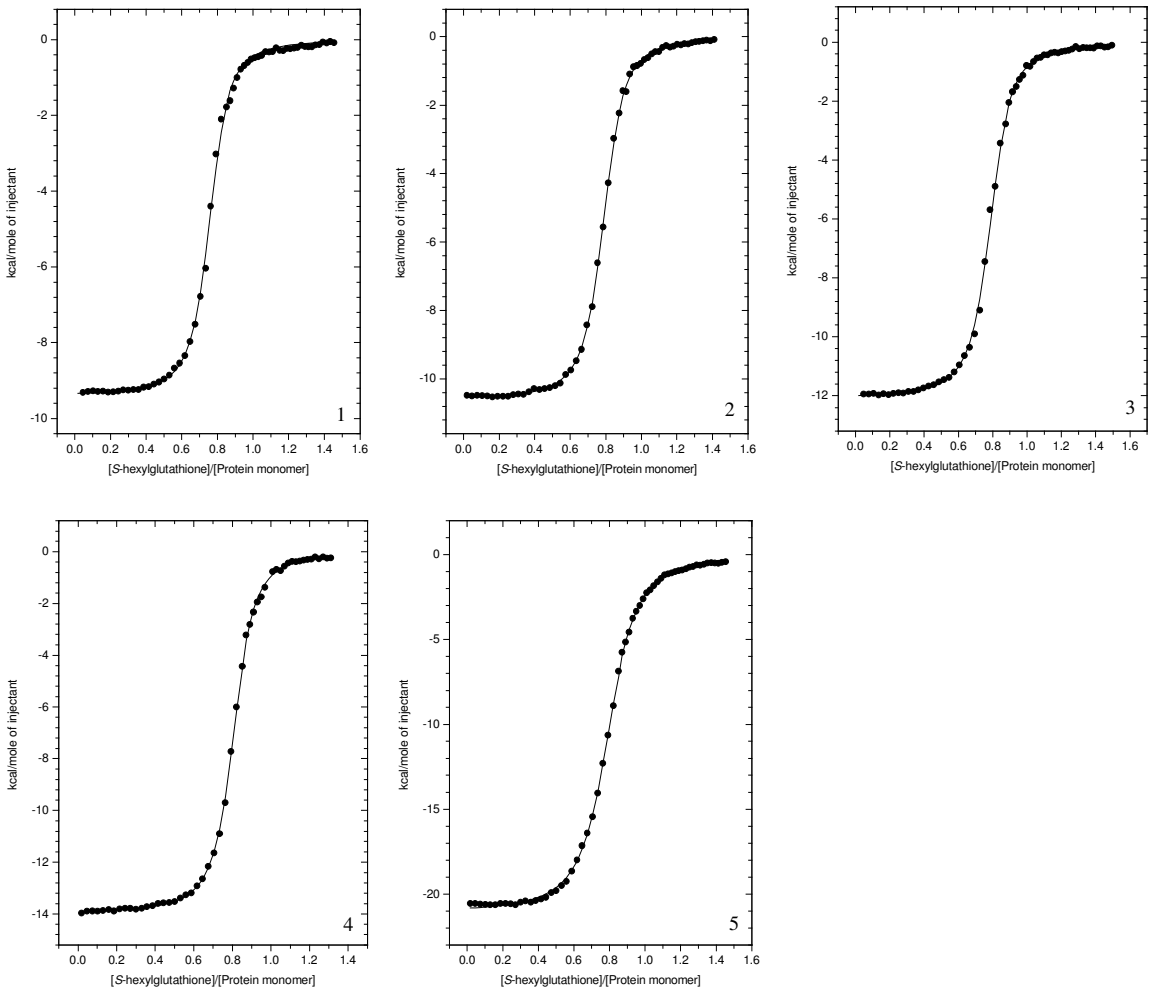

Figure 23: Temperature dependence of the binding of *S*-hexylglutathione to rGST M1-1.

Binding isotherms (1-5) were obtained at 5, 10, 15, 20 and 30 °C, respectively. Experiments were performed in a 20 mM sodium phosphate buffer containing 100 mM NaCl, 1 mM EDTA, 1.3 mM TCEP and 0.02% sodium azide, pH 6.5. Data in each panel represents the integrated exothermic heats generated upon each injection of *S*-hexylglutathione into rGST M1-1 (corrected for heats of dilution). The solid line through the data represents the best non-linear least-squares fit to the experimental data using a one-site binding model.

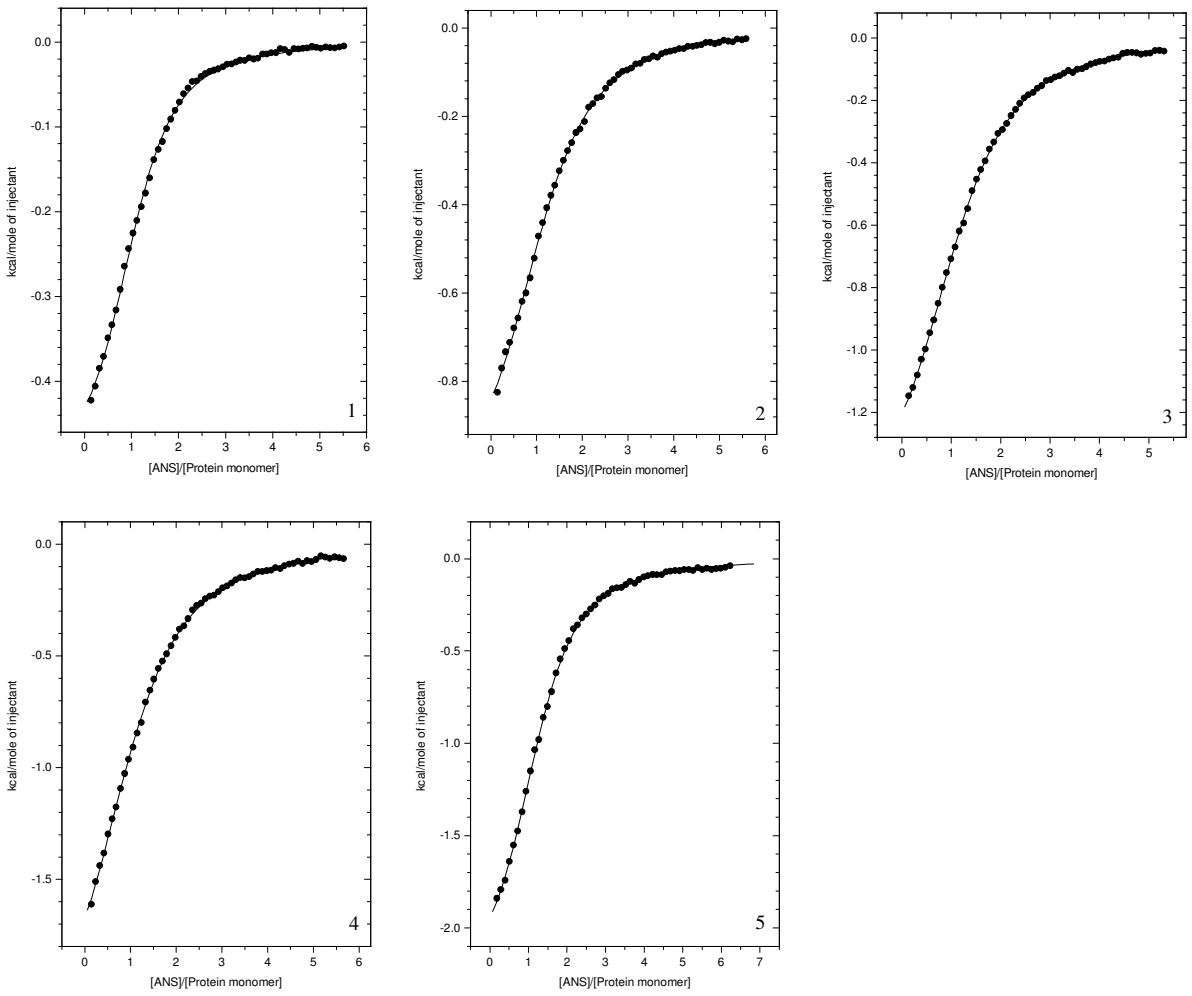

Figure 24: Temperature dependence of the binding of ANS to rGST M1-1.

Binding isotherms (1-5) were obtained at 5, 10, 15, 20 and 30 °C, respectively. Experiments were performed in a 20 mM sodium phosphate buffer containing 100 mM NaCl, 1 mM EDTA, 1.3 mM TCEP and 0.02% sodium azide, pH 6.5. Data in each panel represents the integrated exothermic heats generated upon each injection of ANS into rGST M1-1 (corrected for heats of dilution). The solid line through the data represents the best non-linear least-squares fit to the experimental data using a one-site binding model.

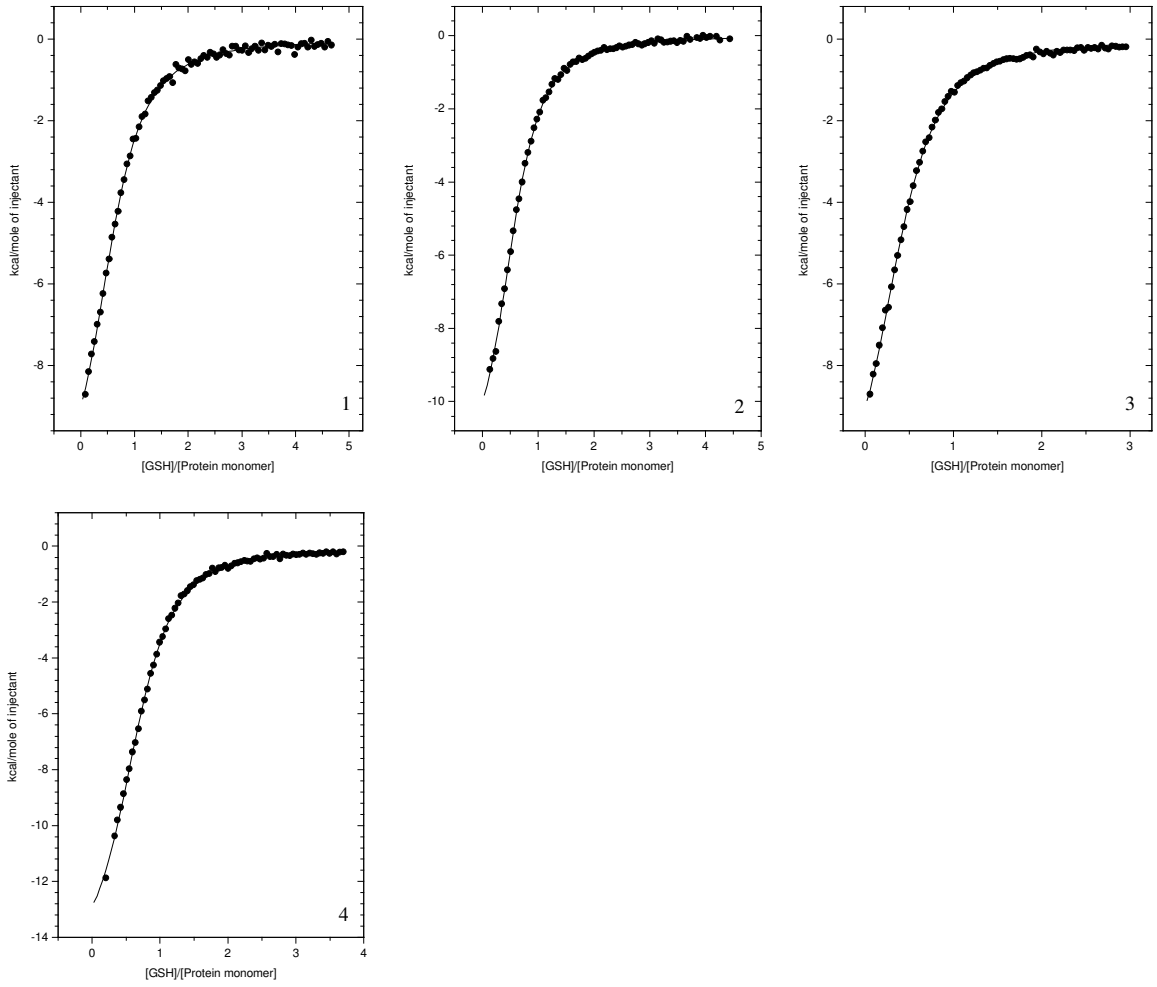

Figure 25: Dependence of the binding of GSH to rGST M1-1 on buffer ionisation.

Binding isotherms were obtained in 20 mM Mes (1), HEPES (2), PIPES (3) and imidazole (4) buffers, at 25 ºC, pH 6.5. All buffers contained 100 mM NaCl, 1 mM EDTA, 1.3 mM TCEP and 0.02% sodium azide. Data in each panel represents the integrated exothermic heats generated upon each injection of GSH into rGST M1-1 (corrected for heats of dilution). The solid line through the data represents the best non-linear least-squares fit to the experimental data using a one-site binding model.

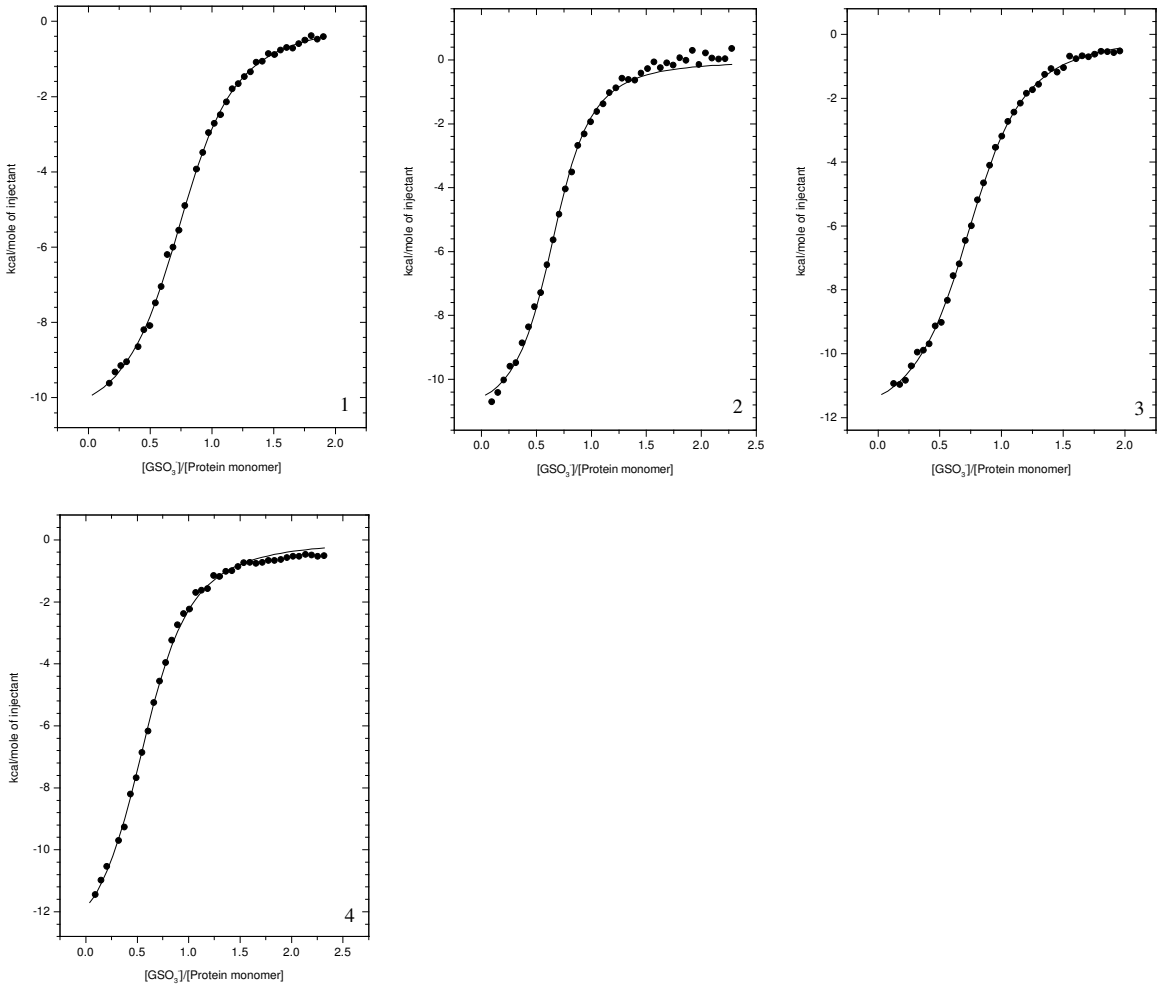

Figure 26: Dependence of the binding of GSO_3^- to rGST M1-1 on buffer ionisation.

Binding isotherms were obtained in 20 mM Mes (1), HEPES (2), PIPES (3) and imidazole (4) buffers, at 25 ºC, pH 6.5. All buffers contained 100 mM NaCl, 1 mM EDTA, 1.3 mM TCEP and 0.02% sodium azide. Data in each panel represents the integrated exothermic heats generated upon each injection of GSO_3^- into rGST M1-1 (corrected for heats of dilution). The solid line through the data represents the best non-linear least-squares fit to the experimental data using a one-site binding model.